Star-Formation Histories, Abundances, and Kinematics of Dwarf Galaxies in the Local Group

Eline Tolstoy,[1] Vanessa Hill,[2] and Monica Tosi[3]

[1]Kapteyn Astronomical Institute, University of Groningen, 9700AV Groningen, The Netherlands; email: etolstoy@astro.rug.nl

[2]Departement Cassiopee, Université de Nice Sophia-Antipolis, Observatoire de la Côte d'Azur, CNRS, F-06304 Nice Cedex 4, France; email: Vanessa.Hill@oca.eu

[3]INAF-Osservatorio Astronomico di Bologna, I-40127 Bologna, Italy; email: monica.tosi@oabo.inaf.it

Annu. Rev. Astron. Astrophys. 2009. 47:371–425

The *Annual Review of Astronomy and Astrophysics* is online at astro.annualreviews.org

This article's doi: 10.1146/annurev-astro-082708-101650

0066-4146/09/0922-0371$20.00

Key Words

Galaxies: dwarf, Galaxies: evolution, Galaxies: formation, Galaxies: stellar content

Abstract

Within the Local Universe galaxies can be studied in great detail star by star, and here we review the results of quantitative studies in nearby dwarf galaxies. The color-magnitude diagram synthesis method is well established as the most accurate way to determine star-formation histories of galaxies back to the earliest times. This approach received a large boost from the exceptional data sets that wide-field CCD imagers on the ground and the *Hubble Space Telescope* could provide. Spectroscopic studies using large ground-based telescopes such as VLT, Magellan, Keck, and HET have allowed the determination of abundances and kinematics for significant samples of stars in nearby dwarf galaxies. These studies have shown how the properties of stellar populations can vary spatially and temporally. This leads to important constraints to theories of galaxy formation and evolution. The combination of spectroscopy and imaging and what they have taught us about dwarf galaxy formation and evolution is the aim of this review.

. . . Les gens ont des étoiles qui ne sont pas les mêmes. Pour les uns, qui voyagent, les étoiles sont des guides. Pour d'autres elle ne sont rien que de petites lumières. Pour d'autres qui sont des savants elles sont des problèmes.

(Antoine de Saint-Exupéry, Le Petit Prince, XXVI)

1. INTRODUCTION

What is a dwarf galaxy? Past definitions always focus on size (e.g., Hodge 1971, Tammann 1994), and the presence of a dark matter halo (e.g., Mateo 1998). Is there any other physical property that distinguishes a dwarf galaxy from bigger galaxies? Are the differences merely due to the amount of baryonic matter that is retained by a system during its evolution? In general, large late-type galaxies sit on the constant central surface brightness ridge defined by Freeman (1970), and appear to have managed to retain most of the baryons they started with. Conversely, for galaxies that lie below this limit, it seems that the fainter they are, the higher the fraction of baryons they have lost. This could be due to Supernova winds and/or tidal interactions, which are effective when a galaxy lacks a suitably deep potential well to be able to hold onto to its gas and/or metals. The galaxies above this central surface brightness limit are either currently forming stars very actively, such as blue compact dwarfs (BCDs), or they have had very active star-formation activity in the past (e.g., elliptical galaxies).

The definition of a galaxy as a dark matter halo naturally excludes globular clusters, which are believed not to contain any dark matter, evidence of extended star-formation histories or associated chemical enrichment. The structural properties of globular clusters (see **Figure 1**) tend to support the idea that they are distinct from galaxies. This definition also excludes tidal dwarfs, and indeed we do not consider them here as they are more a probe of the disruption of large systems. They are a different category of objects that formed much later than the epoch of galaxy formation. There are also no obvious nearby examples of tidal dwarfs where the resolved stellar population can be accurately studied back to the earliest times.

Here we aim to build upon the outstanding review of Mateo (1998) and leave behind the idea that dwarf galaxies are in any way special systems. Many galactic properties (e.g., potential well, metallicity, size) correlate with mass and luminosity, and all types of galaxies show continuous relations in structural, kinematic, and population features between the biggest and the smallest of their kind (e.g., see **Figure 1**). Part of our aim in this review is to investigate these trends and learn from them. The only justification to segregate dwarf galaxies from other types is to study specific aspects of galaxy formation and evolution on a small scale.

Figure 1

Here are plotted the relationships between structural properties for different types of galaxies (after Kormendy 1985, Binggeli 1994), including as dotted lines the classical limits of the dwarf galaxy class as defined by Tammann (1994). (*a*) The absolute magnitude, M_V, versus central surface brightness, μ_V, plane; (*b*) The M_V versus half light radius, $r_{1/2}$, plane. Marked with colored ellipses are the typical locations of elliptical galaxies and bulges (*light red*), spiral galaxy disks (*light blue*), galactic nuclei (*dashed purple*), and large early-(spheroidals) and late-type systems (*dashed gray*). Galactic globular clusters are plotted individually as small gray points. M31, the Milky Way (MW), M33 and LMC are shown as blue open triangles. Some of the blue compact dwarfs with well-studied color-magnitude diagrams are marked as blue solid squares. The peculiar globular clusters ω Cen and NGC 2419 are marked close to the globular cluster ellipse, M32 in the region of elliptical galaxies, and the SMC near the border of the dwarf class. The ultracompact dwarfs (UCDs) studied in the Virgo and Fornax clusters are marked with purple crosses. Local Group dwarf galaxies are plotted as open pentagons, blue for systems with gas, and yellow for systems without gas. The recently discovered ultrafaint dwarfs are given star symbols, and the same color code. For references see text.

The taxonomy of dwarf galaxies typically opens a Pandora's box. At a very influential conference held at the Observatoire de Haute-Provence in 1993, G. Tammann gave a working definition: All galaxies that are fainter than $M_B \leq -16$ ($M_V \leq -17$) and more spatially extended than globular clusters (see *dotted lines* in **Figure 1**) are dwarf galaxies (Tammann 1994). This is broadly consistent

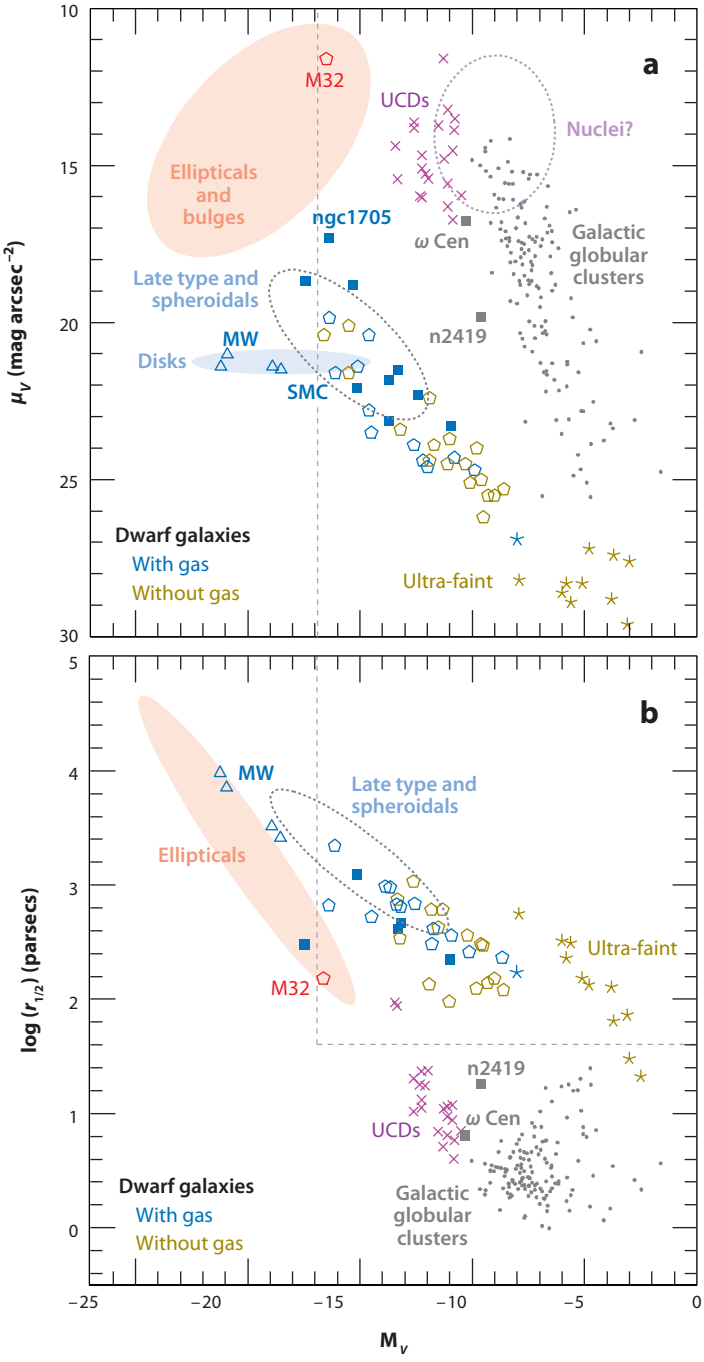

with the limit of mass at which outflows tend to significantly affect the baryonic mass of a galaxy. This includes a number of different types: early-type dwarf spheroidals (dSphs); late-type star-forming dwarf irregulars (dIs); the recently discovered very-low surface brightness, ultrafaint dwarfs (uFd); and centrally concentrated actively star-forming BCDs. The new class of even more extreme ultracompact dwarfs (UCDs) are identified as dwarf galaxies from spectra but are of a similar compactness to globular clusters (see **Figure 1**).

As has been stated throughout the years (Kormendy et al. 2008, and references therein), a morphological classification is only useful if it incorporates a physical understanding of the processes involved. However, at present this understanding is not complete and, hence, structural parameters and their relations may give us clues to the underlying physics. But we also have to be careful not to overinterpret these global measures, especially when we cross over from structurally simple to more complex systems (e.g., from early-type spheroidals to late-type disk-halo star-forming systems). This requires care to establish a meaningful comparison of the same properties of such different systems. This has most commonly been done using basic parameters such as surface brightness and absolute magnitude and physical size of the systems. In **Figure 1** we show these familiar relations. These kinds of plots were first made by Kormendy (1985), and have been used to great effect by Binggeli (1994) and more recently by Belokurov et al. (2007b).

Figure 1 illustrates how dwarfs compare with all other galaxies with no real evidence of a discontinuity, as already noted by Kormendy (1985). From a comparison of the absolute magnitude (M_V) and central surface brightness (μ_V) of galaxies (**Figure 1*a***), the early- and late-type dwarfs (from Irwin & Hatzidimitriou 1995; Mateo 1998; Whiting, Hau & Irwin 1999; Hunter & Elmegreen 2006) appear to fall along similar relations, overlapping with BCDs and other larger late-type systems (from Hunter & Elmegreen 2006) as well as faint spiral galaxy disks and those galaxies defined as spheroidals by Kormendy et al. (2008). This means systems that resemble late-type galaxies in their structural properties but are no longer forming stars. The uFds are clearly separated but arguably follow the same relation as the other dwarfs (from Simon & Geha 2007; Martin, de Jong & Rix 2008). There are clear distinctions in **Figure 1** between elliptical galaxies (from Faber et al. 1997, Kormendy et al. 2008) and other types, with the exception of spiral galaxy bulges. Similarly there are also clear distinctions between Globular clusters (from Harris 1996) and any other type of galaxy, with the exception of galactic nuclei. The position of M32 in the elliptical galaxy region is consistent with it being a low-luminosity elliptical galaxy (e.g., Wirth & Gallagher 1984) and not a dwarf galaxy, or even a tidally stripped larger system. There is evidence that ω Cen, with its clear spread in main sequence turn-offs (MSTOs), red giant branch (RGB) sequences, and chemical abundances, may be the stripped central remnant of an early-type system (e.g., Lee et al. 1999, Pancino et al. 2000, Bekki & Freeman 2003), and its position in **Figure 1** is consistent with that of galactic nuclei. It is interesting to note that ω Cen and nuclei also lie in the same region as the UCDs (from Evstigneeva et al. 2008).

The Magellanic Clouds move in and out of the dwarf galaxy class, which is not surprising as at least the Small Magellanic Cloud (SMC) lies near the boundary of the luminosity definition of dwarf class (see **Figure 1*a***). The fact that the Magellanic Clouds are interacting with each other and our Galaxy makes it more difficult to determine their intrinsic properties. The Large Magellanic Cloud (LMC) appears to be similar to low-luminosity spiral galaxies, such as M33, in terms of mass, luminosity, and size. The SMC, however, more resembles the larger dIs in the Local Group (e.g., NGC 6822, IC 1613), with similar mass, luminosity, and metallicity of star-forming regions.

In **Figure 1*b*** the varying physical size scales of different galaxy types and globular clusters are shown by plotting M_V against the half-light radius $r_{1/2}$, after Belokurov et al. (2007b). In this plot there is a clear (and unsurprising) trend for more luminous galaxies to be larger. The ellipticals clearly fall on a distinct narrow sequence (which is a projection of the fundamental plane). Dwarf

galaxies, that is, BCDs, late-type and spheroidal galaxies fall along a similar, although offset, tilted, and more scattered relation to the elliptical galaxies. Classical Local Group dSphs clearly overlap with irregular and BCD types. The uFds appear in a somewhat offset position. This is perhaps due to difficulties in accurately measuring the size of such diffuse objects, or it may be a real difference with other dwarf galaxies.

From **Figure 1** it can be seen that there is no clear separation between dwarf galaxies and the larger late-type and spheroidal systems. The dIs, BCDs, dSphs, hence late-type and spheroidal galaxies tend to overlap with each other in this parameter space. The overlapping properties of early- and late-type dwarfs have long been shown as convincing evidence that early-type dwarfs are the same as late-type systems that have been stripped of their gas (Kormendy 1985). This is quite different from the distinction between ellipticals and spirals (and spheroidals), which show a more fundamental difference (Kormendy et al. 2008). There is no clear break that distinguishes a dwarf from a larger galaxy and, hence, the most simple definition does not have an obvious physical meaning, as recognized by Tammann (1994).

Whatever the precise definition of subclasses, dwarf galaxies cover a large range of size, surface brightness, and distance, and so they are usually studied with different techniques with varying sensitivity to detail. Some galaxies are just easier to study than others (owing to distance, size, concentration, location in the sky, heliocentric velocity, etc.). This distribution also leads to biases in understanding the full distribution of properties of a complete sample (e.g., Koposov et al. 2008). Because of this the properties and inter-relations of the various types of dwarf galaxies are not always easy to understand.

The classic dichotomy is between early- and late-type dwarf galaxies. It is not easy to compare the properties of dwarf galaxies that have ongoing star formation (e.g., dIs, BCDs), with those that do not (e.g., dSphs). Indeed, the properties that can be measured, and then compared, are often different from one type of galaxy to another. The dSphs do not contain gas and so their internal kinematics can only be determined from stellar velocity dispersions. In gas-rich dIs, instead, the internal kinematics can be easily determined from the gas, and their distance makes them challenging targets to determine stellar velocities from RGB stars. Likewise, abundances in dIs are typically [O/H] measurements in young HII regions, whereas in dSphs they are usually [Fe/H] coming from individual RGB stars over a range of ages.

Galaxies in which the individual stars can be resolved are those that can be studied in the greatest detail. These are primarily to be found in the Local Group, where individual stars can be resolved and photometered down to the oldest MSTOs. This provides the most accurate star-formation histories (SFHs) going back to the earliest times. In the Local Group, spectra can be taken of individual RGB stars at high and intermediate resolution, providing information about the chemical content as well as the kinematics of a stellar population. The most accurate studies of resolved stellar populations have been made in Local Group dwarf galaxies, which are the numerically dominant constituent (e.g., Mateo 1998).

Historically, the first dwarfs to be noticed in the Local Group, leaving out the Magellanic Clouds (which are clearly visible to the naked eye), were the early-type dwarf satellites of M31. M32 and NGC 205 (M110) were first cataloged by C. Messier in 1770, NGC 185 by W. Herschel in 1787, and NGC 147 by J. Herschel in 1829. The spatially extended but low surface brightness dIs were first noticed somewhat later, e.g., NGC 6822 (1881, by E.E. Barnard), and IC 1613 and WLM (early 1900s, by M. Wolf). In all cases these galaxies were cataloged as "faint nebulae." It was not until the discovery (by H. Leavitt in 1912) and application to NGC 6822 (by E. Hubble in 1925) of the Cepheid distance scale that they were realized to be (dwarf) extragalactic systems. In 1938, H. Shapley discovered the first low surface brightness dwarf spheroidal galaxies, Sculptor (Scl) and Fornax (Fnx), around the Milky Way. From the 1930s onward, extensive

observing campaigns led to the compilation of large catalogs of dwarf galaxies extending beyond the Local Group, such as F. Zwicky's catalogs and the Uppsala General Catalog (UGC) initiated by E. Holmberg.

Over the past 50 years, there has been a steady stream of new discoveries of dwarf galaxies in the Local Group, and also in other nearby groups and clusters. The Local Group discovery rate has dramatically increased recently thanks to the Sloan Digital Sky Survey (SDSS; e.g., Adelman-McCarthy et al. 2007), and a new class of uFds (e.g., Willman et al. 2005, Zucker et al. 2006b, Belokurov et al. 2007b) has been found around the Milky Way. However, there remains some uncertainty about the true nature of these systems.

Thus, dwarf galaxies provide an overview of galaxy evolution in miniature that will also be relevant to understanding the early years of their larger cousins and important physical processes that govern star formation and its impact on the surrounding interstellar medium. There remain issues over the inter-relations between different types of dwarf galaxies, and what (if any) is the connection with globular clusters. When these relations are better understood, we will be a significant step closer to understanding the formation and evolution of all galaxies.

2. DETAILED STAR-FORMATION HISTORIES

The field of resolved stellar population studies was initiated by W. Baade in the 1940s when he first resolved dwarf satellites of M31 into individual stars and, from their color distribution, he realized that they were a different "population" from what is typically seen in our Galaxy (Baade 1944a,b). These were simplified using the terms Population I for young stars and Population II for old stars. Thus, the importance of determining accurate SFHs of dwarf galaxies was recognized long ago and, over the years, many different approaches have been followed. The earliest quantitative results came from the determination by Searle, Sargent & Bagnuolo (1973) of how the color of the integrated light of different galaxy types reflected their SFH. This work was extended and improved upon in an extensive series of papers by Gallagher, Hunter and collaborators starting in the early 1980s (e.g., Gallagher, Hunter & Tutukov 1984; Hunter & Gallagher 1986, and references therein). They used various different indicators (e.g., colors and spectrophotometry, Hα luminosity, and emission line ratios) to estimate the star-formation rates (SFRs) at different epochs for large samples of late-type irregular galaxies, including dwarfs.

The transformation in this field occurred around 15 years ago, when the power and resolution of a new generation of telescopes (particularly the *Hubble Space Telescope*, HST) and detectors (large format CCDs) allowed accurate photometry and, thus, detailed color-magnitude diagrams (CMDs) of individual stars in crowded fields of external galaxies to be made. The CMD of a stellar system retains information about the past SFH, as it preserves the imprint of fundamental evolutionary parameters such as age, metallicity, and initial mass function (IMF) in such a way that it is possible to disentangle them.

2.1. Techniques: Synthetic Color-Magnitude Diagram Analysis

At the beginning of the past century, stars were found to group themselves in temperature-luminosity ranges (observed as color and magnitude) in the Hertzsprung-Russell Diagram; and it was later understood that the positions of stars in a CMD represent the evolutionary sequences of stellar populations. Since the 1950s, large numbers of detailed CMDs have been derived for star clusters and nearby dwarf galaxies (e.g., Hodge 1971, and references therein). However, it was not until the advent of modern CCDs and analysis techniques of the early 1980s that the field really took off for complex galactic systems, like dwarf galaxies.

Until about twenty years ago, all stellar age dating used isochrone fitting, which is appropriate for simple stellar populations such as star clusters, but a serious oversimplification for the interpretation of the composite stellar populations of galaxies. In galaxies numerous generations of stars, with different metallicities and ages, contribute to the appearance of the observed CMD. Thus, a new approach was needed to make the most of the new and accurate CMDs, a method to determine a quantitative SFH: the synthetic CMD method.

The synthetic CMD method determines the variation of the SFR within the look-back time reached by the available photometry, namely the SFH. It is based on comparing observed with theoretical CMDs created via Monte-Carlo-based extractions from stellar evolution tracks, or isochrones, for a variety of star-formation laws, IMFs, binary fractions, age-metallicity relations, etc. Photometric errors, incompleteness, and stellar crowding factors also have to be estimated and included in the procedure to fully reproduce an observed CMD (e.g., Tosi et al. 1991, Aparicio et al. 1996, Tolstoy 1996, Dolphin 1997). A combination of assumed parameters is acceptable only if the resulting synthetic CMD satisfactorily reproduces all the main features of the observational one. This means morphology, luminosity, color distribution, and number of stars in specific evolutionary phases. Different researchers use different approaches to assess the quality of the fit, typically using a form of likelihood analysis comparing the model and the data within the uncertainties of the measurement errors. The method is intrinsically statistical in nature and cannot provide a unique solution for the SFH for a number of reasons, but it usefully limits the range of possible scenarios (e.g., Tolstoy & Saha 1996; Hernandez, Gilmore & Valls-Gabaud 2000; Dolphin 2002; Aparicio & Gallart 2004). The theoretical uncertainties in the stellar evolution models also influence the numerical results and have to be treated carefully (see Gallart, Zoccali & Aparicio 2005, for a review).

2.1.1. An example. **Figure 2** shows examples of how CMDs reflect different SFHs in a hypothetical galaxy. Here, we have assumed a distance modulus of $(m\text{-}M)_0 = 19$, reddening $E(B\text{-}V) = 0.08$, and photometric errors and incompleteness typical of HST photometry with the Wide Field Planetary Camera 2 (WFPC2). Thus, these CMDs could apply to a typical SMC field observed with the WFPC2. In all panels, the number of stars and the IMF are the same, and what changes from panel to panel is the metallicity and the SFH. In the top panels, all stellar evolution phases are visible: the blue plume typical of late-type galaxies, populated by massive and intermediate-mass stars on the main sequence, and in the most metal-poor case also by brighter blue-loop stars; the red clumps and blue loops of stars in the core helium-burning phase; the asymptotic giant branch (AGB) and RGB; the subgiant branch; the oldest MSTOs and the main sequence of the lower mass stars. In the lower panels of **Figure 2**, we see a much simpler old SFH. **Figure 2*d*** shows the effect of a burst on top of this old population, and **Figure 2*f*** shows a different metallicity. **Figure 2** (the top panels in particular) emphasizes the challenge in interpreting real CMDs: Observed data points do not have convenient labels indicating their age and metallicity, and unraveling different subpopulations overlying each other is challenging.

One important issue in the derivation of the SFH from a CMD is the metallicity variation of the stellar population. If no spectroscopic abundance information is available (which is, unfortunately, frequently the case), the metallicity is assumed to be that of the stellar evolution models with colors and CMD morphology in best agreement with the empirical CMD. This is often a particularly uncertain assumption, because some of the key evolutionary sequences in the CMD can be heavily affected by age-metallicity degeneracy. For instance, metal-rich RGB stars from a relatively young (a few gigayears old) population can occupy the same region in a CMD as a more metal-poor, but older, population. Without a spectroscopic estimate of the metallicity, it is impossible to break this degeneracy, unless the MSTOs are also observed. This

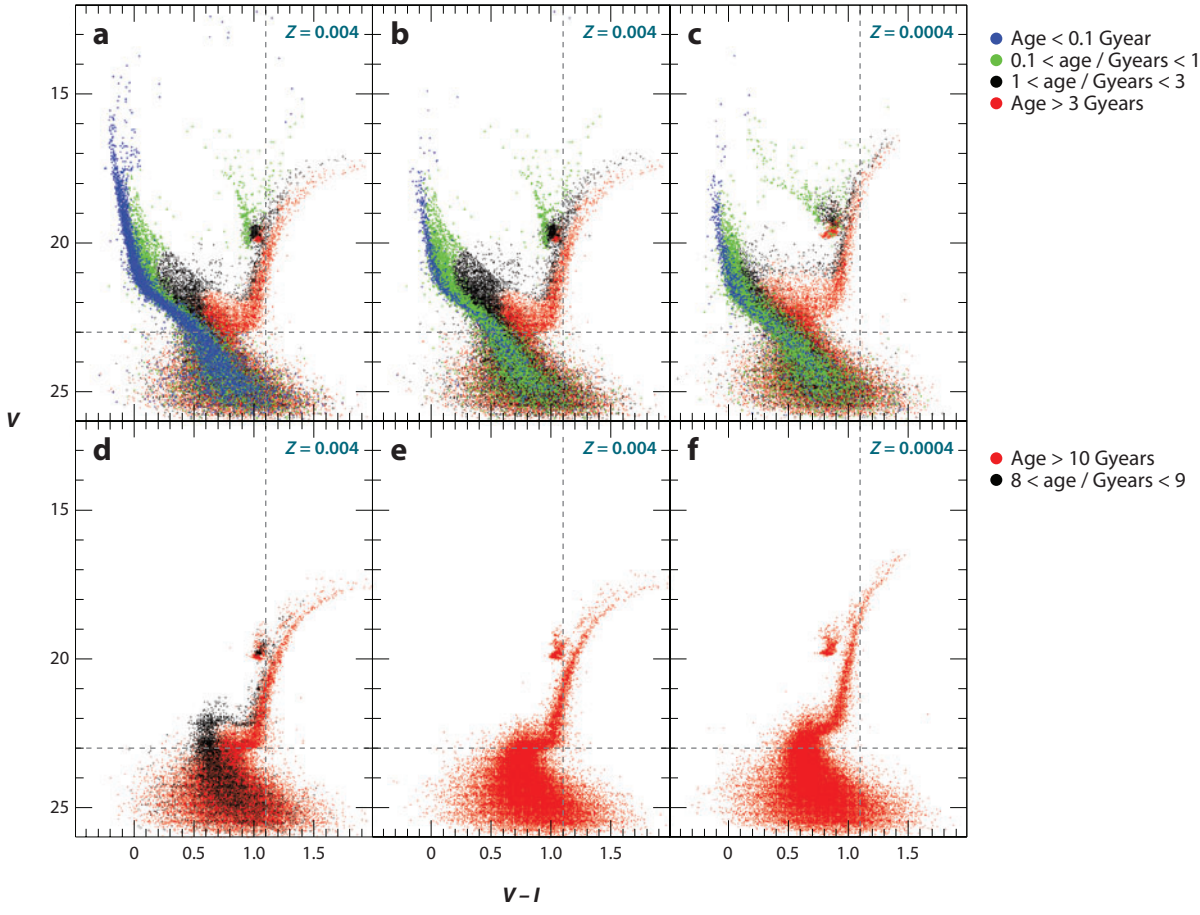

Figure 2

The effect on the color-magnitude diagram (CMD) of different star-formation histories (SFHs) for a hypothetical galaxy. All CMDs contain 50,000 stars, assume Salpeter's initial mass function, and are based on the Padova stellar evolution models (Fagotto et al. 1994a,b). A constant metallicity is assumed, and the value is indicated in the top-right corner of each panel. In all panels, the colors correspond to different stellar ages. The color codes for the top and bottom CMDs are shown in each row. The dotted lines are drawn to help visualize the differences between the various cases. (*b*) The star-formation rate (SFR) is constant from 13 Gyears ago to the present. (*a*) The effect of concentrating recent SFRs into the past 20 Myears. (*c*) The same SFH as in *b*, but with a ten-times lower metallicity. (*e*) An old burst of star formation with a constant SFR from 13 to 10 Gyears ago. (*d*) Two old bursts, one with a constant SFR from 13 to 10 Gyears ago and the other from 9 to 8 Gyears ago, where only 10% of the stars were born in the younger burst. (*f*) The same old SFH as in *e*, but with a ten-times lower metallicity.

is often not the case and one has to deal with the inevitable uncertainty. A further aspect of the effect of metallicity is related to the rather coarse grids of different initial chemical compositions that stellar evolution models are actually computed for. Despite the commendable efforts by stellar evolution modelers, complete sets of homogeneous models covering the entire stellar mass range are limited to a few key metallicities (e.g., Z = 0.02, 0.008, 0.004, 0.0004, 0.00004). Thus, synthetic CMDs assuming a smoothly varying age-metallicity relation have to be created by interpolating between the available metallicities, and this adds to the uncertainty in the derived SFH.

2.1.2. Testing the reliability. In 2001, the different procedures to statistically determine SFHs from about 10 groups, using a variety of different assumptions and stellar evolution models, were compared in the *Coimbra Experiment* (see Skillman & Gallart 2002, and references therein). This experiment showed that, despite all the different assumptions, modeling procedures, and even stellar evolution models, most synthesis methods provided consistent results within their uncertainties. This was again shown in the HST/WFPC2 study of the dI IC 1613 (Skillman et al. 2003), where a synthetic CMD analysis was carried out independently by three different people (representing three independent modeling approaches), and again the results were reassuringly similar (see **Figure 3**). These WFPC2 data, however, did not reach the oldest MSTOs in IC 1613,

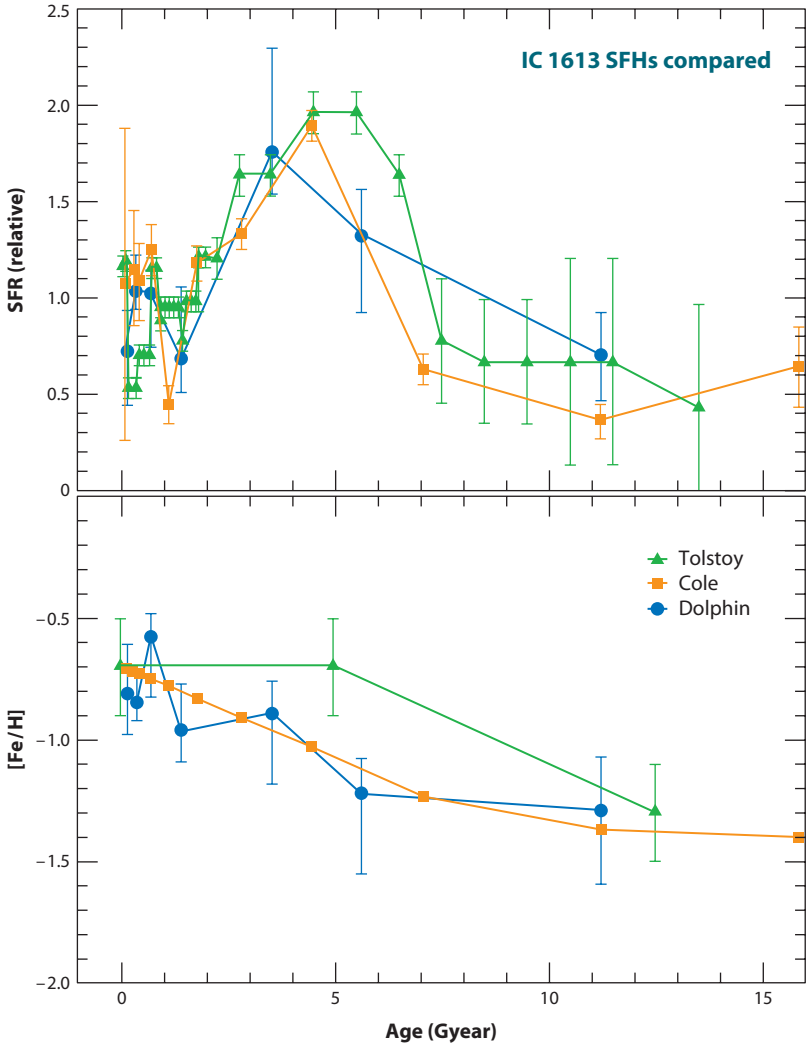

Figure 3

Comparison of star-formation histories for the dwarf-irregular IC 1613 derived via three different methods (by A. Cole, A. Dolphin & E. Tolstoy), as described by Skillman et al. (2003). Note the enhanced levels of star-formation rates between 3 and 6 Gyears ago, which appear in all three models. Also shown are the age-metallicity relations, which were derived in each case. Reprinted from Skillman et al. (2003).

and therefore the SFH at the earliest epochs remained uncertain with these data. More recent deep observations with the HST/ACS, as part of the LCID project (Gallart & the LCID team 2007), do reach the faint oldest MSTOs in IC 1613, but in a different field. Interestingly, its CMD is different from that of Skillman et al. (2003), as it lacks the dominant younger component and it is reproduced by an almost constant SFR with time. This new LCID ACS field is situated at a galacto-centric radius similar to that of the WFPC2 CMD, but, by their nature, irregular galaxies are often asymmetric, and these differences are not surprising. This reminds us of the dangers of looking at a small fraction of these complex systems.

With a sufficient investment in telescope time we can resolve individual stars down to the oldest MSTOs in all the galaxies of the Local Group, and use the resulting CMDs to infer their SFHs over the entire *Hubble* time. This kind of analysis has been obtained for only a handful of galaxies to date. If the oldest MSTOs are not reached, then the look-back time depends on which features of the CMD can be resolved: Horizontal branch (HB) stars are >10 Gyears old but hard to interpret in terms of a SFH, except to say that there are ancient stars. RGB stars are at least 1–2 Gyears old, but without further information it is impossible to be quantitative about the SFH because of the age-metallicity degeneracy. Of course, younger populations are much brighter, and obtaining the SFH over the past gigayear, especially in actively star-forming galaxies, is possible well beyond the Local Group.

2.2. Observations: Dwarf Galaxies in the Local Group

In spite of all the uncertainties, and perhaps because most of them are well treated in a Monte-Carlo approach, the first applications of the synthetic CMD method immediately showed the powerful capability to provide detailed new perspectives (e.g., Ferraro et al. 1989, Tosi et al. 1991, Greggio et al. 1993, Marconi et al. 1995, Gallart et al. 1996, Tolstoy 1996). These early studies found that the SFH not only differs significantly from one galaxy to another, but also according to where one looks within the same galaxy. It was shown that star formation in late-type dwarfs usually occurs in long episodes of moderate intensity separated by short quiescent phases (gasping regime; Marconi et al. 1995), rather than in short episodes of strong intensity separated by long intervals (bursting regime).

When WFPC2 became available after the first HST refurbishment at the end of 1993, it created a tremendous amount of interest and enthusiasm in the field of SFH research (e.g., see reviews, Tolstoy 2003, Dolphin et al. 2005, and references therein), because WFPC2 provided such accurate, well-defined and deep CMDs. In 2002, the Advanced Camera for Surveys (ACS) on HST yet again improved the possibilities, reaching a photometric depth and resolution that is likely to remain unequalled for quite a long time (e.g., see review, Tosi 2007a, and references therein).

To date, a significant fraction of Local Group galaxies have been studied using the synthetic CMD method to infer their SFHs with varying degrees of depth and accuracy (see **Tables 1** and **2**). Many of the galaxies in these tables, and several not included, for which HST/WFPC2 data exist, have been compiled by Holtzman, Afonso & Dolphin (2006), and their SFHs were homogeneously derived by Dolphin et al. (2005). Homogeneous data sets and analyses are valuable to obtain a uniform overview of dwarf galaxy properties in the Local Group.

Tables 1 and **2** are presented in a uniform way to allow an easy comparison between the synthetic CMD analyses for different galaxies over a range of distances. In these tables, we do note if there is supporting evidence for an ancient population (that is, RR Lyr variable stars) that is not clearly seen in the CMD (e.g., the HB and/or the oldest MSTOs are not visible). Leo A is a good example of this, where the presence of RR Lyr variable stars shows that there is an ancient stellar

population that is not unambiguously apparent in the CMD (see **Figure 5*e***). This is also true for NGC 6822, and for some of the early-type galaxies.

In **Tables 1** and **2**, we have included the most recent distance measurements, with references, in column 2. We have then updated the absolute magnitude, M_V, typically from Mateo (1998), in column 3. We include the physical size (the Holmberg radius, r_h) of each galaxy in arcminutes, in column 4. This is to highlight the fraction of the area of the galaxy covered by the instrument used to image the galaxy, which is given in column 5. In columns 6–9, we have given an overview of the depth and detail of the CMD analysis allowed by the different data sets. Sometimes there is more than one data set per galaxy: Column 6 lists the faintest feature detectable in the CMD; column 7 indicates if populations of $\leq$10 Myears were detected or not; column 8 indicates if populations in the range of 2–8 Gyears were detected; and column 9 indicates if populations older than 10 Gyears were detected. In the case where a column contains a "?", this means that the CMD was not deep enough to determine if stars in this age range exist. A column that contains an "x" means that stars of this age were explicitly not detected. In the last three columns, we give an overview of the spectroscopic measurements that exist for individual stars (columns 10 and 11) and HII regions in column 12. Column 10 indicates, with a reference, if individual stars in the galaxy have been observed at low resolution (R < 10,000), typically to determine metallicities, from a single indicator, or kinematics. Column 11 indicates, with a reference, if individual stars in the galaxy have been observed at high resolution (R > 18,000) to determine abundances of different elements. In late-type galaxies, typically these analyses are carried out on young massive stars (e.g., supergiants), and for the closer by early-type galaxies, which do not contain young stars, this typically means RGB stars. In column 12, we indicate if HII-region spectroscopy has been carried out (obviously this is only possible in galaxies with recent star formation). It should be noted that we have not included all synthetic analyses. In some cases, there are multiple studies of one system, and then only the most recent is usually quoted. Sometimes, however, the older study is not superseded (usually because it covers a more significant fraction of the system), and in this case more than one study is listed. In the particular case of studies of several large dSphs (**Table 2**), we have included more than one study based on the same HST data where the results were not the same (e.g., Carina dSph).

The 3D physical spatial distribution of the different types of dwarf galaxies in the Local Group has been displayed in increasing detail over the past years (e.g., Grebel 1999, and most recently by Mateo 2008), including the newly discovered uFds as well as globular clusters and also the most recent version of the morphology-density relation. This shows that galaxies that are currently forming stars are preferentially to be found more than ~300 kpc away from the Milky Way and, thus, the difference between the distribution of dSph and dI around the Milky Way gives a clear indication of the possibility of morphological transformation.

2.2.1. Early-type dwarf galaxies. Early-type galaxies, such as dSphs, are typically associated with large galaxies like our own. They are among the systems closest to us, with the majority at distances <130 kpc, although there are also several more distant examples. Arguably the new uFds are an extension of the dSph class down to much lower luminosities. The dSph systems typically look very much like the old extended stellar populations, which underlie most late-type systems. This suggests that the major difference is that they lack gas and recent star formation, a hypothesis supported by their overlapping structural properties (see **Figure 1**). They have typically not formed stars for at least several hundred million years (e.g., Fnx), and in several cases for much longer (e.g., the Scl dSph apparently formed the majority of its stars more than 10 Gyears ago).

The proximity of dSphs makes it easier to carry out studies of their resolved stellar populations, although this requires wide-field instrumentation to efficiently gain an overview as they

Table 1 Dwarf galaxies with synthetic color-magnitude diagram (CMD) star-formation history analyses: late- and transition-type galaxies in the Local Group

Galaxy	D (kpc)	M_V[a]	r_h (′)[b]	Instrument (fov)	Look-back[c]	≤10 Myr	1–8 Gyr	≥10 Gyr	Spectroscopy		
									LR[d]	HR[d]	HII
(1)	(2)	(3)	(4)	(5)	(6)	(7)	(8)	(9)[e]	(10)	(11)	(12)
WLM	978 ± 20 [1]	−14.6	5.5	WFPC2 (160″) [2]	HB	√	√	√	[3]	[4]	[5]
Sextans B	1370 ± 180 [6]	−14.2	3.9	ESO/2.2m (2′) [7]	RGB	√	√	?	...	...	[8]
NGC 3109	1300 ± 200 [9]	−15.8	13.3	ESO/2.2m (2′) [10]	RGB	√	√	?	...	[11]	[12]
NGC 6822	460 ± 5 [13]	−15.1	40	INT/WFC (23′ × 11′) [14]	RGB	√	√	?	[15]	[16]	[17]
				WFPC2 (160″) [18]	HB	√	√	RRL[19]			
Leo A	800 ± 40 [20]	−11.7	3.9	ACS (195″) [21]	oMSTO	√	√	RRL[20]	[22]	...	[23]
Sextans A	1320 ± 40 [24]	−14.5	4.0	WFPC2 (160″) [25]	HB	√	√	?	...	[26]	[8, 27]
IC 1613	721 ± 5 [28]	−14.6	11 ± 3	WFPC2 (160″) [29]	MSTO	√	√	√	...	[30]	[31]
				ACS (195″) [32]	oMSTO	√	√	√			
SagDIG	1050 ± 50 [33]	−12.2	1.7	ACS (195″) [33]	HB	√	√	√	...	...	[34]
Pegasus	919 ± 30 [35]	−12.8	3.9	WFPC2 (160″) [36]	RGB	√	√	?	...	...	[37]
DDO 210[6]	1071 ± 39 [35]	−10.6	1.6	Subaru (30′)/VLT (7′) [38]	HB	x	√	√	...	...	x
LGS 3[f]	620 ± 20 [39]	−9.9	14.5 ± 4.5	WFPC2 (160″) [39]	HB	x	√	√	[40]	...	x
				ACS (195″) [41]	oMSTO	x	√	√			
Phoenix[f]	406 ± 13 [42]	−10.1	>8.6	WFPC2 (160″) [43]	HB	x	√	√	[44]	...	x
Leo T[f]	400 ± 40 [45]	−8.0 [45]	1.4 [45]	LBT (23′) [46]	HB	x	√	?	[47]	...	...

SMC	59.7 ± 2.2 [48]	−16.1	320	WFPC2 (160″) [49]	oMSTO	√	√	√	[50]	[51]	[52]
				LCO1m drift scan [53]	MSTO	√	√	√			
				WFI (30′) [54]	oMSTO	√	√	√			
				ACS (195″) [55]	oMSTO	√	√	√			
GR 8	2200 ± 400 [56, 57]	−12.3 [58]	1.0 [58]	WFPC2 (160″) [57]	RGB	√	√	?	...	...	[59]

[a]From Mateo 1998, updated using new distances, except where otherwise indicated.
[b]Holmberg limit, from Mateo 1998, except where otherwise indicated.
[c]Faintest main feature visible in the CMD: red giant branch (RGB), horizontal branch (HB), main sequence turn-offs > 2 Gyears old (MSTOs), and oldest main sequence turn-offs (oMSTOs).
[d]Individual RGB stars.
[e]If the CMD is ambiguous as to the presence of an HB, but the presence of ancient stars has been confirmed by the measurement of RR Lyr variable stars, this is noted. A question mark signifies that there is not enough information to determine whether or not an ancient population is present.
[f]Transition types, gas but no star formation

[1] Gieren et al. (2008); [2] Dolphin (2000); [3] Leaman et al. (2009); [4] Urbaneja et al. (2008), Venn et al. (2003); [5] Lee, Skillman & Venn (2005); [6] Sakai, Madore & Freedman (1997); [7] Tosi et al. (1991); [8] Magrini et al. (2005); [9] Soszyński et al. (2006); [10] Greggio et al. (1993); [11] Evans et al. (2006); [12] Peña, Stasińska & Richer (2007); [13] Gieren et al. (2006); [14] Gallart et al. (1996); [15] Tolstoy et al. (2001); [16] Venn et al. (2001); [17] Lee, Skillman & Venn (2006); [18] Wyder (2001, 2003); [19] Clementini et al. (2003); [20] Dolphin et al. (2002); [21] Cole et al. (2007); [22] Brown et al. (2007); [23] van Zee, Skillman & Haynes (2006); [24] Dolphin et al. (2003a); [25] Dolphin et al. (2003b); [26] Kaufer et al. (2004); [27] Kniazev et al. (2005); [28] Pietrzyński et al. (2006); [29] Skillman et al. (2003); [30] Bresolin et al. (2007); Tautvaišienė et al. (2007); [31] Peimbert, Bohigas & Torres-Peimbert (1988); [32] E. Skillman & the LCID team, in preparation; [33] Momany et al. (2005); [34] Skillman, Terlevich & Melnick (1989); [35] McConnachie et al. (2005); [36] Gallagher et al. (1998); [37] Skillman, Bomans & Kobulnicky (1997); [38] McConnachie et al. (2006); [39] Miller et al. (2001); [40] Cook et al. (1999); [41] S. Hildago & the LCID team 2009, in preparation; [42] Held, Saviane & Momany (1999); [43] Holtzman, Smith & Grillmair (2000), Young et al. (2007); [44] Gallart et al. (2001), Irwin & Tolstoy (2002); [45] Irwin et al. (2007); [46] de Jong et al. (2008a); [47] Simon & Geha (2007); [48] Hilditch, Howarth & Harries (2005); [49] Dolphin et al. (2001); [50] Carrera et al. (2008); Harris & Zaritsky (2006); [51] Hill, Barbuy & Spite (1997); Venn (1999); Evans et al. (2005); [52] Vermeij & van der Hulst (2002); [53] Harris & Zaritsky (2004); [54] Noël et al. (2007); [55] Cignoni et al. (2009); [56] Tolstoy et al. (1995); [57] Dohm-Palmer et al. (1998); [58] Mateo 1998; [59] van Zee, Skillman & Haynes (2006).

Table 2 Dwarf galaxies with synthetic color-magnitude diagram (CMD) star-formation history analyses: early-type galaxies in the Local Group

Galaxy	D (kpc)	M_V[a]	r_b (′)[b]	Instrument (fov)	Look-back[c]	≤10 Myr	1–8 Gyr	≥10 Gyr	Spectroscopy		
									LR[d]	HR[d]	HII
(1)	(2)	(3)	(4)	(5)	(6)	(7)	(8)	(9)[e]	(10)	(11)	(12)
Carina	101 ± 5 [1]	−9.3	28.8 ± 3.6	CTIO4m (15′) [2]	oMSTO	x	√	√	[3]	[4, 5]	x
				WFPC2 (160″) [6, 7][f]	oMSTO	x	√	RRL [8]			
Leo I	254 ± 17 [9]	−11.9	12.6 ± 1.5	WFPC2 (160″) [6, 7, 10][f]	oMSTO	x	√	RRL [11]	[12]	[4]	x
Leo II	233 ± 15 [13]	−9.8	8.7 ± 0.9	WFPC2 (160″) [6, 7][f]	oMSTO	x	√	√	[14]	[15]	x
				WFCAM (14′) [16]	HB	x	√	√			
Ursa Min	70 ± 9 [17]	−9.0	50.6 ± 3.6	WFPC2 (160″) [6, 7][f]	oMSTO	x	√	√	[18]	[19]	x
				INT/WFC (23′ × 11′) [20]	oMSTO	x	√	√			
				KPNO0.9m (23′) [21]	oMSTO	x	√	√			
Draco	76 ± 6 [22]	−8.6	28.3 ± 2.4	INT/WFC (23′ × 11′) [23]	oMSTO	x	√	√	[18]	[19, 24]	x
				WFPC2 (160″) [7]	oMSTO	x	√	√			
Sculptor	85.9 ± 5 [25]	−11.2	76.5 ± 5	WFPC2 (160″) [7]	oMSTO	x	√	√	[26]	[4, 27]	x
Fornax	138 ± 5 [28]	−13.2	71 ± 4	ESO/WFI (34′) [29]	oMSTO	x	√	√	[30]	[4, 31]	x
				FORS (7′) [32]	oMSTO	x	√	√			
Cetus	775 ± 50 [33]	−10.1 [33]	4.8 [33]	ACS (195″) [34]	oMSTO	x	√	√	[35]	...	x
Tucana	880 ± 40 [36]	−9.6	3.7 ± 1.2	ACS (195″) [37]	oMSTO	x	√	√	[38]	...	x
NGC 185	616 ± 26 [39]	−15.5	16 ± 2	NOT (3.8′) [40]	TRGB	x	√	RRL [41]	...	...	x
NGC 205	824 ± 27 [39]	−16.6	6.2 ± 0.2	NOT (3.8′) [40]	TRGB	x	√	RRL [42]	[43]	...	x
BooI	62 ± 3 [44, 45]	−5.8 [45]	12.8 ± 0.7 [45]	SDSS (>8000°) [46]	HB	x	√	√	[47, 48]	[50]	x

CVnI	220 ± 20 [45]	−7.9 [45]	8.5 ± 0.5 [45]	SDSS (>8000°) [46]	HB	x	√	√	[48, 49]	...	x
UMaII	32 ± 5 [45]	−3.8 [45]	∼12 [45]	SDSS (> 8000°) [46]	HB	x	√	√	[48]	[51]	x

[a]From Mateo 1998, updated using new distances, except where otherwise indicated.
[b]Holmberg limit, from Mateo 1998, except where otherwise indicated.
[c]Faintest main feature visible in the CMD: tip of the red giant branch (TRGB), horizontal branch (HB), and oldest main sequence turn-offs (oMSTOs).
[d]Individual RGB stars.
[e]If the CMD is ambiguous as to the presence of an HB, but the presence of ancient stars has been confirmed by the measurement of RR Lyr variable stars, this is noted.
[f]Same data set, different analyses.

[1] Mateo, Hurley-Keller & Nemec (1998); [2] Hurley-Keller, Mateo & Nemec (1998); [3] Koch et al. (2006); [4] Shetrone et al. (2003); [5] Koch et al. (2008a); [6] Hernandez, Gilmore & Valls-Gabaud (2000); [7] Dolphin (2002); [8] Saha, Monet & Seitzer (1986); [9] Bellazzini et al. (2004); [10] Gallart et al. (1999); [11] Held et al. (2001); [12] Bosler, Smecker-Hane & Stetson (2007); Koch et al. (2007b); Mateo, Olszewski & Walker (2008); [13] Bellazzini, Gennari & Ferraro (2005); [14] Koch et al. (2007a); [15] Shetrone et al. (2009); [16] Gullieuszik et al. (2008); [17] Nemec, Wehlau & Mendes de Oliveira (1988); [18] Wilkinson et al. (2004); Muñoz et al. (2005); [19] Shetrone, Côté & Sargent (2001); Sadakane et al. (2004); [20] Carrera et al. (2002); [21] Ikuta & Arimoto (2002); [22] Bonanos et al. (2004); [23] Aparicio, Carrera & Martínez-Delgado (2001); [24] Smith et al. (2006); Fulbright, Rich & Castro (2004); [25] Pietrzyński et al. (2008); [26] Tolstoy et al. (2004); Coleman, Da Costa & Bland-Hawthorn (2005); Westfall et al. (2006); Battaglia et al. (2008a); [27] V. Hill & DART 2009, in preparation; [28] Rizzi et al. (2007); [29] Coleman & de Jong (2008); [30] Battaglia et al. (2006); Walker et al. (2006a); [31] Letarte (2007); B. Letarte & DART, in preparation; [32] Gallart et al. (2005) [33] Whiting, Hau & Irwin (1999); [34] M. Monelli & the LCID team (2009), in preparation; [35] Lewis et al. (2007); [36] Castellani, Marconi & Buonanno (1996); Saviane, Held & Piotto (1996); [37] C. Gallart & the LCID team (2009), in preparation; [38] Fraternali et al. (2009); [39] McConnachie et al. (2005); [40] Martínez-Delgado, Aparicio & Gallart (1999); [41] Saha & Hoessel (1990); [42] Saha, Hoessel & Krist (1992); [43] Geha et al. (2006); [44] Siegel (2006); [45] Martin et al. (2008); [46] de Jong et al. (2008b); [47] Muñoz et al. (2006a); [48] Simon & Geha (2007); [49] Ibata et al. (2006); [50] Norris et al. (2008); [51] Frebel et al. (2009).

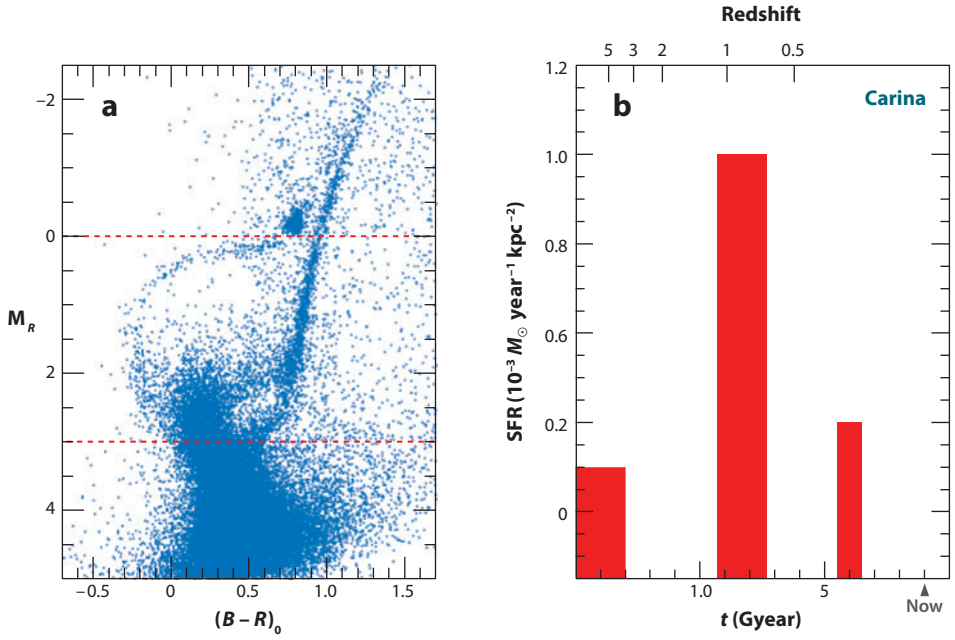

Figure 4

(*a*) A color-magnitude diagram of the Carina dwarf spheroidal (obtained by M. Mateo with the CTIO 4-m and MOSAIC camera, private communication) in the central 30′ of the galaxy. This clearly shows the presence of at least three distinct MSTOs. (*b*) The star-formation history of the central region of Carina determined by Hurley-Keller, Mateo & Nemec (1998), showing the relative strength of the different bursts. The ages are also shown in terms of redshift.

are typically >1° across on the sky. The most famous example is Carina, which has been much studied over the years. It was one of the first galaxies shown, from deep wide-field imaging on the CTIO 4-m telescope, to have completely distinct episodes of star formation (Smecker-Hane et al. 1996; Hurley-Keller, Mateo & Nemec 1998) identified by three distinct MSTOs in the CMD (see **Figure 4*a***). These distinct MSTOs translate into a SFH (see **Figure 4*b***) that consists of three separate episodes of star formation, with the SFR apparently going to zero in between. The existence of a complex SFH was already inferred from the properties of its variable stars (Saha, Hoessel & Krist 1992) and the red clump and HB morphology (Smecker-Hane et al. 1994), but it took synthesis analysis of a CMD going down to the oldest MSTOs to quantify it (Hurley-Keller, Mateo & Nemec 1998).

There have been a number of consistent studies of the Galactic dSphs using HST (Hernandez, Gilmore & Valls-Gabaud 2000; Dolphin 2002). These analyses are typically hampered by the small field of view of HST, compared to the size of the galaxies. Especially as we now know that even these small systems have population gradients, the small field-of-view HST studies are very dependent on where the telescope is pointing.

There are also more distant dSph galaxies, such as Cetus and Tucana, which display all the characteristics found in the closer-by dSphs, but they are at distances well beyond the halo of the Milky Way and M31. Tucana is at a distance of 880 kpc and Cetus is at 775 kpc (see **Table 1**). Both these galaxies have been looked at in great depth by the LCID HST/ACS program (Gallart & the LCID team 2007). Preliminary results for Cetus can be seen in **Figure 5*a,b*** (M. Monelli & the LCID team, in preparation). It looks very similar to a predominantly old dSph,

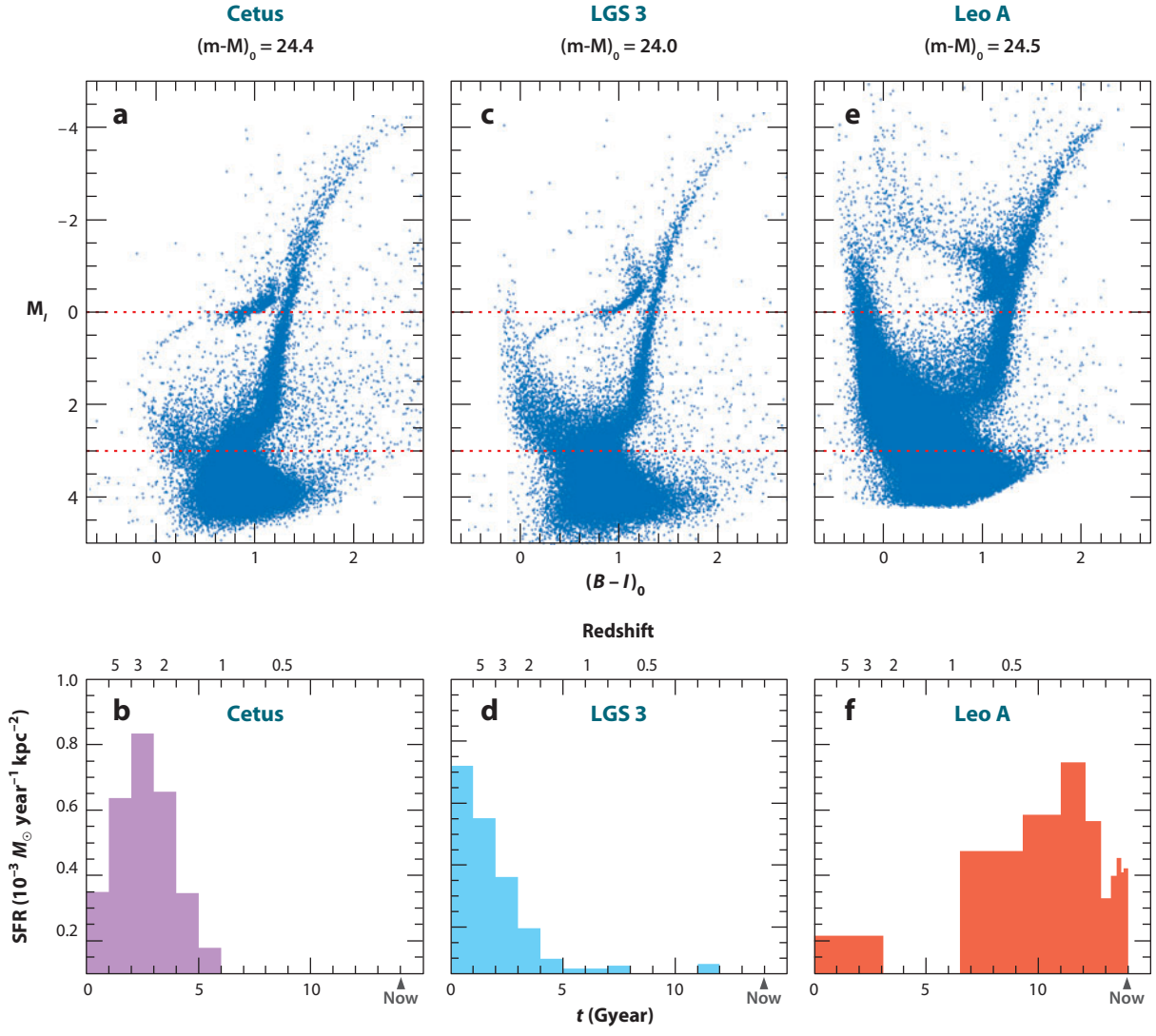

Figure 5

Hubble Space Telescope/Advanced Camera for Surveys (HST/ACS) color-magnitude diagrams (CMDs) and star-formation histories (SFHs) for three Local Group dwarf galaxies: (a,b) Cetus, a distant dwarf spheroidal galaxy (M. Monelli & the LCID team in preparation); (c,d) LGS 3, a transition-type dwarf galaxy (S. Hildago & the LCID team, in preparation); and (e,f) Leo A, a dwarf irregular (Cole et al. 2007). These results come from the LCID project (Gallart & the LCID team 2007, Cole et al. 2007), which is a large program designed to exploit the exquisite image quality of the HST/ACS to obtain uniquely detailed CMDs going back to the oldest main sequence turn offs for a sample of dwarf galaxies. The SFHs come from synthetic CMD analysis and the ages are also shown in terms of redshift.

like Scl, which has not formed any stars over the past 8 Gyears. The blue plume in the CMD (in **Figure 5*a***) is most likely due to blue stragglers. These are old stars that are known to exist in Galactic dSphs (e.g., Mapelli et al. 2007, Momany et al. 2007), and which have undergone mass transfer and appear rejuvenated, but should not be confused with more recent star-formation activity.

Wirth & Gallagher (1984) first made the distinction between diffuse and compact dEs, namely between NGC-205-like and M32-like galaxies, which was immediately confirmed by Kormendy (1985) for a larger sample. The issue has been comprehensively reviewed by Kormendy et al. (2008), who show that the physical properties of M32 are those of a low-luminosity elliptical galaxy (see **Figure 1**). This means that M32, and galaxies like it, are not compact because of any kind of tidal pruning, but because of their intrinsic evolutionary history and/or formation scenario.

Compact objects like M32 are rare (there is only one in the Local Group), whereas more diffuse dwarfs, like dSphs and NGC 205 are much more common. Thus, the three compact systems around M31—NGC 205, NGC 185, and NGC 147—are all big spheroidals, not small ellipticals, as is clear from their position in **Figure 1**. These systems have typically not had much attention from CMD synthesis modeling (see **Table 2**). This is probably due to the fact that they are quite distant, and compact, which makes accurate photometry very challenging even with the help of HST.

There is, in addition, the class of UCDs, which appear to be found only in nearby galaxy clusters, such as Fornax (e.g., Evstigneeva et al. 2008). They may be objects like ω Cen, which is now often considered to be the tidally stripped nucleus of a compact system. The structural properties of ω Cen and UCDs clearly overlap (see **Figure 1**). They have also been proposed to be low-luminosity ellipticals like M32, but **Figure 1** would tend to argue against this.

2.2.2. Late-type dwarf galaxies. These galaxies have long been well studied in the Local Group, and they have proved themselves valuable tools for understanding the wider Universe. This started from the monitoring of Cepheid variable stars in NGC 6822 by E. Hubble in 1925, and the subsequent realization that a larger Universe existed beyond our Milky Way. They have also long been used as probes of metal-poor star formation, both young and old. They still retain HI gas and are, thus— with a few curious exceptions—typically forming stars at the present time as they have probably done over their entire history, with a variety of rates, from extremely low (e.g., Pegasus) to zero (e.g., transition systems DDO 210, LGS 3), to relatively high (e.g., NGC 6822, SMC). The dIs were the first systems to which synthetic CMD analysis was applied (e.g., WLM, Sextans B). They are a numerous and often fairly luminous class within the Local Group. They are typically at distances >400 kpc (the SMC being a notable exception; see **Table 1**). Studies down to the oldest MSTOs of dIs typically require HST-like sensitivity and image stability.

HST has had a large impact on studies of these systems. The exceptionally detailed CMDs from WFPC2 allowed, for the first time, the clear distinction between the main sequence and the blue loop sequence in young metal-poor systems (e.g., Sextans A, Dohm-Palmer et al. 1997). Photometric errors previously blended these sequences in "the blue plume" and there were debates about the reliability of the theoretical predictions of blue-loop stars. These stars have been subsequently shown to be powerful tools for mapping the spatial variations in the SFR over the past 800 Myears (Dohm-Palmer et al. 1998, 2002). The resulting space/time variations are intriguingly reminiscent of the predictions of the stochastic self-propagating star formation proposed by Seiden, Schulman & Gerola (1979), with star formation coming and going in different regions over periods of several hundred million years.

The HST/ACS CMD of Leo A (from Cole et al. 2007; see **Figure 5*e***) is one of the deepest and most accurate ever made for a dI. The SFR as a function of time over the entire history of the galaxy was determined using synthetic CMD analysis (see **Figure 5*f***), and it was found that 90% of the star formation in Leo A happened during the past 8 Gyears. There is a peak in the SFR 1.5–3 Gyears ago, when stars were forming at a level 5–10 times the current rate. The CMD analysis of Leo A only required a very slight metallicity evolution with time (Cole et al. 2007). The mean inferred metallicity in the past is consistent with measurements of the present-day gas-phase

oxygen abundance (van Zee, Skillman & Haynes 2006). There appears to have been only a small and uncertain amount of star formation in Leo A at the earliest times, as the HB is very weak in the CMD in **Figure 5*e***. The error bars on the SFH in **Figure 5*f*** (see Cole et al. 2007) show that from CMD analysis alone, this ancient population is not well defined. The only definite proof of truly ancient stars in Leo A comes from the detection of RR Lyrae variable stars (Dolphin et al. 2002).

Figure 5*c* shows a preliminary HST/ACS CMD and **Figure 5*d*** the SFH derived for LGS 3 (S. Hildago & the LCID team, in preparation), which is a transition-type galaxy. This means that it contains HI gas, but no very young stars (no HII regions, and no supergiants). From the CMD, it looks like it has been forming stars at a low rate for a very long time with a gradually declining rate, and the present-day hiatus is just a normal event in its very low-average SFR.

2.2.3. Ultrafaint dwarf galaxies. An ever increasing number of uFds are being found by SDSS around the Milky Way. As displayed in **Figure 1**, they appear somewhat offset in the $M_V - r_{1/2}$ plane from other dwarf galaxies, although this may be caused by observational difficulties in accurately determining their physical extent. In the M_V-μ_V plane, they appear to be the extension of the dSph sequence to lower luminosity rather than a new class of objects. However, it is clear from both plots in **Figure 1** that especially the fainter of these new systems exist in a region where both the extension of classical dwarf galaxies and the globular cluster sequences may lie. In several cases, the properties of the uFds appear to resemble more diffuse (perhaps tidally disrupted) metal-poor globular clusters rather than dwarf galaxies. From a careful study of the structural properties of uFds (Martin, de Jong & Rix 2008), it can be seen that these new systems range in absolute magnitude from $M_V = -1.5$ (Segue I) to $M_V = -8.0$ (Leo T). Leo T and CVn I ($M_V = -7.9$) are the two brightest of these new systems, although they remain fainter and with lower surface brightness than any of the classical dwarfs, they are consistent with a lower luminosity extension of the dI- and dSph-type galaxies. There are ~8 systems in the range of $-7 < M_V < -4$ (Boo I, UMa I, UMa II, Leo IV, Leo V, CVn II, Coma, and Her), and most of the rest are at $M_V > -3$ (e.g., Wil I, Segue I, Segue II, and Boo II & III). The more luminous and populous CVn I contains a mix of Oosterhoff type I & II RR Lyr variable stars (Kuehn et al. 2008), as is typical for dSphs, whereas the fainter systems do not. So far, most of these new uFds have been found in the immediate vicinity of the Milky Way. The bright systems Leo T, at 410 kpc, and CVn I, at 218 kpc, are the most distant, and the typical distances of the fainter systems range between 23 kpc (Seg I) and 160 kpc (Leo IV, CVn II). These faint and diffuse systems are challenging to study, and it is virtually impossible to detect them beyond these distances.

Some of these new systems have had their stellar populations analyzed using the synthetic CMD method (e.g., de Jong et al. 2008b). However, the SFHs, and even the basic physical properties of the faintest of these systems, can be particularly sensitive to the effect that large and uncertain Galactic contamination brings to small-number statistics (e.g., Martin, de Jong & Rix 2008). In several cases, it is impossible to distinguish the stars that are in uFds from those in the Milky Way without spectroscopic follow-up, and even then they are often found to contain only a few RGB stars or to have kinematics almost indistinguishable from either the Sagittarius (Sgr) tidal streams or the Galaxy (e.g., Geha et al. 2009, Belokurov et al. 2009). This makes separating these systems out from the surrounding stars and determining their properties quite challenging.

Another approach is to look for distinctive stellar populations, such as blue HB (BHB) stars or RR Lyr variable stars, which clearly stand out from the Galactic stellar population. These are usually still small-number tracer populations, but at least they are clear markers of the spatial extent and age of these small and faint systems (e.g., for Boo I, Dall'Ora et al. 2006). In the case of Leo V, it can be seen from the BHB stars that the galaxy has a much more extended stellar component than the half-light radius would suggest (Belokurov et al. 2008; see **Figure 6**). These

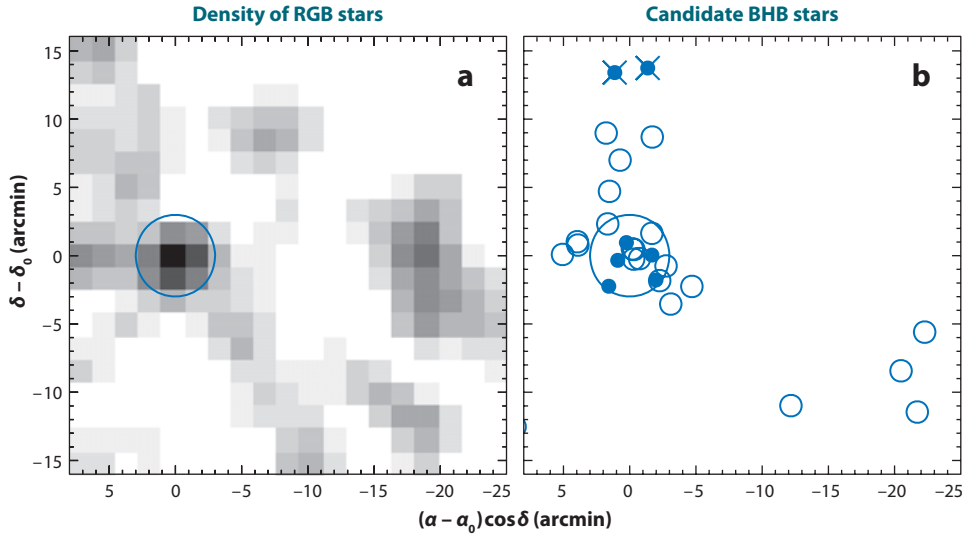

Figure 6

(*a*) The density of red giant branch (RGB) candidate members selected from photometry. The extent of Leo V as judged from two half-light radii is marked. (*b*) The locations of blue horizontal branch (BHB) candidate members. Note that the BHB distribution is elongated and more extended than that of the RGB stars. Filled dots are RGB stars with spectroscopy, $v_\odot \approx 173$ kms^{-1} and low-equivalent width of the MgT feature. Reprinted from Belokurov et al. (2008).

smallest systems are clearly being disrupted, and understanding what they were before this process began is challenging.

It is possible that some of these systems are no more than overdensity enhancements along a stream, and possibly along streams related to Sgr. For example, Segue I has the same space and velocity distribution of a supposed ancient leading arm of Sgr, wrapped 520° around the Milky Way (e.g., Geha et al. 2008). Similarly, Boo II and Coma are believed to lie within streams originating from Sgr. In the case of Leo IV and Leo V, they lie on top of (although clearly behind) the Orphan stream and, thus, kinematic information is needed to hope to disentangle their stars from the complex fore/background stellar populations lying in that direction. The newly discovered Segue II system (Belokurov et al. 2009) is also found to lie along the edge of a Sgr stream and to perhaps be embedded in a stream of its own. In this case, it is postulated to be evidence for groups of galaxies falling onto the Milky Way simultaneously.

2.2.4. The Small Magellanic Cloud. The closest galaxies (excepting some of the new uFds) are the Magellanic Clouds, and their SFHs can be studied in quite some detail. The SMC is an irregular galaxy at the boundary of the dwarf class. As can be seen from **Figure 1**, this does not have a clear physical distinction, as the cut-off is arbitrary. Hence, the SMC can be considered the closest late-type dwarf. It shares key properties with this type of galaxy: high gas content, low current metallicity ($Z \simeq 0.004$ in mass fraction), and low mass (between 1 and $5 \times 10^9\ M_\odot$, Kallivayalil, van der Marel & Alcock 2006) near the upper limit of the range of masses typical of late-type dwarfs.

The SMC hosts several hundred star clusters and several populous clusters covering all ages from 11 Gyears (NGC 121; e.g., Glatt et al. 2008) to a few Myears (e.g., NGC 346 and NGC 602; Sabbi et al. 2007, Cignoni et al. 2009).

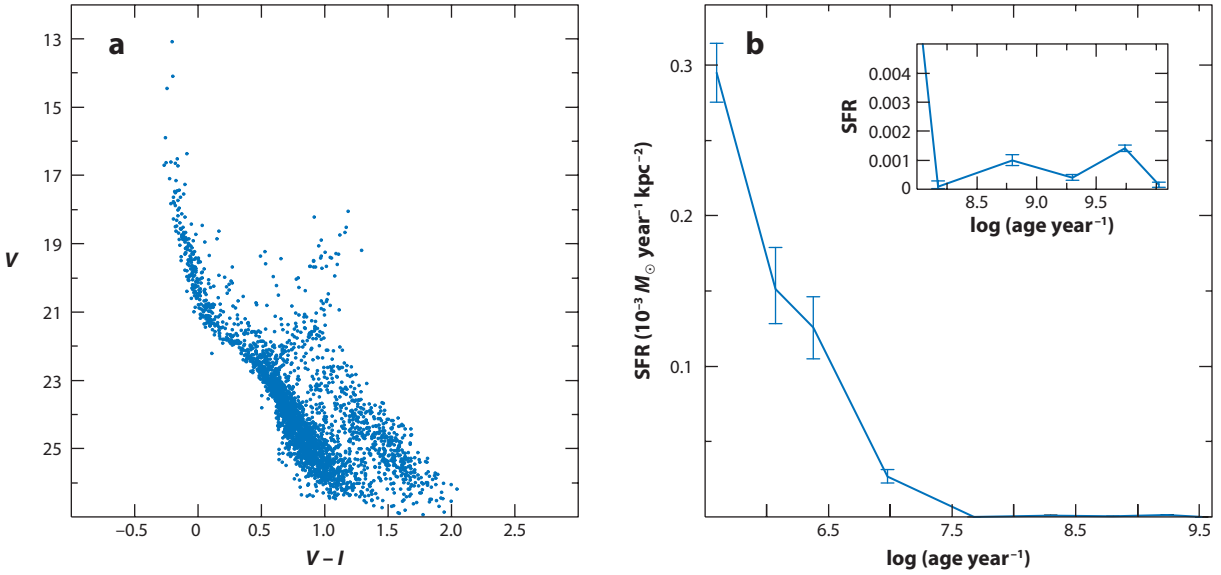

Figure 7

(*a*) Color-magnitude diagram (CMD) of the *Hubble Space Telescope*/Advanced Camera for Surveys field around the young cluster NGC 602 in the SMC. The bright blue plume contains the young cluster stars. The red sequence of pre-main-sequence stars of lower mass that have not yet made it on to the main sequence are also easily recognizable. Also visible are the old main sequence and evolved stars of the SMC field population. Notice that the lower main sequence is only populated by field stars, because the cluster stars with mass below ~1 $M_{\odot}$ have not yet had time to reach it. (*b*) Corresponding star-formation history (SFH) as derived with the synthetic CMD method (Cignoni et al. 2009). The oldest part of the SFH is shown as an inset in the upper right.

Accurate photometry down to the oldest MSTOs is feasible from the ground, although time consuming, and HST allows measurements of both the oldest and the youngest objects, including pre-main-sequence stars, although with fields of view covering only a tiny fraction of the galaxy. Although stars at the oldest MSTOs and subgiant branch are the unique means to firmly establish the SFH at the earliest epochs, pre-main-sequence stars are precious tools to study the details of the most recent star formation (Cignoni et al. 2009), in terms of time and space behavior. The regions of intense recent star formation in the SMC can provide key information on the star-formation mechanisms in environments with metallicity much lower than in any Galactic star-forming region. As an example, **Figure 7** shows the CMD of the young cluster NGC 602 in the Wing of the SMC, observed with HST/ACS. Both very young stars (either on the upper main sequence or still on the pre-main-sequence) and old stars are found. The SFH of the cluster and the surrounding field is also shown, revealing that the cluster has formed most of its stars around 2.5 Myears ago, whereas the surrounding field has formed stars continuously since the earliest epochs. The SFR in this SMC region appears to be quite similar to that of Galactic star-forming regions (Cignoni et al. 2009, and references therein).

Despite being the nearest dI system, the SMC has been less studied than might be expected. For instance, the SFHs derived from synthetic CMDs have, so far, only been based on a few ground-based studies (Harris & Zaritsky 2004, Chiosi et al. 2006, Noël et al. 2007), and a few HST-based ones on small individual regions (Dolphin et al. 2001; McCumber, Garnett & Dufour 2005; Cignoni et al. 2009). New extensive surveys to infer the SFH of the whole SMC back to the earliest epochs are planned (Cioni et al. 2008, Tosi et al. 2008), both at visible and near-infrared wavelengths.

Harris & Zaritsky (2004) were the first to apply the synthetic CMD method to the derivation of the SMC SFH. They mapped the whole SMC from the ground and concluded that 50% of its stars are older than 8.4 Gyears and diffused over the whole body of the galaxy. They also found an indication of a long period of moderate (possibly zero) activity between 3 and 8.4 Gyears ago. Their photometry, however, did not reach the oldest MSTO, and all the studies (Dolphin et al. 2001; McCumber, Garnett & Dufour 2005; Noël et al. 2007; Cignoni et al. 2009; Tosi et al. 2008) that do reach it indicate that, although present, stars older than 8 Gyears do not dominate the SMC population. From the latter studies, the population bulk seems to peak at ages somewhat younger than 6–9 Gyears essentially everywhere in the SMC main body.

2.3. Beyond the Local Group

The dwarf galaxies that have been studied using the CMD synthesis method beyond the Local Group are predominantly actively star-forming BCDs (e.g., I Zw 18, NGC 1705). These galaxies are typically quite distant, but as there are no obvious BCDs in the Local Group (with the possible exception of IC 10 hidden behind a lot of foreground obscuration from the Milky Way), there is no other possibility to study this class of actively star-forming, yet low-metallicity, systems.

In galaxies beyond the Local Group, distance makes crowding more severe, and even HST cannot resolve stars as faint as the MSTO of old populations. The further the distance, the worse the crowding conditions and the shorter the look-back time reachable even with the deepest, highest resolution photometry. Depending on distance and intrinsic crowding, the reachable look-back time in galaxies more than 1 Mpc away ranges from several gigayears (in the best cases, when the RGB or even the HB are clearly identified) to several hundreds of millions of years (when AGB stars are recognized), to a few tens of millions of years (when only the brightest supergiants are resolved). To date, the unique performances of the HST/ACS have allowed us to resolve individual stars on the RGB in some of the most metal-poor BCDs, e.g., SBS 1415+437 at 13.6 Mpc (Aloisi et al. 2005) and I Zw 18 at 18 Mpc (Aloisi et al. 2007). The discovery of stars several gigayears old in these extremely metal-poor galaxies is key information for understanding these systems and placing them in the proper context of galaxy formation and evolution studies.

Not many groups have embarked on the challenging application of the synthetic CMD method beyond the Local Group (for a summary, see Tosi 2007b), and most of them have concentrated their efforts on starbursting late-type dwarfs. In **Figure 8**, some examples of the SFHs of distant late-type dwarfs are shown. All these SFHs have been derived with the synthetic CMD method applied to HST/WFPC2 or NICMOS photometry. The look-back time reached by the photometry is indicated by the dashed vertical line in each panel, and in all cases stars of that age were detected. For those galaxies that have subsequently been observed with the HST/ACS, the look-back time is significantly longer, and the further back we look we always find indisputable evidence of star-formation activity at that increasingly old epoch. This means that there is no evidence that any of these systems is younger than the look-back time. The sample of galaxies shown in **Figure 8** is not homogeneous: UGC 5889 is a low surface brightness galaxy (LSB), whereas NGC 1705, I Zw 18, I Zw 36, and Mrk 178 are BCDs, and NGC 1569 is classified as a dI. Nonetheless, all these dwarfs show qualitatively similar behavior, with a strong current burst superimposed on a moderate and rather continuous underlying star-formation activity. Quantitatively, the actual SFRs differ between galaxies by orders of magnitude. Notice that the least active system is one of the BCDs (Mrk 178), and the most active is a dI (NGC 1569). This is not what one would have expected on the basis of their morphological classification. This highlights the difficulties in making accurate classifications of the structural properties of these active, compact systems. If NGC 1569 were at a distance of 20 Mpc, it would most likely have been classified as a BCD.

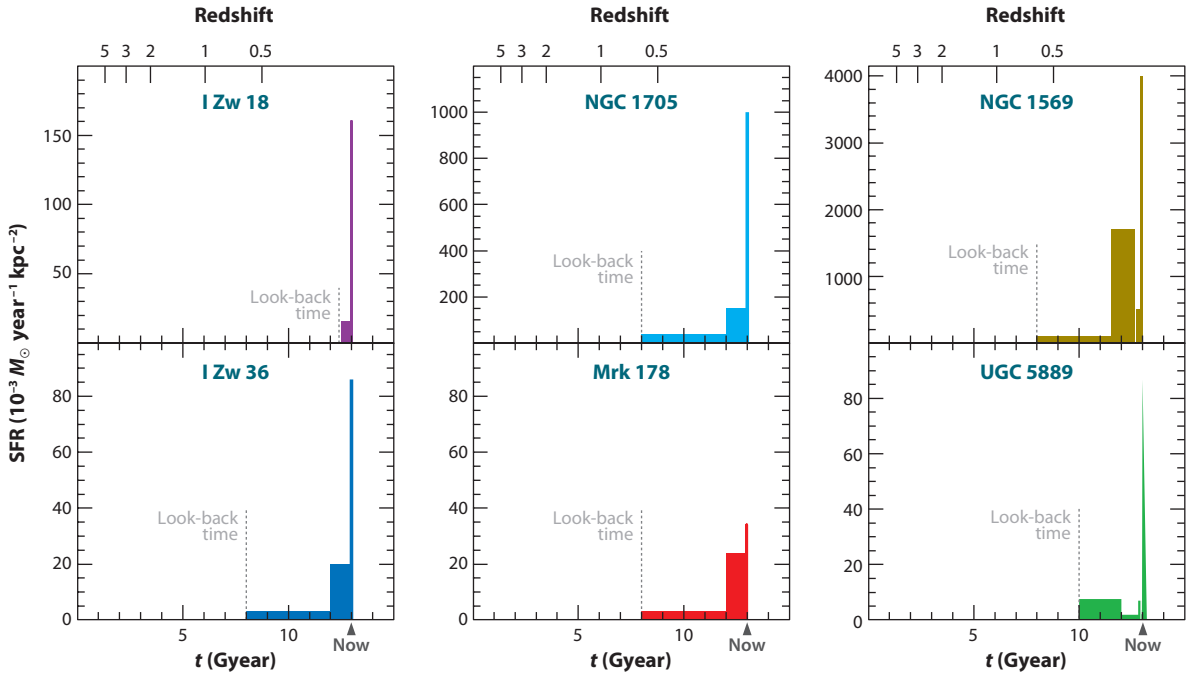

Figure 8

Star-formation histories of late-type dwarfs outside the Local Group. In all panels, the star-formation rate per unit area as a function of time is plotted. The ages are also shown in terms of redshift. The thin gray dashed vertical line in each panel indicates the look-back time reached by the adopted photometry of that galaxy. References: NGC 1569, Greggio et al. (1998), Angeretti et al. (2005); NGC 1705, Annibali et al. (2003); I Zw 18, Aloisi, Tosi & Greggio (1999); I Zw 36, Schulte-Ladbeck et al. (2001); Mrk 178, Schulte-Ladbeck et al. (2000); UGC 5889, Vallenari, Schmidtobreick & Bomans (2005).

The SFR in NGC 1569 is actually about a factor of two higher than shown in **Figure 8**, as more recent HST/ACS imaging has detected the RGB, and made a significant revision of the distance to NGC 1569, to make it almost a magnitude farther away than previously thought (Grocholski et al. 2008).

An interesting result of the SFH studies both in the Local Group and beyond is that the vast majority of dwarfs have, and have always had, fairly moderate star-formation activity. From an extensive Hα study of 94 late-type galaxies, Hunter & Elmegreen (2004) found that the typical SFR of irregular galaxies is $10^{-3}\ M_{\odot}\ \mathrm{year}^{-1}\ \mathrm{kpc}^{-2}$ and that of BCDs is generally higher but not by much. They also found that NGC 1569 and NGC 1705 are among the few systems with unusually high SFRs (see **Figure 8**). Hunter & Elmegreen conclude that the star-formation regions are not intrinsically different in the various galaxy types, but they crowd more closely together in the centers of BCDs.

3. STELLAR KINEMATICS AND METALLICITIES

Stellar abundances and kinematics have been shown to be excellent tools for disentangling the properties of complex stellar systems like our own Galaxy (e.g., Eggen, Lynden-Bell & Sandage 1962). This approach is the only means we have to separate the diverse stellar populations in the Solar Neighborhood. These stars can be split up into disk and halo components on the basis of their 3D velocities, and these subsets can then be studied independently. This concept has

subsequently been expanded and renamed Chemical Tagging (Freeman & Bland-Hawthorn 2002). As large samples of stellar velocities and metallicities have become available for other galaxies, this approach remains the only way to obtain a detailed understanding of a multicomponent stellar system.

The kinematics and metallicities of early- (dSph/dE) and late (dI)-type dwarf galaxies in the Local Group have almost always been measured using different tracers. This is owing to the different distances and stellar densities that are typical for the two types of systems. It is also because dIs contain an easily observable interstellar medium in the form of HI gas and dSphs do not. Because early-type galaxies usually do not contain any (observable) gas nor any young star-forming regions, most of what we know of their internal properties comes from studies of their evolved stellar populations (e.g., RGB stars). Late-type galaxies are typically further away (the SMC being a clear exception), which can make the accurate study of individual RGB stars more challenging, and they contain HI gas and several HII regions. Thus, most of what we know about the kinematics and metallicity of dIs comes from gas and massive (young) star abundances. Red giant branch stars have the advantage that they are all old (>1 Gyear), and their properties are most likely to trace the gravitational potential and chemical evolution throughout the entire galaxy up to the epoch when they formed, and not just the most recent star-formation processes and the final metallicity. It is only with detailed studies of the same tracers that kinematics and metallicities in these different dwarf galaxy types can be accurately compared to make confident global statements about the differences and similarities between early- and late-type galaxies.

3.1. Early-Type Dwarfs

Dwarf spheroidal galaxies are the closest early-type galaxies that contain sufficient numbers of well-distributed RGB stars to provide useful kinematic and metallicity probes. Moreover, dSphs are considered to be interesting places to search for dark matter, because there is so little luminous matter to contribute to the gravitational potential. The velocity dispersion of individual stars can be used to determine the mass of the galaxy. It is also possible to determine metallicities for the same stars. This allows a more careful distinction of the global properties based on structural, kinematic, and metallicity information (e.g., Battaglia 2007).

3.1.1. Galactic dwarf spheroidals. It was originally thought that the luminosity profiles of Galactic dSphs resembled globular clusters and showed systems truncated by the gravitational field of the Milky Way (e.g., Hodge 1971). As measurements improved and the discussion focused on the possible presence of dark matter, Faber & Lin (1983) showed that the profiles are exponentially more like those of galaxy disks and, thus, predicted that Galactic dSphs had a much higher mass-to-light ratio (M/L), $\geq$30, than had previously been thought. In parallel, Aaronson (1983) found observational evidence for this in radial velocity studies of individual stars in the Draco dSph. Thus, it became clear that dSph are small galaxies, related to late-type disk and irregular systems, and not globular clusters.

For a given M/L, the central velocity dispersion of a self-gravitating spheroidal system in equilibrium may scale with the characteristic radial scale length and the central surface brightness (Richstone & Tremaine 1986). Given that globular clusters typically have a central velocity dispersion $\sim$2–8 km s^{-1}, it was expected that dwarf galaxies, which have scale lengths at least 10 times bigger and surface brightnesses about 1000 times smaller (see **Figure 1**), should have central velocity dispersions <2 km s^{-1}. This has been consistently shown not to be the case; all galaxies have stellar velocity dispersions that are typically larger than those of globular clusters ($\sim$8–15 km s^{-1}). This was first shown by Aaronson (1983) for a sample of three stars in the Draco dSph. This early

tentative (and brave!) conclusion has been verified and strengthened significantly over the past decades, with modern samples containing measurements for many hundreds of individual stars in Draco (e.g., Muñoz et al. 2005, Wilkinson et al. 2004) and in all other Galactic dSphs. If it can be assumed that this velocity dispersion is not caused by tidal processes, then this is evidence that dSph galaxies contain a significant amount of unseen (dark) matter (e.g., Mateo 1994, Olszewski 1998, Gilmore et al. 2007), or that we do not understand gravity in these regimes (e.g., Modified Newtonian Dynamics applies). There has been some uncertainty due to the possible presence of binary stars, but a number of studies have carried out observations over multiple epochs, and this effect has been found to be minimal (e.g., Battaglia et al. 2008b, and references therein).

As instrumentation and telescopes improved, a significant amount of work on the kinematic properties of dSphs has become possible. This field has benefited particularly from wide-field multifiber spectrographs on 6–8-m-class telescopes (e.g., VLT/FLAMES and Magellan/MIKE), but also WYFOS on the WHT and AAOmega on the AAT. These facilities have allowed samples of hundreds of stars out to the tidal radii (e.g., Wilkinson et al. 2004; Tolstoy et al. 2004; Muñoz et al. 2005; Kleyna et al. 2005; Walker et al. 2006a,b; Battaglia et al. 2006, 2008a; Battaglia 2007). These velocity measurements often have sufficient signal-to-noise to also obtain metallicities from the CaII triplet, the Mgb index, or a combination of weak lines (e.g., Suntzeff et al. 1993; Tolstoy et al. 2004; Battaglia et al. 2006, 2008b; Muñoz et al. 2006b; Koch et al. 2006; Kirby, Guhathakurta & Sneden 2008; Shetrone et al. 2009). This approach resulted in the discovery of surprising complexity in the "simple" stellar populations in dSphs. It was found that RGB stars of a different metallicity range (and, hence, presumably age range) in dSphs can have noticeably different kinematic properties (e.g., Tolstoy et al. 2004, Battaglia et al. 2006). This has implications for understanding the formation and evolution of the different components in these small galaxies. It is also important for correctly determining the overall potential of the system. The presence of multiple components allows more accurate modeling of the overall potential of the system, and so better constraints on the underlying dark matter profile and the mass content (Battaglia 2007, Battaglia et al. 2008a; see **Figure 9**).

The VLT/FLAMES DART survey (Tolstoy et al. 2006) determined kinematics and metallicities for large samples of individual stars in nearby dSphs. There have also been similar surveys by other teams on VLT and Magellan telescopes (e.g., Gilmore et al. 2007; Walker, Mateo & Olszewski 2009). Traditionally, the mass distribution of stellar systems has been obtained from a Jeans analysis of the line-of-sight velocity dispersion (e.g., Mateo 1994), assuming a single stellar component embedded in a dark matter halo. This analysis suffers from a degeneracy between the mass distribution and the orbital motions presumed for the individual stars, the mass-anisotropy degeneracy. In the DART study of the Scl dSph, the mass was determined by taking advantage of the presence of the two separate components distinguished by metallicity, spatial extent, and kinematics (Battaglia 2007, Battaglia et al. 2008a; see **Figure 9**). Here, it was shown that it is possible to partially break the mass-anisotropy degeneracy when there are two components embedded in the same dark matter halo. The new dynamical mass of the Scl dSph is $M_{\rm dyn} = 3 \times 10^8\, M_\odot$, within 1.8 kpc, which results in an M/L $\sim$ 160. This is a factor $\sim$10 higher than the previous value obtained from a much smaller and more centrally concentrated sample of stars (Queloz, Dubath & Pasquini 1995). This corresponds to a dark matter density within 600 pc for the best-fitting model of 0.22 $M_\odot$ pc^{-3}. This result is largely independent of the exact distribution of dark matter in the central region of the Scl dSph (see **Figure 9**). This same study also found evidence for a velocity gradient, of $7.6^{+3.0}_{-2.2}$ km s^{-1} deg^{-1}, in Scl, which has been interpreted as a signature of intrinsic rotation. This is the first time that rotation has been detected in a nearby dSph, and it was a faint signal that required a large data set going out to the tidal radius.

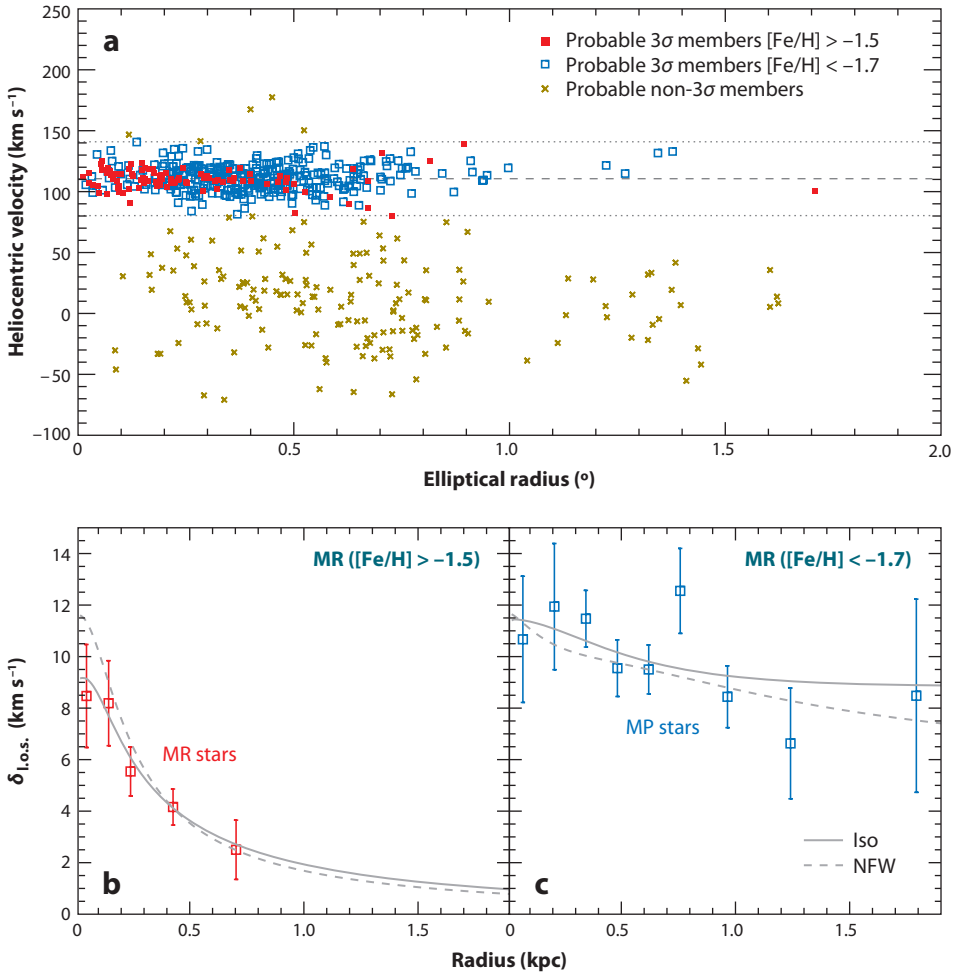

Figure 9

From the DART survey, these are VLT/FLAMES line-of-sight velocity measurements for individual red giant branch stars in the Sculptor dwarf spheroidal galaxy (from Battaglia et al. 2008a). (*a*) Elliptical radii are plotted against velocity for each star. The limits for membership are given by dotted gray lines about $v_{hel} = +110.6$ kms^{-1}, and the heliocentric velocity is shown as a dashed gray line. It is apparent that the velocity dispersion and central concentration of the metal-rich (MR) stars, in red, can clearly distinguish them from the metal-poor (MP) stars, in blue, which have a larger velocity dispersion and are more uniformly distributed over the galaxy. (*b*, *c*) The line-of-sight velocity dispersion profiles, with rotation removed, for the MR (*red*) and MP (*blue*) stars are shown along with the best fitting pseudo-isothermal sphere (*solid gray line*) and Navarro Frenk & White (*dashed gray line*) models.

Another aspect of these surveys has been the determination of metallicity distribution functions (MDFs), typically using the CaII triplet metallicity indicator (Battaglia et al. 2006, Helmi et al. 2006). This uses the empirical relation between the equivalent width of the CaII triplet lines and [Fe/H], and the accuracy of this relation was tested (Battaglia et al. 2008b). It was found that the CaII triplet method may start to fail at low metallicities, [Fe/H] < -2.5, and this is starting to be better understood on physical (e.g., Starkenburg et al. 2008) as well as empirical grounds from following up stars with CaII triplet metallicities, [Fe/H] < -2.5. This means that the effect can

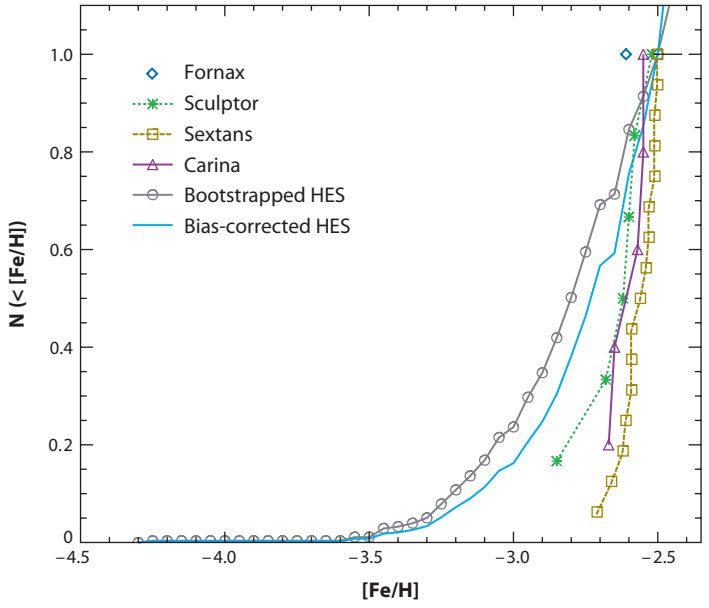

Figure 10

Comparison of the cumulative metallicity distribution functions (MDFs) of the stars in the mean bootstrapped Hamburg-ESO survey sample as a solid gray line, and the new bias-corrected Galactic halo MDF from Schoerck et al. (2008) as a solid light blue line. These are compared to the MDFs for four dwarf spheroidals from the DART survey (Helmi et al. 2006). The halo and the dwarf spheroidal MDFs have been normalized at [Fe/H] = −2.5, which assumes that the completeness of the halo MDF is well understood at this metallicity and below. Note that, at present, the Fornax dwarf spheroidal lacks sufficient stars at [Fe/H] < −2.5 to be properly present on this plot.

be corrected for, and so far there is no significant change to the MDFs presented in Helmi et al. (2006). This is because the fraction of the stellar samples that may be affected by this uncertainty is very small (∼1–2%), and then only a fraction of these actually needs to be corrected. Thus, it seems likely that there are very few extremely metal-poor stars ([Fe/H] < −4) in most classical dSph. However, this result still needs to be verified by careful follow-up of CaII triplet measurements of stars with [Fe/H] < −2.5.

The dSph MDFs found by DART were compared to the Galactic halo MDF from the Hamburg-ESO survey (HES, Beers & Christlieb 2005), and they were found to be significantly different (Helmi et al. 2006; see **Figure 10** for an update). The Galactic halo MDF has recently been revised (Schoerck et al. 2008), and this revision is also shown in **Figure 10**. It can be seen that the difference between the dSphs and the Galactic halo MDFs remains. However, it is obviously of critical importance that the different degrees of incompleteness are well understood, and this is particularly complicated in the halo. What is shown as the Galactic halo MDF in **Figure 10** may still change, but it is most likely that the two halo MDFs shown represent a reasonable range of possibilities. This clear difference between the Galactic halo MDF and those of dSph galaxies provides a challenge to models where all of the Galactic halo builds up from the early merging of dwarf galaxies, because it begs the question: Where have all the most metal-poor stars in the Galactic halo come from? Was there a pre-enrichment of dwarf galaxies, perhaps by the most metal-poor stars, which we appear to find only in the halo (e.g., Salvadori, Ferrara & Schneider 2008)? This mismatch applies equally to any merging scenario that extends over a significant

fraction of a Hubble time, as it means that dSph and dI galaxies could not have merged to form the halo except at very select moments in the past (see Section 4). **Figure 10** does not include uFds, and there is evidence that they may include more metal-poor stars than are to be found in dSphs (e.g., Kirby et al. 2008, Frebel et al. 2009).

3.1.2. More distant dwarf spheroidals. There are also more isolated dSphs, within the Local Group but not obviously associated to the Milky Way or M31, for example, Antlia, Phoenix, Cetus, and Tucana. They have also benefited from spectroscopic studies (e.g., Tolstoy & Irwin 2000, Gallart et al. 2001, Irwin & Tolstoy 2002, Lewis et al. 2007, Fraternali et al. 2009). Antlia, Tucana, and Phoenix have HI gas in their vicinity, but after careful study, only for Phoenix and Antlia has the association been confirmed. These spectroscopic studies have shown evidence for rotation in Cetus and Tucana at a similar magnitude to Scl (Lewis et al. 2007, Fraternali et al. 2009). This rotation is consistent with the flattening of the galaxy. In Phoenix the kinematics and morphology of HI gas compared to the stellar component suggests that the HI is being blown out by a recent star-formation episode (e.g., Young et al. 2007). This supports the theoretical predictions of this effect (e.g., Larson 1974, Mac Low & Ferrara 1999). All these more distant dSphs are far enough away from the Milky Way that any strong tidal influence is likely to have been several gigayears in the past.

3.1.3. Dwarf galaxies around M31. There are also diffuse dEs and dSphs around M31 where spectra have been taken of RGB stars. From a sample of 725 radial velocity measurements in NGC 205, it was found to be rotating at 11 ± 5 km s^{-1} (Geha et al. 2006). A careful study of the structural properties of the dSphs around M31 shows that, on average, the scale radii of the dSphs around M31 are about a factor of two larger than those of dSphs around the Milky Way at all luminosities (McConnachie & Irwin 2006). This could either be due to small-number statistics or it might suggest that the tidal field of M31 is weaker than that of the Milky Way, or the environment in the halo of M31 is different from that of the Milky Way halo.

3.2. Late-Type Dwarfs

Most of what we know about the kinematics of dI galaxies comes from observations of their HI gas (e.g., Lo, Sargent & Young 1993; Young et al. 2003), which is strongly influenced by recent events in the systems. For example, the velocity dispersion measured in the HI gas is predominantly influenced by on-going star-formation processes. Thus, the HI velocity dispersion is almost always $\sim$10 km s^{-1} in any system, from the smallest dIs to the largest spiral galaxies, regardless of the mass or rotation velocity of the HI. This makes it difficult to compare the kinematic properties of dI and dSph galaxies.

Likewise, most of the metallicity information comes from HII region spectroscopy (e.g., Pagel & Edmunds 1981; Hunter & Gallagher 1986; Skillman, Kennicutt & Hodge 1989; Izotov & Thuan 1999; Kunth & Östlin 2000; Hunter & Elmegreen 2004) or spectroscopy of (young) massive stars (e.g., Venn et al. 2001, 2004b; Kaufer et al. 2004). For a few BCDs, the FUSE satellite has also provided abundances for the neutral gas (e.g., Thuan, Lecavelier des Etangs & Izotov 2002; Aloisi et al. 2003; Lebouteiller et al. 2004). Thus, the metallicity measures come from sources that are only a few million years old and the product of the entire SFH in a galaxy. By contrast, in dSphs the abundances are typically measured for stars older than $\sim$1 Gyear, and the value quoted is some form of a mean of the values measured over the entire SFH. This makes it difficult to accurately compare the properties of early- and late-type dwarf galaxies, as there are few common

measurements that can be directly compared. Such comparisons have still been attempted (e.g., Skillman, Kennicutt & Hodge 1989; Grebel, Gallagher & Harbeck 2003) with no consensus on the conclusions.

From studies of the HI gas in these systems, it has been found that, for the smallest and faintest dIs, if rotation is detected at all, it is at or below the velocity dispersion (e.g., Lo, Sargent & Young 1993; Young et al. 2003). Despite this, in all dIs, the HII regions in a single galaxy, even those widely spaced, appear to have, within the margins of error of the observations, identical [O/H] abundances (e.g., Lee, Skillman & Venn 2006). So it appears that either the enrichment process progresses uniformly galaxy wide, or the oxygen abundance within an HII region is affected by some internal, self-pollution process that results in uniform [O/H] values (e.g., Olive et al. 1995). However, the clear gradients in HII-region abundances seen in spiral galaxies argue against this explanation.

One dwarf galaxy that has both HI and stellar kinematic information is the faint transition–type dwarf LGS 3 ($M_V = -9.9$). The stellar component looks like a dSph, dominated by (old) RGB stars (see **Figure 5**). There are no HII regions (Hodge & Miller 1995), and the youngest stars are around 100 Myears old (Miller et al. 2001). However, the galaxy also contains $2 \times 10^5\ M_\odot$ of HI (Lo, Sargent & Young 1993; Young & Lo 1997), which is more extended than the optical galaxy, and has no convincing evidence of rotation. Cook et al. (1999) measured the radial velocities of four RGB stars in LGS 3 at the same systemic velocity as the HI, confirming the association. They found the stellar velocity dispersion of these four stars to be $7.9^{+5.3}_{-2.9}$ km s^{-1}. This leads to a high M/L (>11, perhaps as high as 95), similar to other dSphs. However, this sample of radial velocities is hardly sufficient to reach a firm conclusion.

LGS 3 used to be the lowest luminosity galaxy with HI, but that was before the recent discovery of Leo T (Irwin et al. 2007) from SDSS data. Leo T contains $2.8 \times 10^5\ M_\odot$ of HI gas (Ryan-Weber et al. 2008), and it does not contain HII regions or young stars. The total dynamical mass was determined to be $8.2 \pm 3.6 \times 10^6\ M_\odot$, with M/L ~140. Leo T seems to be a particularly faint dwarf ($M_V = -8$), at a distance of ~420 kpc (see **Table 1**). It is about 2 mag fainter than the other transition-type systems like LGS 3 and Phoenix, and 0.6 mag fainter than the faintest dSph system, Draco.

Leo T is another of the very few systems for which kinematics have been derived from HI and velocities of individual stars. Simon & Geha (2007) measured the radial velocities and metallicities of 19 RGB stars and found the average metallicity to be [Fe/H] ~ −2.3 with a range of ±0.35. They found a central optical velocity of $+38 \pm 2$ km s^{-1}, a velocity dispersion $\sigma = 7.5 \pm 1.6$ km s^{-1}, and no obvious sign of rotation. This is comparable to the HI value, $\sigma_{HI} = 6.9$ km s^{-1}, also with no sign of rotation (Ryan-Weber et al. 2008). This is the smallest and lowest luminosity galaxy with fairly recent star formation known. The inferred past SFR of $1.5 - 2 \times 10^{-5}\ M_\odot$ year^{-1} might be sufficiently low that gas is neither heated nor blown out in this system, thus allowing it to survive (de Jong et al. 2008a).

3.3. Ultrafaint Dwarfs

The stellar kinematics and metallicities of individual stars play an important role in determining what kind of systems uFds are. These measurements can attempt to quantify the degree of disruption uFds may have undergone and if they should be considered faint galaxies or some kind of diffuse globular clusters, such as those seen around M31 (e.g., Mackey et al. 2006). These systems are so embedded in the foreground of our Galaxy, both in position and in velocity, and the total number of their stars is often so small (many have $M_V \gtrsim -4$) that different studies can easily get very different results for even the most fundamental properties, such as their size and their dark

matter content, which depend sensitively upon membership selection criteria (e.g., Ibata et al. 2006; Simon & Geha 2007; Siegel, Shetrone & Irwin 2008; Geha et al. 2009).

From the basic kinematic properties of these systems Simon & Geha (2007) have shown tentative evidence that they are more dark matter–dominated than previously known systems, with M/L ∼140–1700. However, this study did not try to correct for tidal effects, which are almost certainly present. Many of these galaxies also have very small numbers of stars and, thus, test particles, and so the properties of the dark matter content are often extrapolated from a small central region.

Simon & Geha (2007) also determined the average stellar metallicities of uFds and found them to be lower than in most globular clusters ([Fe/H] ≤ -2), and with a scatter that is larger than would be expected in globular clusters. The average metallicities are also lower than in other more luminous dwarf galaxies (see also Kirby et al. 2008), and the lowest metallicity stars appear to be more metal poor than the most metal-poor stars found in the brighter classical dSphs (e.g., Norris et al. 2008, Frebel et al. 2009). Norris et al. (2008) also found evidence for a carbon-rich metal-poor star in Boo I, which suggests that the metal-poor stars in uFds may indeed be more similar to those found in the Milky Way halo, where a large fraction of stars (more metal poor than [Fe/H] <-4) are carbon rich.

CVn I, at a distance of 220 kpc and at $M_V \sim -7.9$ (Zucker et al. 2006b), is one of the brighter examples of uFds and bears much similarity to classical dSphs in structural properties, kinematics, and SFH. From a CMD analysis, Martin et al. (2008) found that the galaxy is dominated by an ancient population (>10 Gyears old), with about 5% of its stars in a young blue plume ∼1.4–2 Gyears old. It has well-populated, broad RGB and HB, which have been studied spectroscopically (Ibata et al. 2006, Simon & Geha 2007). With a sample of 44 stars Ibata et al. (2006) detected the presence of two components with different metallicities and velocities. However, Simon & Geha (2007), with a much larger sample of 212 stars, were not able to reproduce this result.

A recently discovered uFd is Leo V (Belokurov et al. 2008), at a distance of 180 kpc with $M_V = -4.3$. **Figure 6** illustrates how hard it can be to quantify the structural properties and distinctness of these small diffuse systems, several of which may be embedded in Galactic scale streams. Leo V may be related to Leo IV, to which it is very close both spatially and in velocity. They may both be remnants of the same tidal interaction, but given how metal poor their stars appear to be, they would have to be the outer envelopes of dwarf galaxies (several of which are known to have metallicity gradients), like Sgr, and not disrupted globular clusters.

Thus the nature of some of the uFds still remains a mystery, and there is likely to be a range of origins for these systems. The brighter uFds ($M_V < -5$) are relatively easy to study and appear to be a low-mass tail to dSphs (e.g., CVn I) and dI/transition systems (e.g., Leo T). This reduces the sizes of objects in which stars can form in the early Universe (e.g., Bovill & Ricotti 2008, Salvadori & Ferrara 2009), and it follows the trend that these smaller systems could barely enrich themselves. This could be either the result of efficient winds or inefficient star formation, both of which could be caused by a low galactic mass.

It remains a matter of conjecture what the fainter systems, such as Coma and UMa II ($M_V \sim -4$), are. From its highly irregular stellar distribution, UMa II is clearly a disrupted system that sits behind high-velocity cloud complex A (Zucker et al. 2006a, Belokurov et al. 2007a). Coma has very similar properties to UMa II, and it also has an irregular extended shape (Belokurov et al. 2007b). UMa II is one of the few objects that lie in the gap between globular clusters and dwarf galaxies in **Figure 1*a***. This is a region that has so far not been populated by either galaxies or globular clusters, but if the large dark matter masses of the uFds are correct, then they are more likely to be an extension of the galaxy class than of the globular cluster class.

4. DETAILED ABUNDANCES OF RESOLVED STARS

The detailed chemical abundance patterns in individual stars of a stellar population provide a fossil record of chemical enrichment over different timescales. As generations of stars form and evolve, stars of various masses contribute different elements to the system, on timescales directly linked to their mass. Of course, the information encoded in these abundance patterns is always integrated over the lifetime of the system at the time the stars being studied were born. Using a range of stars as tracers provides snapshots of the chemical enrichment stage of the gas in the system throughout the SFH of the galaxy. This approach also assumes that the chemical composition at the stellar surface is unaffected by any connection between interior layers of the star, where material is freshly synthesized, and the photosphere. This assumption is generally true for main-sequence stars, but evolved stars (giants or supergiants) will have experienced mixing episodes that modified the surface composition of the elements involved in hydrogen burning through the CNO cycle, that is, carbon, nitrogen and possibly also oxygen.

These studies require precise measurements of elemental abundances in individual stars, and this can only be done with high-resolution and reasonably high signal-to-noise spectra. It is only very recently that this has become possible beyond our Galaxy. It is efficient high-resolution spectrographs on 8–10-m telescopes that have made it possible to obtain high-resolution ($R > 40{,}000$) spectra of RGB stars in nearby dSphs and O, B, and A supergiants in more distant dIs. These stars typically have magnitudes in the range $V = 17$–19. Before the VLT and Keck, the chemical composition of extragalactic stars could only be measured in supergiants in the nearby Magellanic Clouds (e.g., Wolf 1973; Hill, Andrievsky & Spite 1995; Hill, Barbuy & Spite 1997; Venn 1999), yielding present-day (at most a few 10^7 years ago) measurements of chemical composition. Looking exclusively at young objects, however, makes it virtually impossible to uniquely disentangle how this enrichment built up over time.

4.1. Dwarf Spheroidal Galaxies

The first studies of detailed chemical abundances in dSph galaxies are those of Shetrone, Bolte & Stetson (1998); Shetrone, Côté & Sargent (2001, 17 stars in Draco, Ursa Min, and Sextans) using Keck-HIRES, and Bonifacio et al. (2000, 2 stars in Sgr) using VLT-UVES. These early works were shortly followed by similar studies slowly increasing in size (Shetrone et al. 2003, Bonifacio et al. 2004, Sadakane et al. 2004, Geisler et al. 2005, McWilliam & Smecker-Hane 2005). The total number of stars probed in individual studies remained very low (typically only 3 to 6 in any one galaxy except for Sgr). This was because the stars had to be observed one at a time, and for the most distant dSphs, this required exposure times of up to 5 h per star. Nevertheless, from these small samples it was already clear that dSph galaxies follow unique chemical-evolution paths, which are distinct from that of any of the Milky Way components (e.g., Shetrone, Côté & Sargent 2001; Shetrone et al. 2003; Tolstoy et al. 2003; Venn et al. 2004a).

Most recently, high-resolution spectrographs with high multiplex capabilities have resulted in large samples (>80 stars) of high-resolution spectra of individual stars to determine abundances in a relatively short time. The FLAMES multifiber facility on VLT (Pasquini et al. 2002) has so far been the most productive in this domain. There are a number of FLAMES high-resolution spectroscopy studies in preparation, but some results are already published for Sgr and its stream (Monaco et al. 2005; Sbordone et al. 2007; Monaco et al. 2007, 39 stars), Fnx (Letarte 2007, 81 stars), Carina (Koch et al. 2008a, 18 stars) and Scl (V. Hill & DART, in preparation; 89 stars).

These new extensive studies not only provide abundances with better statistics, but they also allow statistical studies over the total metallicity range in each galaxy. This allows for an almost

complete picture of their chemical evolution over time, with abundance trends as a function of metallicity for each system. Only the most metal-poor regime in these systems is perhaps still somewhat under-represented in these samples, although this is in part because they are rare (Helmi et al. 2006), and in part because these large samples of abundances have been chosen in the inner parts of the galaxies, where younger and/or more metal-rich populations tend to dominate (Tolstoy et al. 2004, Battaglia et al. 2006). New studies to fill in this lack of measured abundances in low-metallicity stars are in preparation (e.g., Aoki et al. 2009). In the following, we consider groups of elements that give particular insights into dwarf-galaxy evolution.

4.1.1. Alpha elements. The α-elements abundances that can easily be measured in RGB spectra includes O, Mg, Si, Ca, and Ti. Although the α-elements have often been considered as a homogeneous group, and their abundances are sometimes averaged to produce a single [α/Fe] ratio, their individual nucleosynthetic origin is not always exactly the same. For example, O and Mg are produced during the hydrostatic He burning in massive stars, and their yields are not expected to be affected by the SN II explosion conditions. However, Si, Ca, and Ti are mostly produced during the SN II explosion. This distinction is also seen in the observations (e.g., Fulbright, McWilliam & Rich 2007), where Si, Ca, and Ti usually track one another, but O and Mg often show different trends with [Fe/H]. It is therefore generally advisable to treat the α-elements, which are well probed in dwarf galaxies separately. **Figure 11** shows a compilation of Mg and Ca abundances of individual stars in those dSphs with more than 15 measurements.

The apparent paucity of α-elements (relative to iron) in dSph galaxies compared to the Milky Way disk or halo was first noted by Shetrone, Bolte & Stetson (1998); Shetrone, Côté & Sargent (2001); Shetrone et al. (2003); Tolstoy et al. (2003); and Venn et al. (2004a) from small samples. **Figure 11** shows this convincingly over most of the metallicity range in each system. However, it also appears that each of these dSphs starts, at low [Fe/H], with [α/Fe] ratios similar to those in the Milky Way halo at low metallicities. These ratios in the dSphs then evolve down to lower values than are seen in the Milky Way at the same metallicities.

The ratio of α-elements to iron, [α/Fe], is commonly used to trace the star-formation timescale in a system, because it is sensitive to the ratio of SNe II (massive stars) to SNe Ia (intermediate-mass binary systems with mass transfer) that have occurred in the past. SNe Ia have a longer timescale than SNe II and as soon as they start to contribute they dominate the iron enrichment and [α/Fe] inevitably decreases. After that, no SFH can ever again result in enhanced [α/Fe], unless coupled with galactic winds removing only the SN Ia ejecta and not that of SNe II. This is seen as a "knee" in a plot of [Fe/H] versus [α/Fe] (see **Figure 11**). The knee position indicates the metal-enrichment achieved by a system at the time SNe Ia start to contribute to the chemical evolution (e.g., Matteucci & Brocato 1990, Matteucci 2003). This is between 10^8 and 10^9 years after the first star-formation episode. A galaxy that efficiently produces and retains metals over this time frame will reach a higher metallicity by the time SNe Ia start to contribute than a galaxy that either loses significant metals in a galactic wind, or simply does not have a very high SFR. The position of this knee is expected to be different for different dSphs because of the wide variety of SFHs. There are already strong hints in the data that not all dSphs have a knee at the same position.

At present, the available data only cover the knee with sufficient statistics to quantify the position in the Scl dSph, a system that stopped forming stars 10 Gyears ago, and the knee occurs at [Fe/H] ≈ -1.8. This is the same break-point as the two kinematically distinct populations in this galaxy (Tolstoy et al. 2004, Battaglia 2007; see **Figure 9**). This means that the metal-poor population has formed before any SN Ia enrichment took place, which means on a timescale shorter than 1 Gyear.

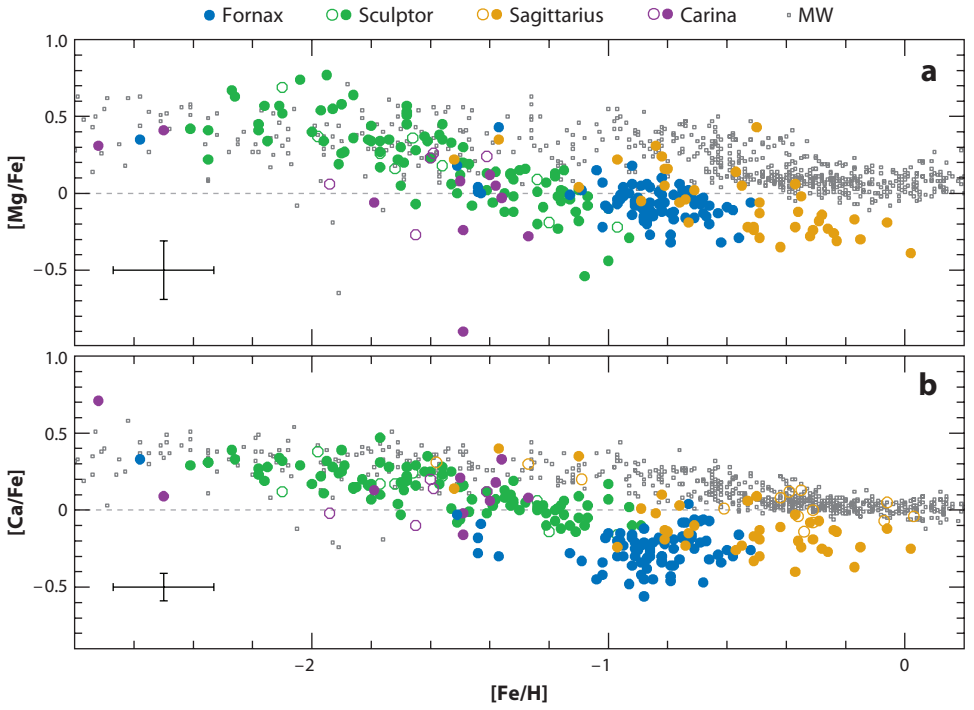

Figure 11

α-elements, (*a*) Mg and (*b*) Ca, in four nearby dwarf spheroidal galaxies: Sgr (*orange*: McWilliam & Smecker-Hane 2005, Monaco et al. 2005, Sbordone et al. 2007), Fnx (*blue*: Shetrone et al. 2003, Letarte 2007), Scl (*green*: V. Hill & DART, in preparation, Shetrone et al. 2003, Geisler et al. 2005), and Carina (*purple*: Shetrone et al. 2003, Koch et al. 2008a). Open symbols refer to single-slit spectroscopy measurements, whereas filled circles refer to multiobject spectroscopy. A representative error-bar for the latter is shown on the left-hand side of the picture. The small gray squares are a compilation of the Milky Way disk and halo star abundances, from Venn et al. (2004a).

In other dSphs, the knee is not well defined owing to a lack of data, but limits can be established. The Sgr dSph has enhanced [α/Fe] up to [Fe/H] ≈ -1.0, which is significantly more metal rich than the position of the knee in the Scl dSph. This is consistent with what we know of the SFH of Sgr, which has steadily formed stars over a period of 8–10 Gyears and only stopped forming stars about 2–3 Gyears ago (e.g., Dolphin 2002). The Carina dSph has had an unusually complex SFH, with at least three separate bursts of star formation (Hurley-Keller, Mateo & Nemec 1998; see **Figure 4**). The abundance measurements in Carina are presently too scarce to have any hope to confidently detect these episodes in the chemical enrichment pattern (e.g., Tolstoy et al. 2003). It appears to possess [α/Fe]-poor stars between [Fe/H] $= -1.7$ and -2.0, which suggests that the knee occurs at lower [Fe/H] than in Scl. It seems that Carina has had the least amount of chemical evolution before the onset of SNe Ia of all galaxies in **Figure 11**. In the Fnx dSph, another galaxy with a complex SFH, the sample does not include a sufficient number of metal-poor stars to determine even an approximate position of the knee. There are abundances for only five stars below [Fe/H] $= -1.2$, and only one below [Fe/H] $= -1.5$. The knee is constrained to be below [Fe/H] < -1.5. From this (small) sample of dSph galaxies, it appears that the position of the knee correlates with the total luminosity of the galaxy, and the mean metallicity of the galaxy. This suggests that the presently most luminous galaxies are those that must have formed

more stars at the earliest times and/or retained metals more efficiently than the less luminous systems.

The abundance ratios observed in all dSphs for stars on the metal-poor side of the knee tend to be indistinguishable from those in the Milky Way halo. From this small sample, it seems that the first billion years of chemical enrichment gave rise to similar enrichment patterns in small dwarf galaxies and in the Milky Way halo. Because the [α/Fe] at early times is sensitive to the IMF of the massive stars, if [α/Fe] in metal-poor stars in dSphs and in the Milky Way halo (or even the bulge) are similar, then there is no need to resort to IMF variations between these systems. Poor IMF sampling has been invoked as a possible cause of lowering [α/Fe] in dwarfs (Tolstoy et al. 2003, Carigi & Hernandez 2008), but these new large samples suggest that this explanation may no longer be necessary, at least in systems as luminous as Sculptor, Fornax, or Sagittarius. However, there is now a hint that the slightly less luminous Sextans ($M_V = -9.5$) could display a scatter in the α/Fe ratios at the lowest metallicities, including [α/Fe] close to solar (Aoki et al. 2009). Such a scatter is so far observed only in this purely old system and suggests a very inhomogeneous metal enrichment in this system that presumably never retained much of the metal it produced. The true extent of this scatter in Sextans remains to be investigated, and extension to other similar systems is needed before general conclusions can be reached on the mechanisms leading to the chemical homogeneity—or not—of dwarf galaxies.

At later times, in those stars that formed ~1 Gyear after the first stars on the metal-rich side of the knee, the decrease of [α/Fe] with increasing metallicity is very well marked. In fact, the end points of the evolution in each of the dSphs investigated has a surprisingly low [α/Fe] (see **Figure 11**). A natural explanation of these low ratios could involve a sudden decrease of star formation, which would make enrichment by massive stars inefficient and leave SNe Ia to drive the chemical evolution. This sudden drop in star formation could be the natural result of galactic winds, which can have a strong impact on dwarf galaxies with relatively shallow potential wells (see Section 5) or perhaps tidal stripping. In this case, one would expect the metal-rich and low [α/Fe] populations to be predominantly young, corresponding to the residual star formation after the sudden decrease. However, the current age determinations for individual giants in these systems are not accurate enough to probe this hypothesis (e.g., Battaglia et al. 2006).

4.1.2. Sodium and nickel. Another example of the low impact of massive stars on the chemical enrichment of dSphs is given by sodium. **Figure 12** shows the compilation of dSph stars compared to the evolution of Na in the Milky Way. According to current stellar models, Na is mostly produced in massive stars (during hydrostatic burning) with a metallicity-dependent yield. The abundance of Na in metal-poor dSph stars is apparently not different from the Milky Way halo stars at the same [Fe/H], but its abundance at later stages in the evolution is distinct from the Milky Way, with the dSph producing (or keeping) too little Na to continue the Milky Way trend above [Fe/H] > -1.

Sodium and nickel underabundances have also been remarked upon by Nissen & Schuster (1997, 2008) in a fraction of halo stars that display low α abundances, thereby producing a [Na/Fe]–[Ni/Fe] correlation. This correlation is tentatively explained as the common sensitivity of both elements to neutron-excesses in supernovae. Fnx is the most striking example that seems to follow the same slope as the Na-Ni relationship in the Milky Way, but extends the trend to much lower [Na/Fe] and [Ni/Fe] values (Letarte 2007; see **Figure 12**). Nickel, unlike sodium, is also largely produced in SNe Ia (Tsujimoto et al. 1995), so the Ni-Na relation can, in theory, be modified by SN Ia nucleosynthesis, especially in the metal-rich populations of dwarfs where the low [α/Fe] ratios point toward a strong SN Ia contribution.

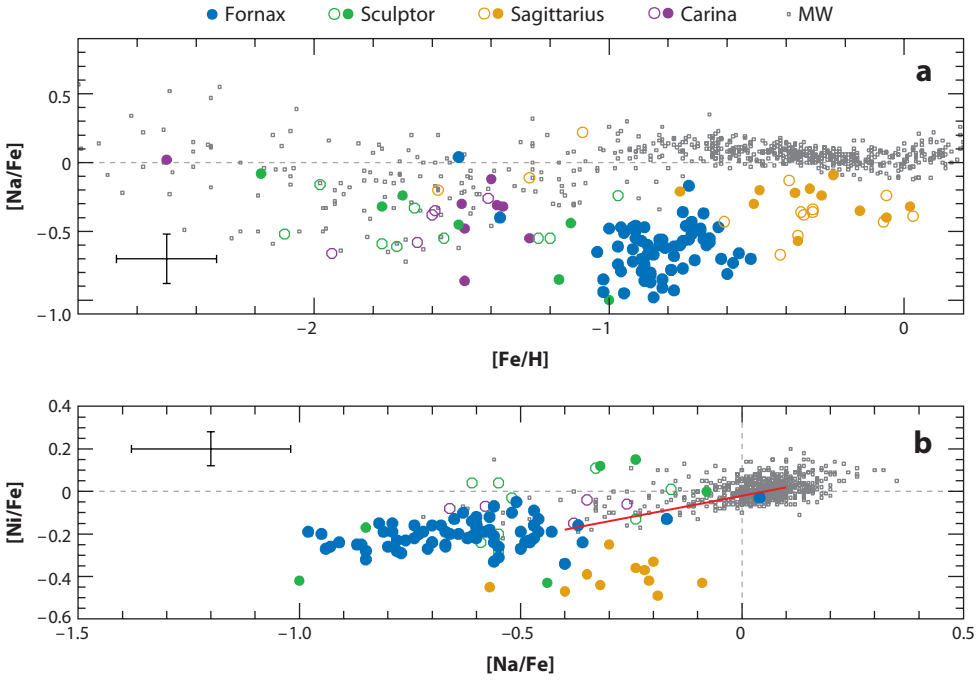

Figure 12

(*a*) Sodium and (*b*) nickel in the same four dwarf spheroidals as in **Figure 11**, compared to the Milky Way. Sgr (*orange*: McWilliam & Smecker-Hane 2005, Monaco et al. 2005, Sbordone et al. 2007), Fnx (*blue*: Shetrone et al. 2003; Letarte 2007), Scl (*green*: V. Hill & DART in preparation; Shetrone et al. 2003, Geisler et al. 2005), and Carina (*purple*: Shetrone et al. 2003; Koch et al. 2008a). Open symbols refer to single-slit spectroscopy measurements, whereas filled circles refer to multiobject spectroscopy. A representative error-bar for the latter is shown on the left-hand side of the picture. The small gray squares are a compilation of the Milky Way disk and halo star abundances, from Venn et al. (2004a), and the solid red line shows the Na-Ni correlation given by Nissen et al. (1997).

4.1.3. Neutron-capture elements. Despite their complicated nucleosynthetic origin, heavy neutron capture elements can provide useful insight into the chemical evolution of galaxies. Nuclei heavier than Z $\sim$ 30 are produced by adding neutrons to iron (and other iron-peak) nuclei. Depending on the rate (relative to β decay) at which these captures occur, and therefore on the neutron densities in the medium, the processes are called either slow or rapid (*s*- or *r*-) processes. The *s*-process is well constrained to occur in low- to intermediate-mass (1–4 $M_{\odot}$) thermally pulsating asymptotic giant branch (AGB) stars (see Travaglio et al. 2004, and references therein), and therefore provide a contribution to chemical enrichment that is delayed by $\sim$100–300 Myears from the time when the stars were born. Thus, *s*-process elements can in principle be used to probe star formation on similar timescales to [α/Fe]. The *r*-process production site is clearly associated with massive-star nucleosynthesis. The most plausible candidates are SNe II, although the exact mechanism to provide the very large neutron densities needed is still under debate (e.g., Sneden, Cowan & Gallino 2008, and references therein). This means that *r*-process elements should contribute to the chemical enrichment of a galaxy with very little, if any, delay. Obviously they need pre-existing Fe-peak seeds and are, therefore, not primary elements such as α elements. One complication arises from the fact that most neutron-capture elements (through their multiple isotopes) can be produced by either the *s*- or the *r*- process, such as yttrium (Y),

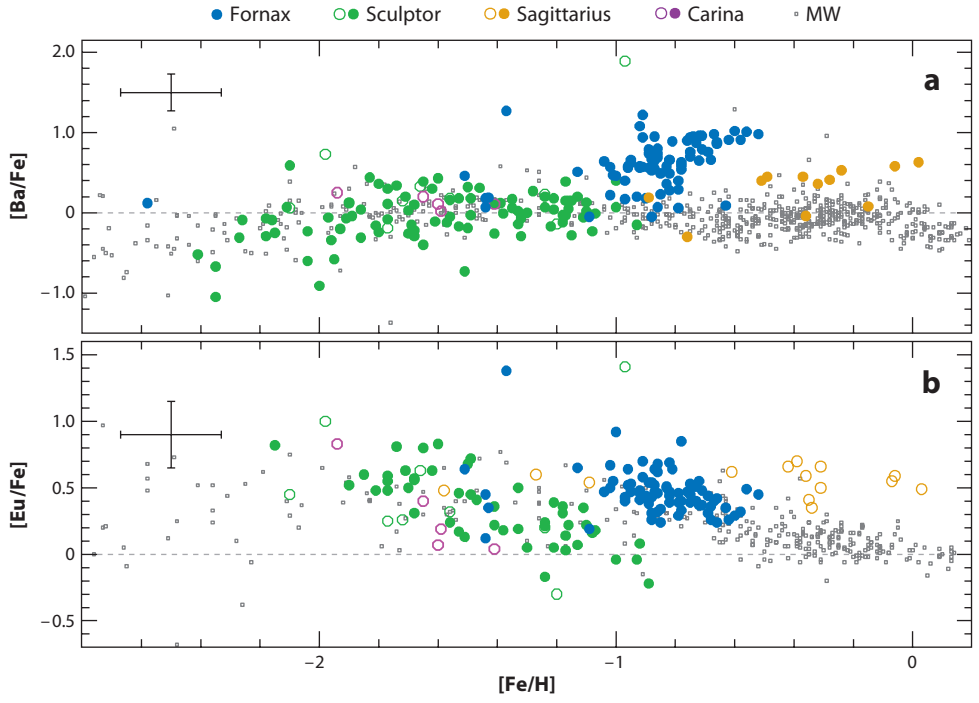

Figure 13

Neutron-capture elements (*a*) Ba, and (*b*) Eu in the same four dSphs as in **Figure 11** compared to the Milky Way. Sgr (*orange*: McWilliam & Smecker-Hane 2005; Monaco et al. 2005; Sbordone et al. 2007), Fnx (*blue*: Shetrone et al. 2003; Letarte 2007), Scl (*green*: V. Hill & DART, in preparation; Shetrone et al. 2003; Geisler et al. 2005), and Carina (*purple*: Shetrone et al. 2003; Koch et al. 2008a). Open symbols refer to single-slit spectroscopy measurements, whereas filled circles refer to multiobject spectroscopy. A representative error-bar for the latter is shown on the left-hand side of the picture. The small gray squares are a compilation of the Milky Way disk and halo star abundances, from Venn et al. (2004a).

barium (Ba) or lanthanum (La). Among the few exceptions is europium (Eu), which is almost exclusively an *r*-process product.

Figure 13 compares Ba and Eu abundances in four dSph galaxies and in the Milky Way. At first glance, the Eu evolution in dSph galaxies resembles that of their respective α-elements (see **Figure 11**), as expected for an *r*-process originating in massive stars. In the Milky Way, Ba and Y are dominated by the *r*-process for [Fe/H] $\lesssim -2.0$ (e.g., Johnson & Bolte 2002, Simmerer et al. 2004), whereas the *s*-process dominates at higher metallicities (e.g., more than 80% of the solar Ba is of *s*-process origin).

At early times (at [Fe/H] < -1), there seems to be little difference between the various dSphs and the Milky Way halo in **Figure 13**. However, there is a hint that at the lowest metallicities ([Fe/H] < -1.8), [Ba/Fe] increases in scatter and starts to turn down. This hint is confirmed in the plot in Section 4.2, which includes other dSphs, although from much smaller samples (Shetrone, Côté & Sargent 2001; Fulbright, Rich & Castro 2004; Aoki et al. 2009). In fact, this scatter and downturn of [Ba/Fe] is a well-known feature in the Milky Way halo (François et al. 2007; Barklem et al. 2005, and references therein), where it occurs at much lower metallicities ([Fe/H] < -3.0). So far we have extremely low number statistics for dSphs, and these results need to be confirmed in larger samples of low-metallicity stars. These low *r*-process values at higher [Fe/H]

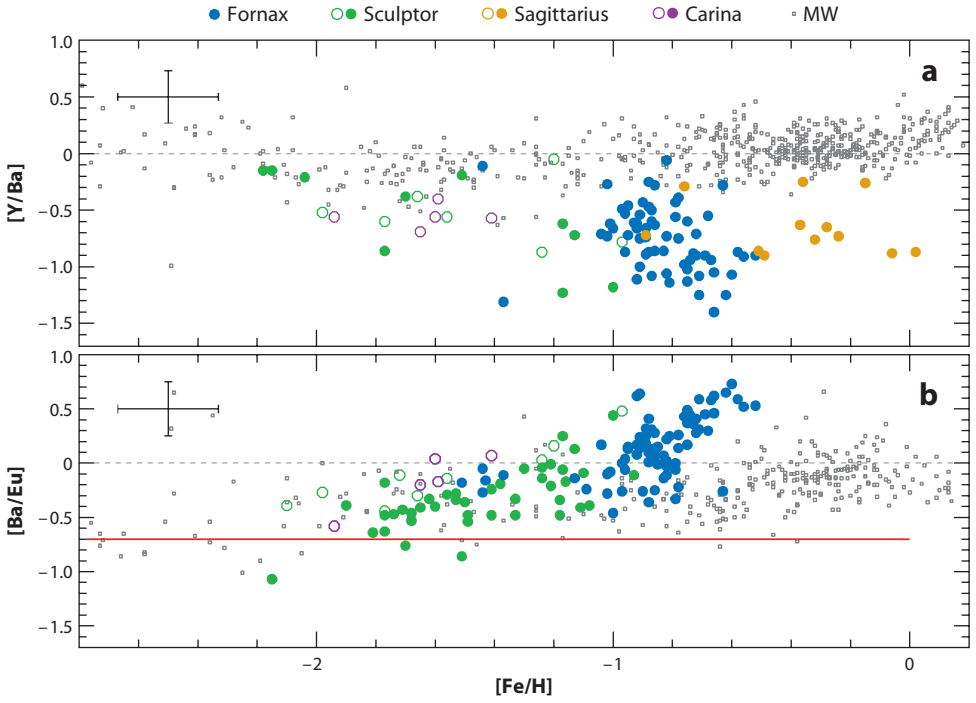

Figure 14

Ratios of (*a*) first to second *s*-process peak elements [Y/Ba] and (*b*) *r*- to *s*-process element production [Ba/Eu] in the same four dwarf spheroidals as in **Figure 11** compared to the Milky Way. The solid red line indicates the pure r-process [Ba/Eu] production ratio. Sgr (*orange*: McWilliam & Smecker-Hane 2005, Monaco et al. 2005, Sbordone et al. 2007), Fnx (*blue*: Shetrone et al. 2003, Letarte 2007), Scl (*green*: V. Hill & DART, in preparation; Shetrone et al. 2003; Geisler et al. 2005), and Carina (*purple*: Shetrone et al. 2003, Koch et al. 2008a). Open symbols refer to single-slit spectroscopy measurements, whereas filled circles refer to multiobject spectroscopy. A representative error-bar for the latter is shown on the left-hand side of the picture. The small gray squares are a compilation of the Milky Way disk and halo star abundances, from Venn et al. (2004a).

than in the Galactic halo either mean that the dwarf galaxies enriched faster than the halo at the earliest times or that the site for the *r*-process is less common (or less efficient) in dSphs. The *r*-process elements are clearly useful tracers of early timescales, because unlike the α-elements (in the halo and in dSphs), they show significant scatter in the lowest metallicity stars. The *r*-process is, thus, produced in much rarer events than the α-elements, and so it can be a much finer tracer of timescales and enrichment (and mixing) processes.

The ratio of [Ba/Eu], shown in **Figure 14**, indicates the fraction of Ba produced by the *s*-process to that produced by the *r*-process. In dSphs, as in the Milky Way, the early evolution of all neutron-capture elements is dominated by the *r*-process (this was already noted by Shetrone, Côté & Sargent 2001; Shetrone et al. 2003). In each system, however, the low- and intermediate-mass AGB stars contribute *s*-process elements, which soon start to dominate the Ba (and other neutron capture elements) production. The metallicity of this switch from *r*- to *s*-process ([Fe/H] ~ -1.8, the same as the [α/Fe] knee) is only somewhat constrained in the Scl dSph. This turnover needs to be better constrained in Scl and even more so in other galaxies to provide timing constraints on the chemical enrichment rate. It could reveal the metallicity reached by the system at the time when the *s*-process produced in AGBs starts to contribute.

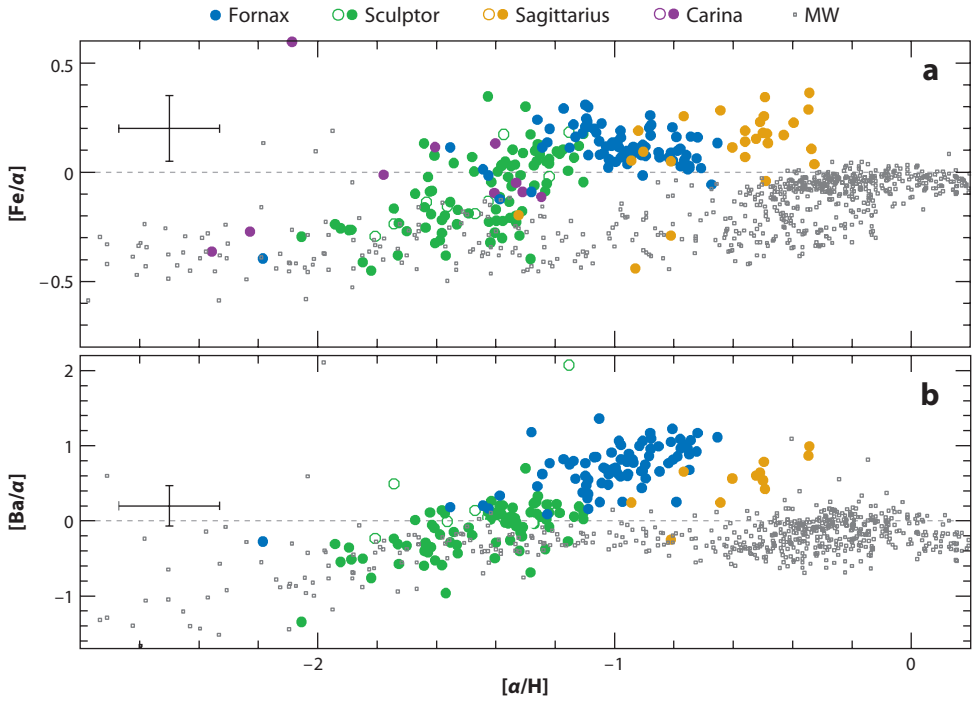

Figure 15

Trends of (*a*) iron as a function of α elements and (*b*) neutron-capture element, Ba, as a function of α elements in the same four dwarf spheroidals as in **Figure 11** compared to the Milky Way. Sgr (*orange*: McWilliam & Smecker-Hane 2005, Monaco et al. 2005, Sbordone et al. 2007), Fnx (*blue*: Shetrone et al. 2003, Letarte 2007), Scl (*green*: V. Hill & DART, in preparation; Shetrone et al. 2003; Geisler et al. 2005), and Carina (*purple*: Shetrone et al. 2003; Koch et al. 2008a). Open symbols refer to single-slit spectroscopy measurements, whereas filled circles refer to multiobject spectroscopy. A representative error-bar for the latter is shown on the left-hand side of the picture. The small gray squares are a compilation of the Milky Way disk and halo star abundances, from Venn et al. (2004a).

For the more metal-rich stars ([Fe/H] > -1), there is also a distinctive behavior of [Ba/Fe] in dSphs (**Figure 13**). In the Scl dSph, the [Ba/Fe] values never leave the Milky Way trend, but this galaxy also has almost no stars more metal rich than [Fe/H] < -1. Fnx, however, and to a lesser extent Sgr, display large excesses of barium for [Fe/H] > -1. This is now barium produced by the *s*-process, and it shows the clear dominance of the *s*-process at late times in dSphs.

Figure 15 shows the trends of [Fe/α], and [Ba/α] against [α/H]. The fact that [α/H] keeps increasing significantly after the knee in the Scl dSph demonstrates that even in this system, which has no significant intermediate-age population, there was still ongoing star formation contributing α enrichment from massive stars well after SNe Ia started contributing. This is also confirmed by the presence of stars that have [Fe/H] > -1.8 (the knee), and were therefore formed after SNe Ia started exploding. In Fnx or Sgr, the very flat, extended and high [Fe/α] plateau also shows that massive stars have kept feeding the chemical enrichment all along the evolution, even though they do not dominate the Fe enrichment. As for the *s*-process, the widely different behavior of Scl, Fnx, and Sgr and the Milky Way are even more striking viewed in this representation than they were in **Figure 13**; this illustrates the total disconnect of massive star nucleosynthesis to Ba, and the strong influence of AGB stars at a time when massive stars do not drive the metallicity evolution anymore.

4.2. Ultrafaint Dwarf Galaxies

Individual stars in the uFds that have recently been discovered around the Milky Way have so far been little observed at high spectral resolution. This is probably owing to the difficulty in confirming membership for the brighter stars in these systems. However, several groups are currently following up confirmed members (typically selected from lower resolution CaII triplet observations) to derive abundances. So far, Koch et al. (2008b) have observed two RGB stars in Herc ($M_V \sim -6.6$), and Frebel et al. (2009) are following up RGB stars in the even fainter uFds UMa II and Coma (both with, $M_V \sim -4$). The latter study confirms that uFds do contain very metal-poor stars, [Fe/H] < -3 (as found by Kirby et al. 2008), unlike the more luminous classical dSphs (Helmi et al. 2006). It also appears that these uFds extend the metallicity-luminosity relation down to the lower luminosities (Simon & Geha 2007; see Section 4.1).

The two stars in Herc seem to have particularly peculiar abundance patterns, with high Mg and O abundances (hydrostatic burning in massive stars) and normal Ca and Ti abundances (explosive nucleosynthesis in massive stars), but exceedingly unenriched levels of Ba (Koch et al. 2008b). However, elemental ratios in the extremely metal-poor stars in the two fainter dwarfs UMa II and Coma (Frebel et al. 2009) are remarkably similar to the Milky Way halo's extremely metal-poor stars. **Figure 16** compares Mg and Ba measurements in faint dSphs, with more luminous dSph stars that have [Fe/H] $\lesssim -2$, including a new sample of six very metal-poor stars in Sextans by Aoki et al. (2009) and the Milky Way. In fact, only Sextans seems to have scattered and low [Mg/Fe] ratios, whereas other dSphs and uFds all show similar [Mg/Fe] enhancements. The similarity between stars with metallicities below [Fe/H] $\lesssim -2$ in the Milky Way and faint dwarfs is seen also in other light elements, such as Na, Sc, Cr, Mn, Ni, or Zn. This may also be true of more luminous dSphs (see Section 4.1).

The overall similarity between all the most metal-poor stars for element ratios up to the iron-peak can be taken as an indication that star formation and metal-enrichment, even at the earliest times, and even in the smallest systems, has proceeded in a similar manner. This may lead to the net yield of the very first stars. The very low dispersion found in abundance ratios of these elements in Galactic extremely metal-poor stars (EMPS), down to metallicities of [Fe/H] ~ -4, came as a surprise (Cayrel et al. 2004); because it was thought that one or a few SNe II were sufficient to enrich the gas to those metallicities, the expectation was that among EMPS the variety of metal-production sites (SNe II of different masses) would appear as dispersed abundance ratios. We are now adding to this puzzle the fact that these well-defined abundance ratios are also achieved by considerably smaller halos.

The only discrepancy among the most metal-poor stars concerns the *r*-process element Ba, which stands out below the Milky Way halo distribution both for faint and somewhat more luminous dSph galaxies. The most extreme low-Ba abundances are found so far in Herc (Koch et al. 2008b) and Draco (Fulbright, Rich & Castro 2004), where only upper limits were detected.

4.3. Dwarf Irregulars

The dIs are all (except the SMC) located at rather large distances from the Milky Way and so far, the only probes that could be used to derive chemical abundances in these objects were HII regions and a few supergiant stars. Both types of probes allow a look-back time of at most a few tens of millions of years, and this is the end-point of a Hubble-time's worth of chemical evolution for any galaxy. This limitation makes it difficult to gather relevant information to constrain the chemical enrichment over time in these systems. However, abundances in HII regions and supergiants (see references in **Table 1**) are useful to understand how dIs fit in the general picture of dwarf galaxies, and how they compare to larger late-type galaxies. First, they give the present-day metallicity

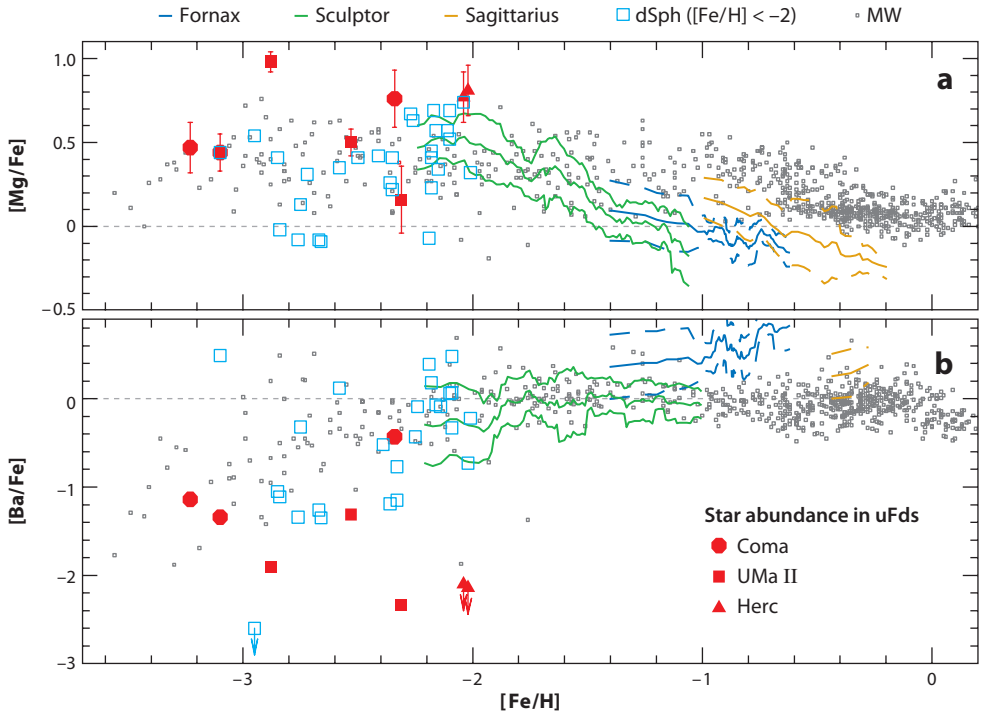

Figure 16

(*a*) Mg (α-element) and (*b*) Ba (*s*-process element) abundances in dwarf spheroidals (dSphs), ultra-faint dwarfs (uFds) and the Galactic halo. The red symbols are abundances of stars in uFds as measured by Frebel et al. (2009) for stars in UMa II (*squares*) and Coma (*circles*) and by Koch et al. (2008b, *triangles*) in Herc. These are compared to the trends derived from **Figures 11** and **13** for Scl, Fnx, and Sgr as well as individual stellar abundances for all very metal-poor stars ([Fe/H] < -2) in dSphs (Fulbright, Rich & Castro 2004; Sadakane et al. 2004; Venn et al. 2004a; Koch et al. 2008a; Aoki et al. 2009; *light blue open squares*), and the Milky Way from the compilation by Venn et al. (2004a) and complemented by Cayrel et al. (2004) and François et al. (2007) (*small gray squares*). The dSph trends were derived by a simple 10-point running average on the data for each dSph galaxy with sufficient statistics (more than 20 measurements).

of these systems, and all are more metal poor than the Milky Way–disk young population, in agreement with the metallicity-luminosity relation (see, for example, van Zee & Haynes 2006 for a relation based on dIs within 5 Mpc), and range between $12 + \log(\mathrm{O/H}) \sim 8.1$ (e.g., NGC 6822, IC 1613) to $12 + \log(\mathrm{O/H}) \sim 7.30$ (Leo A), or $[\mathrm{O/H}] \sim -0.6$ to -1.4. Both HII regions and supergiants typically agree on the oxygen abundances of the systems, within the respective measurement uncertainties (Venn et al. 2003, Kaufer et al. 2004), with little metallicity dispersion within a galaxy, and no spatial gradient (e.g., Kobulnicky & Skillman 1997; van Zee, Skillman & Haynes 2006; van Zee & Haynes 2006). This holds even in the most metal-poor galaxies and suggests a very efficient mix of metals across the galaxy despite the clumpiness of the interstellar medium and ongoing star formation. The shear within these systems is expected to be very low, and this has been taken as an indication that mixing occurs in the gaseous hot phase, before the gas cools down to form new stars (e.g., van Zee, Skillman & Haynes 2006).

A- to M-type supergiants have a further interest as they provide the present-day [α/Fe] ratios in dIs, which are not accessible from HII regions where typically only light elements (e.g., He, N, O, Ne, S, Ar), and no iron (nor any other element that would trace SNe Ia), can be measured.

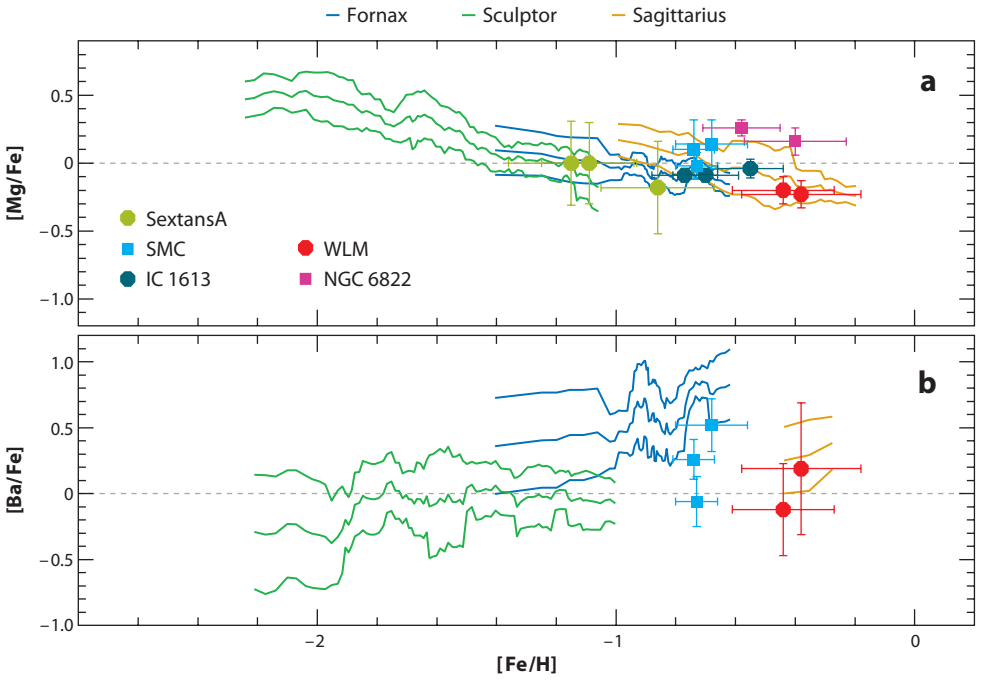

Figure 17

(*a*) Mg (α-element) and (*b*) Ba (*s*-process element) abundances in individual supergiants in the dwarf irregular galaxies Sex A (Kaufer et al. 2004), SMC (Hill, Barbuy & Spite 1997; Luck et al. 1998; Venn 1999), NGC 6822 (Venn et al. 2001), and WLM (Venn et al. 2003) compared to the trends derived from **Figures 11** and **13** for Scl, Fnx, and Sgr (see **Figure 16** for details on the trends). For the SMC, the points are, in fact, the mean and dispersion of the samples studied in the references given (~6–10 A, K, and Cepheids supergiants, respectively).

The first dI where abundances of stars were measured was, of course, the SMC in our backyard. The largest samples to date with abundances in the SMC are of supergiants that are discussed by Hill, Barbuy & Spite (1997, K-type stars), Luck et al. (1998, F-type stars), and Venn (1999, A-type stars). Similar studies in more distant dIs needed efficient spectrographs on 8–10-m telescopes and, at the expense of observing for many hours, the detailed abundances of a few stars have been observed in A-type supergiants out to distances of 1.3 Mpc. This work has been pioneered by K. Venn and collaborators using A-type stars (Venn et al. 2001, 2003; Kaufer et al. 2004) in NGC 6822, Sextans A, and WLM. There has also been a more recent study using M-type stars in IC 1613 by Tautvaišienė et al. (2007).

Figure 17 illustrates the observed low [α/Fe] in these systems and compares them to the observed trends of older populations (RGB stars) in dSph galaxies, as defined in **Figures 11** and **16**. These low [α/Fe] are expected in galaxies that have formed stars over a long period of time, however; they clearly occur at much lower metallicities than in larger systems such as the Milky Way or the LMC, pointing toward an inefficient metal enrichment of the galaxy (low star-formation rate and/or metal losses through winds). It is interesting to see in **Figure 17** how dIs actually prolong the trends of dSph galaxies, not only for α elements but also for neutron-capture elements. From these diagnostics, dSphs are entirely consistent with dIs that lost their gas at a late stage of their evolution. The Fnx dSph and the SMC, which are both dominated by

intermediate-age populations, are also quite similar in their chemical enrichment, except that Fnx ran out of gas (or lost its gas) and stopped star formation about 10^8 years ago.

5. CHEMICAL-EVOLUTION MODELS

The detailed evolutionary histories of dwarf galaxies have intrigued astronomers for decades. One of the main reasons of interest is that they are often extremely low-metallicity systems and, thus, assumed to be highly unevolved. Their low abundances of metals and helium, derived from HII region spectra, allow the determination of the primordial helium abundance with a minimum of extrapolation (e.g., Peimbert & Torres-Peimbert 1974; Olive, Steigman & Skillman 1997; Izotov & Thuan 1998; Izotov, Thuan & Stasińska 2007), and thus provide insights into Big Bang nucleosynthesis.

Recently, dwarf galaxies have been of interest owing to their cosmological importance as potential building blocks of larger systems. Nearby dwarf galaxies are the closest we can get to the detailed study of a primordial system. They typically have relatively simple structures and often very low metallicities. We assume that, because small systems are believed to be the first to collapse in the early Universe, it was galaxies like these that were the first to form and are, thus, potential hosts of the first stars. Their widespread distribution throughout the early Universe also makes them suitable candidates to be able to reionize the Universe uniformly and rapidly (e.g., Stark et al. 2007; Choudhury, Ferrara & Gallerani 2008). Recently, there have been large samples of stellar abundances of individual stars obtained in nearby dwarf galaxies (e.g., V. Hill & DART 2009, in preparation; Letarte 2007; Monaco et al. 2007). These will provide a wealth of information on chemical evolution through time and determine the accurate evolutionary path of these small systems and their contribution to universal processes such as the build-up of metals in the Universe.

Beatrice Tinsley, beginning in the mid-1960s pioneered the field of galactic chemical-evolution modeling. The cornerstones were laid by E. Salpeter in 1955 in his paper on the IMF and in 1959 with his first determination of the effects of stellar evolution on the metallicity evolution of stellar populations. This work was extended by M. Schmidt in 1959 and 1963 to determine universal predictions for the SFR in a galaxy. Tinsley, however, provided the first full description of the theoretical modeling of galactic chemical evolution and of its relevance to many astrophysical topics. In 1968, she was already studying the evolutionary properties of galaxies of different morphological types (Tinsley 1968), and with subsequent seminal papers (Audouze & Tinsley 1976, Tinsley 1980), she set the stage for all future studies of galactic chemical evolution. Since the late seventies (e.g., Lequeux et al. 1979), a wealth of chemical-evolution models have been computed for dwarf galaxies in general and for late-type dwarfs in particular (see e.g., Matteucci & Chiosi 1983; Pilyugin 1993; Marconi, Matteucci & Tosi 1994; Carigi et al. 1995; Tosi 1998, and references therein).

The predictions of early models of the chemical evolution of dwarf galaxies were far from unique (as reviewed, e.g., by Tosi 1998), because few observational constraints were available: the interstellar medium chemical abundances (helium, nitrogen, and oxygen as derived from the emission lines of HII regions), and the gas and total mass (mainly from 21-cm radio observations). These data define present-day galaxy properties and do not constrain the early epochs. This allows for little discrimination between different models, which may have very different paths to the same end point. Star-formation laws, IMF, and gas flows could be treated as free parameters and, with their uncertainties, it was inconceivable to model the evolution of individual galaxies, unless unusually rich in observational data. In practice, until recently, only the Magellanic Clouds were modeled individually (e.g., Gilmore & Wyse 1991, Pagel & Tautvaisiene 1998), even though many

constraints were still missing (e.g., accurate field star metallicity distribution, detailed abundances in older populations, etc.). It is fair to ask how good the predictions of some of these models were, because 30 years later we are still arguing about whether or not dIs and BCDs differ only in the recent SFH, and if BCDs are actually ancient systems with a recent burst, as already suggested by Lequeux et al. (1979), or something entirely different.

Detailed chemical-evolution models of individual dwarf galaxies have recently become possible as more accurate SFHs become available combined with large samples of stellar abundances for individual stars over a range of ages. This provides an accurate age-metallicity relation, which is a key constraint for chemical-evolution models.

5.1. Explaining Low Metallicity

One of the major challenges for chemical-evolution models of dwarf galaxies has always been to reconcile their low observed metallicity with the fairly high SFR of the most metal-poor systems, many of which are actively star-forming BCDs. Historically, three mechanisms have been envisaged to accomplish this task (Matteucci & Chiosi 1983):

- variations in the IMF; steeper IMF slopes and/or mass range cut-offs have been proposed to reduce the chemical enrichment from massive stars;
- accretion of metal-free, or very metal-poor, gas to dilute the enrichment of the galaxy; and
- metal-rich gas outflows, such as galactic winds, triggered by supernova explosions in systems with shallow potential wells, or gas stripping due to interactions with other galaxies or with the intergalactic medium to efficiently remove the metal-enriched gas from the system.

Whether one of these mechanisms is preferable or a combination of any or all of them is required is still a matter of debate. When detailed numerical models were computed it was immediately recognized that metal-enriched winds are the most straightforward mechanism to recreate the observed properties of dwarf galaxies (Matteucci & Tosi 1985; Pilyugin 1993; Marconi, Matteucci & Tosi 1994; Carigi et al. 1995). The infall of metal-poor gas can, in principle, explain the evolution of gas-rich dwarfs, but gas accretion is also likely to trigger more star formation and chemical enrichment. This can quickly lead to more rapid enrichment of small dwarf galaxies. Bottom-heavy IMFs imply abundance ratios for elements produced by stars of different mass that are at odds with the observed values (see Section 4.1.1).

5.2. Galactic Winds

It was first proposed by Larson (1974) that gas could be blown out by internal energetic events related to star formation, such as stellar winds and supernova explosions. These processes can accelerate metal-rich stellar and supernova ejecta beyond the escape velocity of small dwarf galaxies (e.g., Heiles 1990, Tenorio-Tagle 1996, Rieschick & Hensler 2003, Fujita et al. 2004). The theory is periodically further developed (e.g., Dekel & Silk 1986; D'Ercole & Brighenti 1999; Mac Low & Ferrara 1999; Ferrara & Tolstoy 2000; Legrand et al. 2001; Tassis et al. 2003; Marcolini et al. 2006; Salvadori, Ferrara & Schneider 2008), and naturally explains the well-established correlation between luminosity and metallicity (e.g., Skillman, Kennicutt & Hodge 1989; Gallazzi et al. 2005), as smaller galaxies are less able to retain their heavy elements. It can also explain the structural similarities observed by Kormendy (1985), and it has even been suggested that many dwarf galaxies have lost most of the gas mass they originally possessed and, hence, follow the structural relations regardless of the current gas mass fraction (Dekel & Silk 1986; Skillman & Bender 1995). However, this theory cannot explain why some galaxies lose all their gas very early and some relatively

recently. There has been no global parameter, such as mass, found to explain this. Hence, the influence of tidal effects is considered to play an important, but hard to verify, role (e.g., Lin & Faber 1983). It may also be related to the varying initial conditions under which different galaxies may have formed, or perhaps also the density of the dark matter halo in which they reside.

Galactic winds have been predicted by hydrodynamical simulations (D'Ercole & Brighenti 1999, Mac Low & Ferrara 1999) to be able to remove a large fraction of the elements synthesized by SNe II as well as a fraction of the galaxy's interstellar medium. Thus, galactic winds can be quite effective and lead to a significant reduction of the interstellar medium enrichment. The strength of this effect depends both upon the galaxy mass—or the depth of the potential well—and on the intensity of the star formation, and thus the number of supernova explosions that can be expected. This is precisely what is needed by chemical-evolution models to reproduce the observed properties of dwarfs. Moreover, there is increasing observational evidence for starburst-driven metal-enriched outflows (e.g., Meurer et al. 1992; Heckman et al. 2001; Martin, Kobulnicky & Heckman 2002; Veilleux, Cecil & Bland-Hawthorn 2005; Westmoquette, Smith & Gallagher 2008). Whether early-type dwarfs are connected to late-type dwarfs, as the extreme consequence of tremendous winds from originally gas-rich dwarfs or gas stripping or ram pressure in harsh environments, is difficult to say. The evidence that gas-poor dwarfs are preferentially located in denser environments than gas-rich ones (Binggeli, Tarenghi & Sandage 1990) seems, however, to favor the stripping scenario.

5.3. Modeling Individual Systems

Two kinds of models for individual galaxies are commonly used: standard chemical-evolution models and chemodynamical models. The standard models follow the evolution of individual elements, taking into account global parameters such as mass of the system, gas flows, and IMF, and stellar parameters such as their chemical yields and lifetimes, but make very simplistic assumptions (if any) on stellar and gas dynamics (see Tinsley 1980 for a comprehensive and still relevant review). The chemodynamical models deal with the dynamical processes in great detail. Standard models are quite successful in predicting large-scale, long-term phenomena, but their simplistic treatment of stellar and supernova feedbacks and of gas motions, is an obvious drawback. Chemodynamical models are more able to account for small-scale, short-term phenomena, but the timescales required to run hydrodynamic codes and the errors that start to creep in have made them less successful to follow galactic-scale evolution over more than a gigayear. The challenge in the next few years is to improve both types of approaches and get a more realistic insight into how stars and gas evolve, chemically and dynamically, in their host galaxies.

5.3.1. Standard models. A number of standard models have been computed for nearby dSphs adopting the individual SFHs derived from deep HST photometry and comparing the model predictions with the stellar chemical abundances inferred from new generation spectroscopy. Carigi, Hernandez & Gilmore (2002) analyzed Carina, Ursa Min, Leo I, and Leo II and suggested a relation between the duration of the star-formation activity and the size of the dark matter halo. Lanfranchi & Matteucci (e.g., Lanfranchi, Matteucci & Cescutti 2008, and references therein) devoted a series of papers to the chemical evolution of Carina, Draco, Sgr, Sextans, Scl, and Ursa Min, reaching the conclusion that, to reproduce the observed stellar abundance ratios and age-metallicity relations, they need low star formation and high wind efficiencies. They suggest that a connection between dSphs and BCDs is unlikely.

Owing to the lack of stellar spectroscopy available for more distant dI galaxies, chemical-evolution models with the detailed approach applied to nearby dSphs have been computed only for

NGC 6822 (Carigi, Colín & Peimbert 2006), the closest dI in the Local Group beyond the Clouds. Models assuming the SFH derived from HST CMDs have been computed also for the starburst dwarfs NGC 1569 and NGC 1705 (Romano, Tosi & Matteucci 2006), a few megaparsecs outside the Local Group. Projects are in progress to model the chemical evolution of the Magellanic Clouds with the level of detail and reliability achieved so far only for the Solar Neighborhood, as soon as their SFHs and age-metallicity relations are derived (e.g., Tosi et al. 2008). The situation is expected to improve significantly with the advent of new generation instruments on HST, VLT, and eventually Extremely Large Telescopes, which will allow measurement of reliable stellar metallicities at larger distances.

5.3.2. Chemodynamical models. To date chemodynamical models have mainly been used to study the effects of feedback from supernova explosions in a variety of conditions. They can analyze in detail the heating and cooling processes and put important constraints on the onset and fate of galactic winds, stripping, and ram pressure. However, they are not yet able to follow the evolution of a galaxy over the entire Hubble time assuming empirically derived SFHs. They have been applied to resolved starburst dwarfs with SFH derived from HST photometry [e.g., Recchi et al. (2004, 2006) for I Zw 18 and NGC 1569] and to a few nearby dSphs [see Fenner et al. (2006), Marcolini et al. (2006, 2008) for Draco, Scl, and Fnx).

5.3.3. Model predictions and observed abundances. The different timescales for the chemical enrichment of elements produced by different stellar processes are particularly useful to constrain chemical-evolution models. This is especially true for *r*- and *s*-process elements, and for Ba in particular. Only a few models (Fenner et al. 2006, Lanfranchi, Matteucci & Cescutti 2008, and references therein) are recent enough to have their predictions compared with the abundance patterns measured in dwarfs (as shown in Section 4). They thus deserve a few more words of comment. Both types of models reproduce fairly well the observed properties of the galaxies they are applied to, although sometimes they need to assume chemical yields different from those available in the literature (Lanfranchi, Matteucci & Cescutti 2008, and references therein).

[Ba/Fe] is one of the few elements known to have a very large spread at low metallicities (e.g., François et al. 2007; see **Figure 16**). At early times, Ba is produced by the *r*-process, which must be a rare occurrence and, thus, a sensitive probe of enrichment timescales. The strong rise of [Ba/Fe] seen in Fnx or Sgr (and the LMC; Pompeia et al. 2008) is clearly attributable to the *s*-process that comes from AGB stellar wind pollution. This is currently not well predicted by chemical-evolution models of dSphs such as those of Lanfranchi, Matteucci & Cescutti (2008) and Fenner et al. (2006), probably because of the lack of adequate stellar yields. In these models, the galactic wind removes the gas and makes the SFR drop suddenly, preventing high-mass stars from contributing to the enrichment and thereby lowering the *r*-process contribution to the neutron capture elements. But the wind does not prevent low- and intermediate-mass AGBs from contributing significantly to the ISM. The decreasing *r*-process contribution is indeed observed in **Figure 14** with the continuous rise of [Ba/Eu] in Fnx in the range [Fe/H] > -0.8, but this decrease of the *r*-process also acts to prevent [Ba/Fe] from rising: In fact, in these models, [Ba/Fe] (or [La/Fe]) decrease slightly at high metallicities. The models of Fenner et al. (2006) aim to reproduce the abundances of the Scl dSph, and indeed there is a turn-up of [Ba/Fe] that is linked to the rise of the *s*-process, but [Ba/Fe] at low metallicities in Scl is strongly underestimated in the models compared to observations. This is probably due to the strong winds in these models, efficiently removing metals produced by massive stars, including the *r*-process that makes Ba at low metallicities. These models also predict low α-elements down to the lowest metallicities in the systems, which are also not observed. In

these models, the low-metallicity AGB stars that produce the *s*-process responsible for the [Ba/Fe] upturn, also produce the correct [Ba/Y].

Finally, **Figure 14** shows that, in the domain where the neutron-capture enrichment is dominated by the *s*-process, [Y/Ba] in dSphs is exceedingly low. The most straight-forward interpretation assumes that low-metallicity AGB stars dominate the *s*-process. Suggesting that in these stars nucleosynthesis favors high-mass nuclei over lower mass ones, as the result of less numerous seed nuclei (iron mostly) being bombarded by similar neutron fluxes to those at higher metallicities. However, this simple-minded explanation has so far lacked any quantitative prediction to be tested against observations, owing largely to the uncertainties plaguing the detailed *s*-process computations (thermal pulses in AGBs are a challenge to model). Another interpretation put forward by Lanfranchi, Matteucci & Cescutti (2008) is that low [Y/Ba] are reached by simply decreasing the *r*-/*s*-fractions at late times (as above, owing to galactic winds losing preferentially *r*-process elements). Again, the models are not able to reproduce the steep rise in heavier *s*-process elements such as Ba. This shows us that yields inferred from the Solar Neighborhood are not adequate. Although they can reproduce the abundance patterns in the halo and disk of the Milky Way, they cannot easily also reproduce the abundances of dSphs, such as Fnx and Sgr, nor the LMC.

6. CONCLUDING REMARKS

In this review, we have provided an overview of the current understanding of the detailed properties of dwarf galaxies from studies of their resolved stellar populations. This includes CMD analysis, to determine accurate SFHs, as well as low- and high-resolution spectroscopy, to determine kinematic and chemical properties of stars over a range of ages.

Most dwarf galaxies in the Local Group have structural properties similar to each other and to larger late-type and spheroidal systems (Section 1). Early-type dwarfs tend to extend to fainter magnitudes, with transition types being found at the faint end of the dI distribution. The fact that there exists a transition type, intermediate in properties between a dSph and a dI, supports the idea that there is an evolutionary pathway. The transition between early and late types may indicate the average mass at which galaxies will always lose their gas, especially if they spend time in the vicinity of a large galaxy. But, of course, this mass will be dependent on the environment that a galaxy has passed through, which could explain why this is not a sharp cut-off. Despite numerous caveats and regardless of size, luminosity, and SFH, all dSph and dI galaxies in the Local Group (and beyond) appear to overlap along a straight line in the $M_V - \mu_V$ plane (**Figure 1*a***), a relationship that is unchanged over a range of $\approx$15 mag in M_V.

The continuity of structural properties from dwarf galaxies to larger spheroidal and late-type systems is most likely dominated by physical processes that scale with mass, for example, the efficiency with which gas and/or metals can be lost from a system during its evolution through supernova winds and/or interactions. Thus, early-type dwarf galaxies in the Local Group must have suffered the largest effect owing to interactions with large galaxies, as has already been suggested from the morphology-density relation. Accurate SFHs have been determined for a range of dwarf galaxy types (see Section 2). The different classes of dwarf galaxies have different rates of present-day star-formation activity and possibly also different degrees of past disruption. However, the past SFHs of early- and late-type systems bear strong similarities to each other (see **Figure 5**). There is evidence for interruptions and enhancements in the SFHs of dwarf galaxies. This is especially true of early-type systems, a few of which have experienced star-formation activity only at the earliest epochs, but most have had extended or recurrent star-formation activity. No genuinely young galaxy (of any type) has ever been found; stars are always found at the oldest look-back times observed.

The SFHs of BCDs are also broadly similar to dIs (that is, comparing **Figure 5** with **Figure 8**). However, the recent SFRs in BCDs are usually higher than in dIs. The SFRs in BCDs are more similar to those found in active star-forming zones with HII regions in the SMC (**Figure 7**), or in the Milky Way, with the difference that the BCDs are forming stars globally, dominating the entire galaxy. All the BCDs that have been studied in detail (see Section 2.3) have apparently had their strongest star-formation episode recently, unlike dIs. This is most likely a selection effect owing to the difficulty in finding distant low-luminosity dwarf galaxies, unless they happen to be currently actively forming stars.

Spectroscopy of individual stars has helped to define the detailed chemical and kinematic properties of stellar populations of different ages in nearby dSph systems and in comparison to larger systems such as the Milky Way and the LMC (Sections 3 and 4). The chemical enrichment of dwarf galaxies seems to be dominated by effects that are most likely dominated by gas and metal loss. The least massive systems actually seem to lose such a large fraction of their metals during star-formation episodes that star formation has a slow effect on the global chemical evolution (see Section 5). This means that galaxies with the same mass but quite different SFHs end up with the same final metallicity, consistent with the well-known mass/luminosity-metallicity relation for dwarf galaxies.

One clear mismatch in the physical properties between early- and late-type dwarfs is that the HI gas in the brighter late-types, such as SMC, NGC 6822, and IC 1613, is rotating with ∼20–60 km s^{-1}. Such high rotation values are never seen in the stars of early-type dwarfs. However, we really do not know if old and young stars in dwarf galaxies can have different kinematic properties, such as those seen in the Milky Way. The kinematics of late-type galaxies have always been measured using HI gas, out of which their young populations are currently forming. Early-type galaxies, however, are of necessity probed using only their old or even ancient stellar populations. A careful comparison of the kinematics and metallicity distributions of equivalent tracers in early- and late-type galaxies has yet to be made.

The abundance patterns of RGB stars for large samples of individual stars, typically in dSph galaxies (Section 4), show that there are distinct differences in the chemical-evolution paths between galaxies. The rate at which α-enrichment occurs varies between systems. There are not yet large enough samples in a diversity of environments to really say how this may or may not relate to the mass of a system, its SFH, or the rate of mass and/or metal loss. But stars do appear to retain a clear abundance signature of the galactic environment in which they were born. These patterns also extend to younger stars in late-type systems (see **Figure 17**).

The hierarchical theory of galaxy formation contains at its heart the concept of smaller systems continuously merging to form larger ones. This leads to the general expectation that the properties of the smaller systems will be reflected in the larger. Thus, the relationship between the properties of individual stars in small dwarf galaxies around the Milky Way, and stars in the Milky Way, is a recurrent theme (see Section 4). From recent abundance studies of low-metallicity stars in dSphs (see **Figure 16**), it seems likely that there exist only narrow windows of opportunity when the merging of dwarf galaxies to form larger systems would not lead to inconsistencies. Properly understanding the constraints that these kinds of data can put on the merger history of the Milky Way requires more extensive abundance studies of metal-poor stars in dwarf galaxies, as well as a better theoretical understanding of supernovae yields (including the *r*-process) and the mixing of ejecta into interstellar gas. It also remains an open question of how the uFds may relate to the merger history of the Milky Way and if they can fully account for the deficiencies of the larger types of dwarf galaxies as building blocks of the Milky Way.

The dark matter content of dwarf galaxies is also of importance for the verification of cosmological theories, as it indicates how galaxies we see today, which may have lost a significant

fraction of their initial baryons, relate to structures in cosmological simulations. For an accurate determination of the dynamical properties, it must be realized that dwarf galaxies are not the simple systems they were once thought to be. Making assessments of the total mass of small galaxies is complicated, not least because the dark matter halos are likely to extend beyond the baryonic tracers, but also because there are multiple components in the baryonic matter.

This review shows the inherent complexities that are involved in understanding even the smallest galaxies. These low-metallicity systems show a wealth of variety in their properties, such as luminosity, surface brightness, SFH (both past and present), kinematics, and abundances. However, there is strong evidence that they are all part of a continuous distribution of galaxies from small to large.

. . .E quindi uscimmo a riveder le stelle.

(Dante Alighieri, La Divina Commedia, Inferno XXXIV, 139)

DISCLOSURE STATEMENT

The authors are not aware of any affiliations, memberships, funding, or financial holdings that might be perceived as affecting the objectivity of this review.

ACKNOWLEDGMENTS

The authors are grateful to M. Cignoni, A. Frebel, C. Gallart, S. Hildago, M. Mateo, and M. Monelli for providing data and analyses ahead of publication or as private communication.

We thank G. Battaglia, V. Belokurov, M. Cignoni, A. Cole, A. Helmi, and D. Romano, for useful comments and help in the preparation of figures and tables. We thank F. Matteucci, M. Irwin, R. Sancisi, F. Fraternali, G. Clementini, and P. Jablonka for useful conversations, and E. Skillman S. Salvadori, M. Breddels, E. Starkenburg, T. de Boer, and P. van der Kruit for careful comments on early drafts. Very detailed and useful comments from the editor, J. Kormendy, were also highly appreciated.

E.T. thanks Bologna Observatory for hospitality and Paris Observatory for hospitality and financial support. E.T. gratefully acknowledges support from an NWO-VICI grant. V.H. acknowledges the financial support of Program National Galaxies (PNG) of CNRS/INSU, France.

This research has made use of the NASA/IPAC Extragalactic Database (NED), which is operated by the Jet Propulsion Laboratory, California Institute of Technology, under contract with the National Aeronautics and Space Administration.

LITERATURE CITED

Aaronson M. 1983. *Ap. J. Lett.* 266:L11–15

Adelman-McCarthy JK, Agüeros MA, Allam SS, Anderson KSJ, Anderson SF, et al. 2007. *Ap. J. Suppl.* 172:634–44

Aloisi A, Clementini G, Tosi M, Annibali F, Contreras R, et al. 2007. *Ap. J. Lett.* 667:L151–54

Aloisi A, Savaglio S, Heckman TM, Hoopes CG, Leitherer C, Sembach KR. 2003. *Ap. J.* 595:760–78

Aloisi A, Tosi M, Greggio L. 1999. *Astron. J.* 118:302–22

Aloisi A, van der Marel RP, Mack J, Leitherer C, Sirianni M, Tosi M. 2005. *Ap. J. Lett.* 631:L45–48

Angeretti L, Tosi M, Greggio L, Sabbi E, Aloisi A, Leitherer C. 2005. *Astron. J.* 129:2203–16

Annibali F, Greggio L, Tosi M, Aloisi A, Leitherer C. 2003. *Astron. J.* 126:2752–73

Aoki W, Arimoto N, Sadakane K, Tolstoy E, Battaglia G, et al. 2009. *Astron. Astrophys.* In press. arXiv:0904.4307

Aparicio A, Carrera R, Martínez-Delgado D. 2001. *Astron. J.* 122:2524–37
Aparicio A, Gallart C. 2004. *Astron. J.* 128:1465–77
Aparicio A, Gallart C, Chiosi C, Bertelli G. 1996. *Ap. J. Lett.* 469:L97–100
Audouze J, Tinsley BM. 1976. *Annu. Rev. Astron. Astrophys.* 14:43–79
Baade W. 1944a. *Ap. J.* 100:137–46
Baade W. 1944b. *Ap. J.* 100:147–50
Barklem PS, Christlieb N, Beers TC, Hill V, Bessell MS, et al. 2005. *Astron. Astrophys.* 439:129–51
Battaglia G. 2007. *Chemistry and kinematics of stars in Local Group galaxies*. PhD thesis. Univ. Groningen, The Netherlands
Battaglia G, Helmi A, Tolstoy E, Irwin M, Hill V, Jablonka P. 2008a. *Ap. J. Lett.* 681:L13–16
Battaglia G, Irwin M, Tolstoy E, Hill V, Helmi A, et al. 2008b. *MNRAS* 383:183–99
Battaglia G, Tolstoy E, Helmi A, Irwin MJ, Letarte B, et al. 2006. *Astron. Astrophys.* 459:423–40
Beers TC, Christlieb N. 2005. *Annu. Rev. Astron. Astrophys.* 43:531–80
Bekki K, Freeman KC. 2003. *MNRAS* 346:L11–15
Bellazzini M, Gennari N, Ferraro FR. 2005. *MNRAS* 360:185–93
Bellazzini M, Gennari N, Ferraro FR, Sollima A. 2004. *MNRAS* 354:708–12
Belokurov V, Evans NW, Irwin MJ, Lynden-Bell D, Yanny B, et al. 2007a. *Ap. J.* 658:337–44
Belokurov V, Walker MG, Evans NW, Faria DC, Gilmore G, et al. 2008. *Ap. J. Lett.* 686:L83–86
Belokurov V, Walker MG, Evans NW, Gilmore G, Irwin M, et al. 2009. *MNRAS*. In press. arXiv:0903.0818
Belokurov V, Zucker DB, Evans NW, Kleyna JT, Koposov S, et al. 2007b. *Ap. J.* 654:897–906
Binggeli B. 1994. In *Dwarf Galaxies*, ed. G Meylan, P Prugniel. *Eur. South. Obs. Astrophys. Symp.*, 49:13–18. Garching: ESO
Binggeli B, Tarenghi M, Sandage A. 1990. *Astron. Astrophys.* 228:42–60
Bonanos AZ, Stanek KZ, Szentgyorgyi AH, Sasselov DD, Bakos GÁ. 2004. *Astron. J.* 127:861–67
Bonifacio P, Hill V, Molaro P, Pasquini L, Di Marcantonio P, Santin P. 2000. *Astron. Astrophys.* 359:663–68
Bonifacio P, Sbordone L, Marconi G, Pasquini L, Hill V. 2004. *Astron. Astrophys.* 414:503–14
Bosler TL, Smecker-Hane TA, Stetson PB. 2007. *MNRAS* 378:318–38
Bovill MS, Ricotti M. 2009. *Ap. J.* 693:1859–70
Bresolin F, Urbaneja MA, Gieren W, Pietrzyński G, Kudritzki RP. 2007. *Ap. J.* 671:2028–39
Brown WR, Geller MJ, Kenyon SJ, Kurtz MJ. 2007. *Ap. J.* 666:231–35
Carigi L, Colín P, Peimbert M. 2006. *Ap. J.* 644:924–39
Carigi L, Colín P, Peimbert M, Sarmiento A. 1995. *Ap. J.* 445:98–107
Carigi L, Hernandez X. 2008. *MNRAS 390*:582–94
Carigi L, Hernandez X, Gilmore G. 2002. *MNRAS* 334:117–28
Carrera R, Aparicio A, Martínez-Delgado D, Alonso-García J. 2002. *Astron. J.* 123:3199–209
Carrera R, Gallart C, Aparicio A, Costa E, Méndez RA, Noël NED. 2008. *Astron. J.* 136:1039–48
Castellani M, Marconi G, Buonanno R. 1996. *Astron. Astrophys.* 310:715–21
Cayrel R, Depagne E, Spite M, Hill V, Spite F, et al. 2004. *Astron. Astrophys.* 416:1117–38
Chiosi E, Vallenari A, Held EV, Rizzi L, Moretti A. 2006. *Astron. Astrophys.* 452:179–93
Choudhury TR, Ferrara A, Gallerani S. 2008. *MNRAS* 385:L58–62
Cignoni M, Sabbi E, Nota A, Tosi M, Degl'Innocenti S, et al. 2009. *Astron. J.* 137:3668–84
Cioni MRL, Bekki K, Clementini G, de Blok WJG, Emerson JP, et al. 2008. *PASA* 25:121–28
Clementini G, Held EV, Baldacci L, Rizzi L. 2003. *Ap. J. Lett.* 588:L85–88
Cole AA, Skillman ED, Tolstoy E, Gallagher JS III, Aparicio A, et al. 2007. *Ap. J. Lett.* 659:L17–20
Coleman MG, Da Costa GS, Bland-Hawthorn J. 2005. *Astron. J.* 130:1065–82
Coleman MG, de Jong JTA. 2008. *Ap. J.* 685:933–46
Cook KH, Mateo M, Olszewski EW, Vogt SS, Stubbs C, Diercks A. 1999. *Publ. Astron. Soc. Pac.* 111:306–12
Dall'Ora M, Clementini G, Kinemuchi K, Ripepi V, Marconi M, et al. 2006. *Ap. J. Lett.* 653:L109–12
de Jong JTA, Harris J, Coleman MG, Martin NF, Bell EF, et al. 2008a. *Ap. J.* 680:1112–19
de Jong JTA, Rix HW, Martin NF, Zucker DB, Dolphin AE, et al. 2008b. *Astron. J.* 135:1361–83
Dekel A, Silk J. 1986. *Ap. J.* 303:39–55
D'Ercole A, Brighenti F. 1999. *MNRAS* 309:941–54
Dohm-Palmer RC, Skillman ED, Gallagher J, Tolstoy E, Mateo M, et al. 1998. *Astron. J.* 116:1227–43

Dohm-Palmer RC, Skillman ED, Mateo M, Saha A, Dolphin A, et al. 2002. *Astron. J.* 123:813–31
Dohm-Palmer RC, Skillman ED, Saha A, Tolstoy E, Mateo M, et al. 1997. *Astron. J.* 114:2527–44
Dolphin AE. 1997. *New Astron.* 2:397–409
Dolphin AE. 2000. *Ap. J.* 531:804–12
Dolphin AE. 2002. *MNRAS* 332:91–108
Dolphin AE, Saha A, Claver J, Skillman ED, Cole AA, et al. 2002. *Astron. J.* 123:3154–98
Dolphin AE, Saha A, Skillman ED, Dohm-Palmer RC, Tolstoy E, et al. 2003a. *Astron. J.* 125:1261–90
Dolphin AE, Saha A, Skillman ED, Dohm-Palmer RC, Tolstoy E, et al. 2003b. *Astron. J.* 126:187–96
Dolphin AE, Walker AR, Hodge PW, Mateo M, Olszewski EW, et al. 2001. *Ap. J.* 562:303–13
Dolphin AE, Weisz DR, Skillman ED, Holtzman JA. 2005. In *Resolved Stellar Populations*, ed. D Valls-Gabaud, M Chavez. ASP Conf. Ser. In press. arXiv:astro-ph/0506430
Eggen OJ, Lynden-Bell D, Sandage AR. 1962. *Ap. J.* 136:748–66
Evans C, Bresolin F, Urbaneja M, Peitrzyński G, Gieren W, Kudritzki RP. 2006. *The Messenger* 126:5–6
Evans C, Smartt S, Lennon D, Dufton P, Hunter I, et al. 2005. *The Messenger* 122:36–38
Evstigneeva EA, Drinkwater MJ, Peng CY, Hilker M, DePropris R, et al. 2008. *Astron. J.* 136:461–78
Faber SM, Lin DNC. 1983. *Ap. J. Lett.* 266:L17–20
Faber SM, Tremaine S, Ajhar EA, Byun YI, Dressler A, et al. 1997. *Astron. J.* 114:1771–96
Fagotto F, Bressan A, Bertelli G, Chiosi C. 1994a. *Astron. Astrophys. Suppl.* 104:365–76
Fagotto F, Bressan A, Bertelli G, Chiosi C. 1994b. *Astron. Astrophys. Suppl.* 105:29–38
Fenner Y, Gibson BK, Gallino R, Lugaro M. 2006. *Ap. J.* 646:184–91
Ferrara A, Tolstoy E. 2000. *MNRAS* 313:291–309
Ferraro FR, Fusi Pecci F, Tosi M, Buonanno R. 1989. *MNRAS* 241:433–52
François P, Depagne E, Hill V, Spite M, Spite F, et al. 2007. *Astron. Astrophys.* 476:935–50
Fraternali F, Tolstoy E, Irwin M, Cole A. 2009. *Astron. Astrophys.* 499:121–28
Frebel A, Simon JD, Geha M, Willman B. 2009. *Ap. J.* In press. arXiv:0902.2395
Freeman K, Bland-Hawthorn J. 2002. *Annu. Rev. Astron. Astrophys.* 40:487–537
Freeman KC. 1970. *Ap. J.* 160:811–30
Fujita A, Mac Low MM, Ferrara A, Meiksin A. 2004. *Ap. J.* 613:159–79
Fulbright JP, McWilliam A, Rich RM. 2007. *Ap. J.* 661:1152–79
Fulbright JP, Rich RM, Castro S. 2004. *Ap. J.* 612:447–53
Gallagher JS III, Hunter DA, Tutukov AV. 1984. *Ap. J.* 284:544–56
Gallagher JS III, Tolstoy E, Dohm-Palmer RC, Skillman ED, Cole AA, et al. 1998. *Astron. J.* 115:1869–87
Gallart C, Aparicio A, Bertelli G, Chiosi C. 1996. *Astron. J.* 112:1950–68
Gallart C, Aparicio A, Zinn R, Buonanno R, Hardy E, Marconi G. 2005. In *IAU Colloq. 198: Near-Field Cosmology with Dwarf Elliptical Galaxies*, ed. H Jerjen, B Binggeli, pp. 25–29. Cambridge, UK: Cambridge Univ. Press
Gallart C, Freedman WL, Aparicio A, Bertelli G, Chiosi C. 1999. *Astron. J.* 118:2245–61
Gallart C, the LCID team. 2007. In *Stellar Populations as Building Blocks of Galaxies*, ed. A Vazdekis, R Peletier, 241:290–94. Cambridge, UK: Cambridge Univ. Press
Gallart C, Martínez-Delgado D, Gómez-Flechoso MA, Mateo M. 2001. *Astron. J.* 121:2572–83
Gallart C, Zoccali M, Aparicio A. 2005. *Annu. Rev. Astron. Astrophys.* 43:387–434
Gallazzi A, Charlot S, Brinchmann J, White SDM, Tremonti CA. 2005. *MNRAS* 362:41–58
Geha M, Guhathakurta P, Rich RM, Cooper MC. 2006. *Astron. J.* 131:332–42
Geha M, Willman B, Simon JD, Strigari LE, Kirby EN, et al. 2009. *Ap. J.* 692:1464–75
Geisler D, Smith VV, Wallerstein G, Gonzalez G, Charbonnel C. 2005. *Astron. J.* 129:1428–42
Gieren W, Pietrzyński G, Nalewajko K, Soszyński I, Bresolin F, et al. 2006. *Ap. J.* 647:1056–64
Gieren W, Pietrzyński G, Szewczyk O, Soszyński I, Bresolin F, et al. 2008. *Ap. J.* 683:611–19
Gilmore G, Wilkinson MI, Wyse RFG, Kleyna JT, Koch A, et al. 2007. *Ap. J.* 663:948–59
Gilmore G, Wyse RFG. 1991. *Ap. J. Lett.* 367:L55–58
Glatt K, Gallagher JS III, Grebel EK, Nota A, Sabbi E, et al. 2008. *Astron. J.* 135:1106–16
Grebel EK. 1999. In *The Stellar Content of Local Group Galaxies*, eds. P Whitelock, R Cannon, *IAU Symp.* 192:17–38. San Francisco, CA: Astron. Soc. Pac.
Grebel EK, Gallagher JS III, Harbeck D. 2003. *Astron. J.* 125:1926–39

Greggio L, Marconi G, Tosi M, Focardi P. 1993. *Astron. J.* 105:894–932
Greggio L, Tosi M, Clampin M, de Marchi G, Leitherer C, et al. 1998. *Ap. J.* 504:725–42
Grocholski AJ, Aloisi A, van der Marel RP, Mack J, Annibali F, et al. 2008. *Ap. J. Lett.* 686:L79–82
Gullieuszik M, Held EV, Rizzi L, Girardi L, Marigo P, Momany Y. 2008. *MNRAS* 388:1185–97
Harris J, Zaritsky D. 2004. *Astron. J.* 127:1531–44
Harris J, Zaritsky D. 2006. *Astron. J.* 131:2514–24
Harris WE. 1996. *Astron. J.* 112:1487–88
Heckman TM, Sembach KR, Meurer GR, Strickland DK, Martin CL, et al. 2001. *Ap. J.* 554:1021–34
Heiles C. 1990. *Ap. J.* 354:483–91
Held EV, Clementini G, Rizzi L, Momany Y, Saviane I, Di Fabrizio L. 2001. *Ap. J. Lett.* 562:L39–42
Held EV, Saviane I, Momany Y. 1999. *Astron. Astrophys.* 345:747–59
Helmi A, Irwin MJ, Tolstoy E, Battaglia G, Hill V, et al. 2006. *Ap. J. Lett.* 651:L121–24
Hernandez X, Gilmore G, Valls-Gabaud D. 2000. *MNRAS* 317:831–42
Hilditch RW, Howarth ID, Harries TJ. 2005. *MNRAS* 357:304–24
Hill V, Andrievsky S, Spite M. 1995. *Astron. Astrophys.* 293:347–59
Hill V, Barbuy B, Spite M. 1997. *Astron. Astrophys.* 323:461–68
Hodge P, Miller BW. 1995. *Ap. J.* 451:176–87
Hodge PW. 1971. *Annu. Rev. Astron. Astrophys.* 9:35–66
Holtzman JA, Afonso C, Dolphin A. 2006. *Ap. J. Suppl.* 166:534–48
Holtzman JA, Smith GH, Grillmair C. 2000. *Astron. J.* 120:3060–69
Hunter DA, Elmegreen BG. 2004. *Astron. J.* 128:2170–205
Hunter DA, Elmegreen BG. 2006. *Ap. J. Suppl.* 162:49–79
Hunter DA, Gallagher JS III. 1986. *Publ. Astron. Soc. Pac.* 98:5–28
Hurley-Keller D, Mateo M, Nemec J. 1998. *Astron. J.* 115:1840–55
Ibata R, Chapman S, Irwin M, Lewis G, Martin N. 2006. *MNRAS* 373:L70–74
Ikuta C, Arimoto N. 2002. *Astron. Astrophys.* 391:55–65
Irwin M, Hatzidimitriou D. 1995. *MNRAS* 277:1354–78
Irwin M, Tolstoy E. 2002. *MNRAS* 336:643–48
Irwin MJ, Belokurov V, Evans NW, Ryan-Weber EV, de Jong JTA, et al. 2007. *Ap. J. Lett.* 656:L13–16
Izotov YI, Thuan TX. 1998. *Ap. J.* 500:188–216
Izotov YI, Thuan TX. 1999. *Ap. J.* 511:639–59
Izotov YI, Thuan TX, Stasińska G. 2007. *Ap. J.* 662:15–38
Johnson JA, Bolte M. 2002. *Ap. J.* 579:616–25
Kallivayalil N, van der Marel RP, Alcock C. 2006. *Ap. J.* 652:1213–29
Kaufer A, Venn KA, Tolstoy E, Pinte C, Kudritzki RP. 2004. *Astron. J.* 127:2723–37
Kirby EN, Guhathakurta P, Sneden C. 2008. *Ap. J.* 682:1217–33
Kirby EN, Simon JD, Geha M, Guhathakurta P, Frebel A. 2008. *Ap. J. Lett.* 685:L43–46
Kleyna JT, Wilkinson MI, Evans NW, Gilmore G. 2005. *Ap. J. Lett.* 630:L141–44
Kniazev AY, Grebel EK, Pustilnik SA, Pramskij AG, Zucker DB. 2005. *Astron. J.* 130:1558–73
Kobulnicky HA, Skillman ED. 1997. *Ap. J.* 489:636–55
Koch A, Grebel EK, Gilmore GF, Wyse RFG, Kleyna JT, et al. 2008a. *Astron. J.* 135:1580–97
Koch A, Grebel EK, Kleyna JT, Wilkinson MI, Harbeck DR, et al. 2007a. *Astron. J.* 133:270–83
Koch A, Grebel EK, Wyse RFG, Kleyna JT, Wilkinson MI, et al. 2006. *Astron. J.* 131:895–911
Koch A, McWilliam A, Grebel EK, Zucker DB, Belokurov V. 2008b. *Ap. J. Lett.* 688:L13–16
Koch A, Wilkinson MI, Kleyna JT, Gilmore GF, Grebel EK, et al. 2007b. *Ap. J.* 657:241–61
Koposov S, Belokurov V, Evans NW, Hewett PC, Irwin MJ, et al. 2008. *Ap. J.* 686:279–91
Kormendy J. 1985. *Ap. J.* 295:73–79
Kormendy J, Fisher DB, Cornell ME, Bender R. 2008. *Ap. J. Suppl.* In press. arXiv:0810.1681
Kuehn C, Kinemuchi K, Ripepi V, Clementini G, Dall'Ora M, et al. 2008. *Ap. J. Lett.* 674:L81–84
Kunth D, Östlin G. 2000. *Astron. Astrophys. Rev.* 10:1–79
Lanfranchi GA, Matteucci F, Cescutti G. 2008. *Astron. Astrophys.* 481:635–44
Larson RB. 1974. *MNRAS* 169:229–46
Leaman R, Cole AA, Venn KA, Tolstoy E, Irwin MJ, et al. 2009. *Ap. J.* In press. arXiv0904.0657

Lebouteiller V, Kunth D, Lequeux J, Lecavelier des Etangs A, Désert JM, et al. 2004. *Astron. Astrophys.* 415:55–61
Lee H, Skillman ED, Venn KA. 2005. *Ap. J.* 620:223–37
Lee H, Skillman ED, Venn KA. 2006. *Ap. J.* 642:813–33
Lee YW, Joo JM, Sohn YJ, Rey SC, Lee HC, Walker AR. 1999. *Nature* 402:55–57
Legrand F, Tenorio-Tagle G, Silich S, Kunth D, Cerviño M. 2001. *Ap. J.* 560:630–35
Lequeux J, Peimbert M, Rayo JF, Serrano A, Torres-Peimbert S. 1979. *Astron. Astrophys.* 80:155–66
Letarte B. 2007. *Chemical analysis of the Fornax dwarf galaxy*. PhD thesis. Univ. Groningen, The Netherlands
Lewis GF, Ibata RA, Chapman SC, McConnachie A, Irwin MJ, et al. 2007. *MNRAS* 375:1364–70
Lin DNC, Faber SM. 1983. *Ap. J. Lett.* 266:L21–25
Lo KY, Sargent WLW, Young K. 1993. *Astron. J.* 106:507–29
Luck RE, Moffett TJ, Barnes TG III, Gieren WP. 1998. *Astron. J.* 115:605–34
Mackey AD, Huxor A, Ferguson AMN, Tanvir NR, Irwin M, et al. 2006. *Ap. J. Lett.* 653:L105–8
Mac Low MM, Ferrara A. 1999. *Ap. J.* 513:142–55
Magrini L, Leisy P, Corradi RLM, Perinotto M, Mampaso A, Vílchez JM. 2005. *Astron. Astrophys.* 443:115–32
Mapelli M, Ripamonti E, Tolstoy E, Sigurdsson S, Irwin MJ, Battaglia G. 2007. *MNRAS* 380:1127–40
Marcolini A, D'Ercole A, Battaglia G, Gibson BK. 2008. *MNRAS* 386:2173–80
Marcolini A, D'Ercole A, Brighenti F, Recchi S. 2006. *MNRAS* 371:643–58
Marconi G, Matteucci F, Tosi M. 1994. *MNRAS* 270:35–45
Marconi G, Tosi M, Greggio L, Focardi P. 1995. *Astron. J.* 109:173–99
Martin CL, Kobulnicky HA, Heckman TM. 2002. *Ap. J.* 574:663–92
Martin NF, Coleman MG, de Jong JTA, Rix HW, Bell EF, et al. 2008. *Ap. J. Lett.* 672:L13–16
Martin NF, de Jong JTA, Rix HW. 2008. *Ap. J.* 684:1075–92
Martínez-Delgado D, Aparicio A, Gallart C. 1999. *Astron. J.* 118:2229–44
Mateo M. 1994. In *Dwarf Galaxies*, ed. G Meylan, P Prugniel, *Eur. South. Obs. Astrophys. Symp.*, 49:309–22. Garching: ESO
Mateo M. 2008. *The Messenger* 134:3–8
Mateo M, Hurley-Keller D, Nemec J. 1998. *Astron. J.* 115:1856–68
Mateo M, Olszewski EW, Walker MG. 2008. *Ap. J.* 675:201–33
Mateo ML. 1998. *Annu. Rev. Astron. Astrophys.* 36:435–506
Matteucci F. 2003. *Ap. Space Sci.* 284:539–48
Matteucci F, Brocato E. 1990. *Ap. J.* 365:539–43
Matteucci F, Chiosi C. 1983. *Astron. Astrophys.* 123:121–34
Matteucci F, Tosi M. 1985. *MNRAS* 217:391–405
McConnachie AW, Arimoto N, Irwin M, Tolstoy E. 2006. *MNRAS* 373:715–28
McConnachie AW, Irwin MJ. 2006. *MNRAS* 365:1263–76
McConnachie AW, Irwin MJ, Ferguson AMN, Ibata RA, Lewis GF, Tanvir N. 2005. *MNRAS* 356:979–97
McCumber MP, Garnett DR, Dufour RJ. 2005. *Astron. J.* 130:1083–96
McWilliam A, Smecker-Hane TA. 2005. In *Cosmic Abundances as Records of Stellar Evolution and Nucleosynthesis*, ed. TG Barnes III, FN Bash, *ASP Conf. Ser.*, 36:221–34. San Francisco, CA: ASP
Meurer GR, Freeman KC, Dopita MA, Cacciari C. 1992. *Astron. J.* 103:60–80
Miller BW, Dolphin AE, Lee MG, Kim SC, Hodge P. 2001. *Ap. J.* 562:713–26
Momany Y, Held EV, Saviane I, Bedin LR, Gullieuszik M, et al. 2005. *Astron. Astrophys.* 439:111–27
Momany Y, Held EV, Saviane I, Zaggia S, Rizzi L, Gullieuszik M. 2007. *Astron. Astrophys.* 468:973–78
Monaco L, Bellazzini M, Bonifacio P, Buzzoni A, Ferraro FR, et al. 2007. *Astron. Astrophys.* 464:201–9
Monaco L, Bellazzini M, Bonifacio P, Ferraro FR, Marconi G, et al. 2005. *Astron. Astrophys.* 441:141–51
Muñoz RR, Carlin JL, Frinchaboy PM, Nidever DL, Majewski SR, Patterson RJ. 2006a. *Ap. J. Lett.* 650:L51–54
Muñoz RR, Frinchaboy PM, Majewski SR, Kuhn JR, Chou MY, et al. 2005. *Ap. J. Lett.* 631:L137–41
Muñoz RR, Majewski SR, Zaggia S, Kunkel WE, Frinchaboy PM, et al. 2006b. *Ap. J.* 649:201–23
Nemec JM, Wehlau A, Mendes de Oliveira C. 1988. *Astron. J.* 96:528–59
Nissen PE, Schuster WJ. 1997. *Astron. Astrophys.* 326:751–62

Nissen PE, Schuster WJ. 2008. In *The Galaxy Disk in Cosmological Context, Proc. Int. Astron. Union*, ed. J Andersen, J Bland-Hawthorn, B Nordström. IAU Symp., 254:103–8
Noël NED, Gallart C, Costa E, Méndez RA. 2007. *Astron. J.* 133:2037–52
Norris JE, Gilmore G, Wyse RFG, Wilkinson MI, Belokurov V, et al. 2008. *Ap. J. Lett.* 689:L113–16
Olive KA, Rood RT, Schramm DN, Truran J, Vangioni-Flam E. 1995. *Ap. J.* 444:680–85
Olive KA, Steigman G, Skillman ED. 1997. *Ap. J.* 483:788–97
Olszewski EW. 1998. In *Galactic Halos*, ed. D Zaritsky, *ASP Conf. Ser.*, 136:70–77. San Francisco, CA: ASP
Pagel BEJ, Edmunds MG. 1981. *Annu. Rev. Astron. Astrophys.* 19:77–113
Pagel BEJ, Tautvaisiene G. 1998. *MNRAS* 299:535–44
Pancino E, Ferraro FR, Bellazzini M, Piotto G, Zoccali M. 2000. *Ap. J. Lett.* 534:L83–87
Pasquini L, Avila G, Blecha A, Cacciari C, Cayatte V, et al. 2002. *The Messenger* 110:1–9
Peña M, Stasińska G, Richer MG. 2007. *Astron. Astrophys.* 476:745–58
Peimbert M, Bohigas J, Torres-Peimbert S. 1988. *Rev. Mex. Astron. Astrofis.* 16:45–54
Peimbert M, Torres-Peimbert S. 1974. *Ap. J.* 193:327–33
Pietrzyński G, Gieren W, Soszyński I, Bresolin F, Kudritzki RP, et al. 2006. *Ap. J.* 642:216–24
Pietrzyński G, Gieren W, Szewczyk O, Walker A, Rizzi L, et al. 2008. *Astron. J.* 135:1993–97
Pilyugin LS. 1993. *Astron. Astrophys.* 277:42–52
Pompeia L, Hill V, Spite M, Cole A, Primas F, et al. 2008. *Astron. Astrophys.* 480:379–95
Queloz D, Dubath P, Pasquini L. 1995. *Astron. Astrophys.* 300:31–42
Recchi S, Hensler G, Angeretti L, Matteucci F. 2006. *Astron. Astrophys.* 445:875–88
Recchi S, Matteucci F, D'Ercole A, Tosi M. 2004. *Astron. Astrophys.* 426:37–51
Richstone DO, Tremaine S. 1986. *Astron. J.* 92:72–74
Rieschick A, Hensler G. 2003. *Ap. Space Sci.* 284:861–64
Rizzi L, Held EV, Saviane I, Tully RB, Gullieuszik M. 2007. *MNRAS* 380:1255–60
Romano D, Tosi M, Matteucci F. 2006. *MNRAS* 365:759–78
Ryan-Weber EV, Begum A, Oosterloo T, Pal S, Irwin MJ, et al. 2008. *MNRAS* 384:535–40
Sabbi E, Sirianni M, Nota A, Tosi M, Gallagher JS III, et al. 2007. *Astron. J.* 133:44–57
Sadakane K, Arimoto N, Ikuta C, Aoki W, Jablonka P, Tajitsu A. 2004. *Publ. Astron. Soc. Jpn.* 56:1041–58
Saha A, Hoessel JG. 1990. *Astron. J.* 99:97–148
Saha A, Hoessel JG, Krist J. 1992. *Astron. J.* 103:84–103
Saha A, Monet DG, Seitzer P. 1986. *Astron. J.* 92:302–27
Sakai S, Madore BF, Freedman WL. 1997. *Ap. J.* 480:589–95
Salvadori S, Ferrara A. 2009. *MNRAS* 395:L6–10
Salvadori S, Ferrara A, Schneider R. 2008. *MNRAS* 386:348–58
Saviane I, Held EV, Piotto G. 1996. *Astron. Astrophys.* 315:40–51
Sbordone L, Bonifacio P, Buonanno R, Marconi G, Monaco L, Zaggia S. 2007. *Astron. Astrophys.* 465:815–24
Schoerck T, Christlieb N, Cohen JG, Beers TC, Shectman S, et al. 2008. *Astron. Astrophys.* Submitted. arXiv:0809.1172
Schulte-Ladbeck RE, Hopp U, Greggio L, Crone MM. 2000. *Astron. J.* 120:1713–30
Schulte-Ladbeck RE, Hopp U, Greggio L, Crone MM, Drozdovsky IO. 2001. *Astron. J.* 121:3007–25
Searle L, Sargent WLW, Bagnuolo WG. 1973. *Ap. J.* 179:427–38
Seiden PE, Schulman LS, Gerola H. 1979. *Ap. J.* 232:702–6
Shetrone M, Venn KA, Tolstoy E, Primas F, Hill V, Kaufer A. 2003. *Astron. J.* 125:684–706
Shetrone MD, Bolte M, Stetson PB. 1998. *Astron. J.* 115:1888–93
Shetrone MD, Côté P, Sargent WLW. 2001. *Ap. J.* 548:592–608
Shetrone MD, Siegel MH, Cook DO, Bosler T. 2009. *Astron. J.* 137:62–71
Siegel MH. 2006. *Ap. J. Lett.* 649:L83–86
Siegel MH, Shetrone MD, Irwin M. 2008. *Astron. J.* 135:2084–94
Simmerer J, Sneden C, Cowan JJ, Collier J, Woolf VM, Lawler JE. 2004. *Ap. J.* 617:1091–114
Simon JD, Geha M. 2007. *Ap. J.* 670:313–31
Skillman ED, Bender R. 1995. *Rev. Mex. Astron. Astrof. Conf. Ser.* 3:25–30
Skillman ED, Bomans DJ, Kobulnicky HA. 1997. *Ap. J.* 474:205–16

Skillman ED, Gallart C. 2002. In *Observed HR Diagrams and Stellar Evolution*, ed. T Lejeune, J Fernandes, *ASP Conf. Ser.*, 274:535–44. San Francisco, CA: ASP
Skillman ED, Kennicutt RC, Hodge PW. 1989. *Ap. J.* 347:875–82
Skillman ED, Terlevich R, Melnick J. 1989. *MNRAS* 240:563–72
Skillman ED, Tolstoy E, Cole AA, Dolphin AE, Saha A, et al. 2003. *Ap. J.* 596:253–72
Smecker-Hane TA, Stetson PB, Hesser JE, Lehnert MD. 1994. *Astron. J.* 108:507–13
Smecker-Hane TA, Stetson PB, Hesser JE, Vandenberg DA. 1996. In *From Stars to Galaxies: the Impact of Stellar Physics on Galaxy Evolution*, ed. C Leitherer, U Fritze-von Alvensleben, J Huchra, *ASP Conf. Ser.*, 98:328–32. San Francisco, CA: ASP
Smith GH, Siegel MH, Shetrone MD, Winnick R. 2006. *Publ. Astron. Soc. Pac.* 118:1361–72
Sneden C, Cowan JJ, Gallino R. 2008. *Annu. Rev. Astron. Astrophys.* 46:241–88
Soszyński I, Gieren W, Pietrzyński G, Bresolin F, Kudritzki RP, Storm J. 2006. *Ap. J.* 648:375–82
Stark DP, Bunker AJ, Ellis RS, Eyles LP, Lacy M. 2007. *Ap. J.* 659:84–97
Starkenburg E, Hill V, Tolstoy E, Irwin M, Battaglia G, Helmi A. 2008. *GARCON08, Chemical Evolution of Dwarf Galaxies and Stellar Clusters*. On-line proc. **http://www.mpa-garching.mpg.de/mpa/conferences/garcon08/posters.html**
Suntzeff NB, Mateo M, Terndrup DM, Olszewski EW, Geisler D, Weller W. 1993. *Ap. J.* 418:208–28
Tammann GA. 1994. In *Dwarf Galaxies*, ed. G Meylan, P Prugniel, *Eur. South. Obs. Astrophys. Symp.*, 49:3–9. Garching: ESO
Tassis K, Abel T, Bryan GL, Norman ML. 2003. *Ap. J.* 587:13–24
Tautvaišienė G, Geisler D, Wallerstein G, Borissova J, Bizyaev D, et al. 2007. *Astron. J.* 134:2318–27
Tenorio-Tagle G. 1996. *Astron. J.* 111:1641–50
Thuan TX, Lecavelier des Etangs A, Izotov YI. 2002. *Ap. J.* 565:941–51
Tinsley BM. 1968. *Ap. J.* 151:547–65
Tinsley BM. 1980. *Fund. Cosmic Phys.* 5:287–388
Tolstoy E. 1996. *Ap. J.* 462:684–704
Tolstoy E. 2003. In *A Decade of Hubble Space Telescope Science*, ed. M Livio, K Noll, M Stiavelli, pp. 128–52. Cambridge, UK: Cambridge Univ. Press
Tolstoy E, Hill V, Irwin M, Helmi A, Battaglia G, et al. 2006. *The Messenger* 123:33–37
Tolstoy E, Irwin M. 2000. *MNRAS* 318:1241–48
Tolstoy E, Irwin MJ, Cole AA, Pasquini L, Gilmozzi R, Gallagher JS. 2001. *MNRAS* 327:918–38
Tolstoy E, Irwin MJ, Helmi A, Battaglia G, Jablonka P, et al. 2004. *Ap. J. Lett.* 617:L119–22
Tolstoy E, Saha A. 1996. *Ap. J.* 462:672–83
Tolstoy E, Saha A, Hoessel JG, Danielson GE. 1995. *Astron. J.* 109:579–87
Tolstoy E, Venn KA, Shetrone M, Primas F, Hill V, et al. 2003. *Astron. J.* 125:707–26
Tosi M. 1998. In *Dwarf Galaxies and Cosmology*, ed. TX Thuan, C Balkowski, V Cayatte, JTT Van. *Rencontres Moriond* 33:443–52. Gyf-sur-Yvette, Paris: Ed. Front.
Tosi M. 2007a. *41st ESLAB Symp. The Impact of HST on European Astronomy*. In press. arXiv:0707.3057
Tosi M. 2007b. In *From Stars to Galaxies: Building the Pieces to Build Up the Universe*, ed. A Vallenari, R Tantalo, L Portinari, A Moretti, *ASP Conf. Ser.*, 374:221–29. San Francisco, CA: ASP
Tosi M, Gallagher JS III, Sabbi E, Glatt K, Grebel EK, et al. 2008. IAU Symp.: *Low- Metallicity Star Formation: From the First Stars to Dwarf Galaxies*, Proc. Int. Astron. Union, 255:381–86
Tosi M, Greggio L, Marconi G, Focardi P. 1991. *Astron. J.* 102:951–74
Travaglio C, Gallino R, Arnone E, Cowan J, Jordan F, Sneden C. 2004. *Ap. J.* 601:864–84
Tsujimoto T, Nomoto K, Yoshii Y, Hashimoto M, Yanagida S, Thielemann FK. 1995. *MNRAS* 277:945–58
Urbaneja MA, Kudritzki RP, Bresolin F, Przybilla N, Gieren W, Pietrzyński G. 2008. *Ap. J.* 684:118–35
Vallenari A, Schmidtobreick L, Bomans DJ. 2005. *Astron. Astrophys.* 435:821–29
van Zee L, Haynes MP. 2006. *Ap. J.* 636:214–39
van Zee L, Skillman ED, Haynes MP. 2006. *Ap. J.* 637:269–82
Veilleux S, Cecil G, Bland-Hawthorn J. 2005. *Annu. Rev. Astron. Astrophys.* 43:769–826
Venn KA. 1999. *Ap. J.* 518:405–21
Venn KA, Irwin M, Shetrone MD, Tout CA, Hill V, Tolstoy E. 2004a. *Astron. J.* 128:1177–95

Venn KA, Lennon DJ, Kaufer A, McCarthy JK, Przybilla N, et al. 2001. *Ap. J.* 547:765–76
Venn KA, Tolstoy E, Kaufer A, Kudritzki RP. 2004b. In C*arnegie Obs. Astrophys. Ser.*, Vol. 4: *Origin and Evolution of the Elements*, ed. A McWilliam, M Rauch, p. 58. Cambridge, UK: Cambridge Univ. Press
Venn KA, Tolstoy E, Kaufer A, Skillman ED, Clarkson SM, et al. 2003. *Astron. J.* 126:1326–45
Vermeij R, van der Hulst JM. 2002. *Astron. Astrophys.* 391:1081–95
Walker MG, Mateo M, Olszewski E. 2009. *Astron. J.* 137:3100–8
Walker MG, Mateo M, Olszewski EW, Bernstein R, Wang X, Woodroofe M. 2006a. *Astron. J.* 131:2114–39
Walker MG, Mateo M, Olszewski EW, Pal JK, Sen B, Woodroofe M. 2006b. *Ap. J. Lett.* 642:L41–44
Westfall KB, Majewski SR, Ostheimer JC, Frinchaboy PM, Kunkel WE, et al. 2006. *Astron. J.* 131:375–406
Westmoquette MS, Smith LJ, Gallagher JS. 2008. *MNRAS* 383:864–78
Whiting AB, Hau GKT, Irwin M. 1999. *Astron. J.* 118:2767–74
Wilkinson MI, Kleyna JT, Evans NW, Gilmore GF, Irwin MJ, Grebel EK. 2004. *Ap. J. Lett.* 611:L21–24
Willman B, Dalcanton JJ, Martinez-Delgado D, West AA, Blanton MR, et al. 2005. *Ap. J. Lett.* 626:L85–88
Wirth A, Gallagher JS III. 1984. *Ap. J.* 282:85–94
Wolf B. 1973. *Astron. Astrophys.* 28:335–48
Wyder TK. 2001. *Astron. J.* 122:2490–523
Wyder TK. 2003. *Astron. J.* 125:3097–110
Young LM, Lo KY. 1997. *Ap. J.* 490:710–28
Young LM, Skillman ED, Weisz DR, Dolphin AE. 2007. *Ap. J.* 659:331–38
Young LM, van Zee L, Lo KY, Dohm-Palmer RC, Beierle ME. 2003. *Ap. J.* 592:111–28
Zucker DB, Belokurov V, Evans NW, Kleyna JT, Irwin MJ, et al. 2006a. *Ap. J. Lett.* 650:L41–44
Zucker DB, Belokurov V, Evans NW, Wilkinson MI, Irwin MJ, et al. 2006b. *Ap. J. Lett.* 643:L103–6

Annual Review of Astronomy and Astrophysics

Volume 47, 2009

Contents

Indexes

Errata

An online log of corrections to *Annual Review of Astronomy and Astrophysics* articles may be found at http://astro.annualreviews.org/errata.shtml